Available online at www.sciencedirect.com
ScienceDirect
Nuclear Physics A 810 (2008) 13–76
NUCLEAR PHYSICS A
www.elsevier.com/locate/nuclphysa

Global and local level density models

A.J. Koning [a,*], S. Hilaire [b], S. Goriely

[a] *Nuclear Research and Consultancy Group NRG, PO Box 25, 1755 ZG Petten, The Netherlands*
[b] *Commissariat à l'Energie Atomique, Centre DAM – Ile de France, Service de Physique Nucléaire, Bruyères-le-Châtel, 91297 Arpajon cedex, France*
[c] *Institut d'Astronomie et d'Astrophysique, Université Libre de Bruxelles, Campus de la Plaine CP 226, B-1050 Brussels, Belgium*

Received 4 January 2008; received in revised form 30 May 2008; accepted 10 June 2008

Available online 21 June 2008

Abstract

Four different level density models, three phenomenological and one microscopic, are consistently parameterized using the same set of experimental observables. For each of the phenomenological models, the Constant Temperature Model, the Back-shifted Fermi gas Model and the Generalized Superfluid Model, a version without and with explicit collective enhancement is considered. Moreover, a recently published microscopic combinatorial model is compared with the phenomenological approaches and with the same set of experimental data. For each nuclide for which sufficient experimental data exists, a local level density parameterization is constructed for each model. Next, these local models have helped to construct global level density prescriptions, to be used for cases for which no experimental data exists. Altogether, this yields a collection of level density formulae and parameters that can be used with confidence in nuclear model calculations. To demonstrate this, a large-scale validation with experimental discrete level schemes and experimental cross sections and neutron emission spectra for various different reaction channels has been performed.

1. Introduction

In statistical models for predicting nuclear reactions, level densities are needed at excitation energies where discrete level information is not available or incomplete. Together with the optical model potential, a correct level density is perhaps the most crucial ingredient for a reliable

* Corresponding author.
E-mail address: koning@nrg-nl.com (A.J. Koning).

0375-9474/$ – see front matter
doi:10.1016/j.nuclphysa.2008.06.005

theoretical analysis of cross sections, spectra, angular distributions, and other nuclear reaction observables. This is one of the reasons why level densities have been thoroughly studied in the past and the existing literature on the subject consists of a panoply of models ranging from microscopic level densities that are directly obtained from combinatorial methods and Hartree–Fock approaches to phenomenological analytical expressions. From a physical point of view, microscopic approaches are obviously to be preferred, and the combination of advances in theoretical nuclear physics and dramatically increased computer power has indeed led to very promising results, see e.g. [1,2]. It is now possible to tabulate level density values for both parities and a wide range of spins on a dense energy grid for nuclides spanning the entire nuclide chart. On the other hand, phenomenological, analytical level density formulae are still routinely used in nuclear reaction calculations. Often, especially for the stable nuclides, experimental information such as discrete level energies and spins and mean resonance spacings is available, which is not reproduced by microscopic approaches. As usual, adjustable parameters are then welcome to account for our current inability to perfectly describe these observables. To optimize between the best possible physics and the best possible results, either microscopic, tabulated level densities may be multiplied by simple empirical adjustment expressions (which should do not deviate too much from unity) that allow us to fit basic observables, or microscopic level densities should inspire the development of adjustable, analytical expressions. In this paper, we follow both approaches, resulting in various level density descriptions and parameters which can directly be used in nuclear reaction calculations.

Level density studies that only address the low energy region of discrete levels, or only the energy region around and above the neutron separation energy, where resonance information is available, are of limited value to modern nuclear reaction calculations. What is required is a reliable, continuous prescription over a large energy range, 0–10 MeV, 0–50 MeV or even 0–200 MeV, depending on the application. Hereby, one should realize that issues such as the proper damping mechanism for collective effects at high energies are still unsolved, which obviously affects the reliability of level density models. Another recurring issue that we have encountered too often is the completeness of the formalism and parameterization. This is very important when it comes to actual implementation in nuclear reaction software. Many expressions and parameters enter the phenomenological level density models, with different prescriptions for different energy regimes, and failure to precise them all does not allow reproduction of the results by others. In this paper, we will remove several of these problems by providing a consistent parameterization of four level density models, namely the

- Back-shifted Fermi gas Model (BFM)
- Constant Temperature Model (CTM)
- Generalized Superfluid Model (GSM)
- Skyrme–Hartree–Fock–Bogolyubov combinatorial Model (HFM)

The parameterizations will extend over a large energy range, taking into account experimental information from both discrete levels and mean resonance spacings.

In the past, all phenomenological level density models have come with their own set of particular problems. For example, the CTM [3] requires solving the problem of matching the constant temperature part at low energies and the Fermi gas expression at high energies. Since this matching depends on experimental information (discrete levels, mean resonance spacings, shell corrections, separation energies, etc.) it may occur that the solution of the matching problem yields hard to believe, and sometimes unphysical, values for the matching parameters. Now that

nuclear reaction calculations can be performed for many nuclides in a relatively short time span, it is essential that the level density model is robust, since often not every individual case can be subjected to a detailed inspection. Here we have verified that no anomalous parameters occur, for any model, not only by careful inspection of the resulting level densities, but also through direct validation in our nuclear reaction code. Another phenomenological approach is to treat the pairing energy as an adjustable parameter, which is the basis of the BFM [4]. This removes the matching problem, since all observables are fitted with only two parameters, but the standard version of the Fermi gas expression leads to numerical divergence when used at low excitation energy. Although that problem has been solved about 20 years ago, the use of the BFM is not as widespread as the CTM. Instead, the CTM is often invoked for the lowest energies, at the expense of using more parameters, while it remains to be seen whether it produces results better than the BFM. Finally, for the GSM [5] the problem apparently has been its inaccessibility and relative obscurity, when compared with the other two approaches. There are however no basic unsolvable problems in the parameterization of this model, as has been shown for individual cases in the past and as we will show here for the entire periodic table.

Before we start the description of the various models, an issue to mention already now is nomenclature. The first versions of the CTM and BFM models have been constructed more than 30 years ago. Refinements such as energy-dependent shell effects and explicit treatment of collective effects were not yet included in those first studies. However, when we speak of the CTM, BFM, or GSM in this paper, it should be understood that such effects are always, for energy-dependent shell effects, or optionally, for collective effects, included. The basic distinction between the various models thus only concerns differences in basic methodology (e.g. constant temperature vs. back-shifted pairing corrections). All other aspects will be treated equally for all models, to enable consistent comparisons.

For each of the models, we have produced local level density parameters, i.e. parameters that are optimized per nucleus, which give the best average description of all observables (discrete levels, mean resonance spacing, etc.) for the nucleus under consideration. Simultaneously, we have also produced a global level density parameterization for all models, which can be used for any nucleus, especially if no experimental information is available. In sum, various novelties are presented here:

- A modern experimental database: Use of the large compilation of mean resonance spacings, D_0, of the RIPL library [6], and the most recent version of the Evaluated Nuclear Structure Data File (ENSDF), available in processed form as discrete level file in the RIPL library.
- All level density models are compared on the same consistent basis. By simultaneously adopting a local and a global approach, we ensure that level density estimates for nuclides with and without experimental information are founded on the same basis. All necessary ingredients are completely specified, so that all our models can be reproduced by others.
- A direct comparison with microscopical level densities based on Skyrme–Hartree–Fock–Bogolyubov calculations, which themselves are optionally adjusted to reproduce the basic observables.
- Direct level density validation with nuclear reaction calculations. For non-fissile nuclides (at least), two important ingredients, namely the optical model potential [7] and the pre-equilibrium model [8], are now relatively well under control, leaving the level density parameterization as the major remaining uncertainty. We will present a consistent study of the effects of various level density models on nuclear reaction calculations.

A good reason to provide more than one level density model is that while no single model is the most appropriate for all nuclides, having various approaches that are all assumed to be more or less reliable offer the possibility to do sensitivity and uncertainty analyses of nuclear reaction calculations.

This paper is set up as follows. In Section 2 we provide the theoretical formulation of the level density. It includes the level density expression, the general forms for the level density parameter and the spin cut-off parameter and collective effects. In Section 3 we describe the experimental information that our models will be validated with. In Section 4 we make the distinction between the different level density models that we treat in this paper. Section 5 describes the optimization procedure for the obtained parameters and in Section 6 we discuss the results. Finally, the paper is summarized in Section 7.

2. Theory

The derivation of analytical level density expressions for independent nucleons from a grand partition function, using the saddle-point approximation, is well known [9] and will not be repeated here. However, we feel that we should give a complete presentation of all level density formulae used, including a precise description of all ingredients, for any energy regime that may occur in statistical reaction calculations. This should ensure reproduction of our results by others.

To set the notation, we first give some general definitions. The *level density* $\rho(E_x, J, \Pi)$ corresponds to the number of nuclear levels per MeV around an excitation energy E_x, for a certain spin J and parity Π. The *total level density* $\rho^{\mathrm{tot}}(E_x)$ corresponds to the total number of levels per MeV around E_x, and is obtained by summing the level density over spin and parity:

$$\rho^{\mathrm{tot}}(E_x) = \sum_J \sum_{\Pi} \rho(E_x, J, \Pi). \tag{1}$$

The nuclear levels are degenerate in M, the magnetic quantum number, which gives rise to the *total state density* $\omega^{\mathrm{tot}}(E_x)$ which includes the $2J + 1$ states for each level, i.e.

$$\omega^{\mathrm{tot}}(E_x) = \sum_J \sum_{\Pi} (2J+1)\rho(E_x, J, \Pi). \tag{2}$$

When level densities are given by analytical expressions they are usually factorized as follows

$$\rho(E_x, J, \Pi) = P(E_x, J, \Pi) R(E_x, J) \rho^{\mathrm{tot}}(E_x), \tag{3}$$

where $P(E_x, J, \Pi)$ is the parity distribution and $R(E_x, J)$ the spin distribution. In this work the parity equipartition is assumed for the three phenomenological models,

$$P(E_x, J, \Pi) = \frac{1}{2}, \tag{4}$$

which is quite a good approximation at energies of a few MeV and higher. We note that recent progress is being made to turn this statement into a quantitative model [10,11]. Finally, for future reference we provide the general expression for the total state density, as obtained from the methods of statistical mechanics [12],

$$\omega^{\mathrm{tot}}(E_x) = \frac{\exp[S(E_x)]}{\sqrt{D(E_x)}}, \tag{5}$$

where S is the entropy and D is the determinant related to the saddle-point approximation. Appropriate choices for S and D lead to the various analytical level density expressions detailed in this paper.

2.1. The Fermi gas model

Arguably the best known analytical level density expression is that of the Fermi gas model (FGM) [13]. It is based on the assumption that the single particle states which construct the excited levels of the nucleus are equally spaced, and in fact holds for non-interacting nucleons generally, and that collective levels are absent. For a two-fermion system, i.e. distinguishing between excited neutrons and protons, the total Fermi gas state density reads

$$\omega_F^{\mathrm{tot}}(E_x) = \frac{\sqrt{\pi}}{12}\frac{\exp[2\sqrt{aU}]}{a^{1/4}U^{5/4}}, \tag{6}$$

where a is the level density parameter, which theoretically is given by $a = \frac{\pi^2}{6}(g_\pi + g_\nu)$, with g_π (g_ν) denoting the spacing of the proton (neutron) single particle states near the Fermi energy. In practice a is determined, through Eq. (6), from experimental information of the specific nucleus under consideration or from global systematics. In contemporary analytical models, it is energy-dependent. This will be discussed in more detail below. Eq. (6) also contains the *effective* excitation energy

$$U = E_x - \Delta, \tag{7}$$

where the energy shift Δ is an empirical parameter which is equal to, or for some models closely related to, the pairing energy which is included to simulate the known odd–even effects in nuclei. The underlying idea is that Δ accounts for the fact that pairs of nucleons must be separated before each component can be excited individually. In practice, Δ plays an important role as adjustable parameter to reproduce observables, and its definition can be different for the various models we discuss here. Eq. (6) indicates that throughout this paper we will use both the *true* excitation energy E_x, as basic running variable and for expressions related to discrete levels, and U, mostly for expressions related to the continuum. When implementing level density models, particular care is required for the case $E_x < \Delta$, when Eq. (6) and some other related quantities become undefined. In such cases, the state density prescription (6) is usually replaced by alternatives (e.g. expressions calculated directly from the number of discrete levels) or appropriate actions need to be taken. Such cases will be explicitly mentioned throughout this paper.

Anticipating an analogous derivation for the GSM, we note that the total Fermi gas state density of Eq. (6) is obtained from Eq. (5) by inserting the thermodynamic relations for the entropy

$$S = 2at, \tag{8}$$

and the determinant

$$D = \frac{144}{\pi}a^3t^5, \tag{9}$$

where the thermodynamic temperature t is given by

$$t = \sqrt{\frac{U}{a}}, \tag{10}$$

while we use $t = 0$ for $U < 0$, when necessary.

Under the assumption that the projections of the total angular momentum are randomly coupled, it can be derived [9,13] that the Fermi gas level density is

$$\rho_F(E_x, J, \Pi) = \frac{1}{2}\frac{2J+1}{2\sqrt{2\pi}\sigma^3}\exp\left[-\frac{(J+\frac{1}{2})^2}{2\sigma^2}\right]\frac{\sqrt{\pi}}{12}\frac{\exp[2\sqrt{aU}]}{a^{1/4}U^{5/4}}, \tag{11}$$

where the first factor $\frac{1}{2}$ represents the equiparity distribution and σ^2 is the spin cut-off parameter, which represents the width of the angular momentum distribution. It depends on excitation energy and will also be discussed in more detail below. Eq. (11) is a special case of the factorization of Eq. (3), with the Fermi gas spin distribution given by,

$$R_F(E_x, J) = \frac{2J+1}{2\sigma^2} \exp\left[-\frac{(J+\frac{1}{2})^2}{2\sigma^2}\right]. \tag{12}$$

Summing $\rho_F(E_x, J, \Pi)$ over all spins and parities yields for the total Fermi gas level density

$$\rho_F^{\mathrm{tot}}(E_x) = \frac{1}{\sqrt{2\pi}\sigma} \frac{\sqrt{\pi}}{12} \frac{\exp[2\sqrt{aU}]}{a^{1/4}U^{5/4}}, \tag{13}$$

which is, through Eqs. (5) and (6), related to the total Fermi gas state density as

$$\rho_F^{\mathrm{tot}}(E_x) = \frac{1}{\sqrt{2\pi}\sigma} \frac{e^S}{\sqrt{D}} = \frac{\omega_F^{\mathrm{tot}}(E_x)}{\sqrt{2\pi}\sigma}. \tag{14}$$

These equations show that ρ_F^{tot} and ρ_F are determined by three parameters, a, σ and Δ. The first two of these have specific energy dependencies that will now be discussed separately, while we postpone the discussion of Δ to the section on the various specific level density models.

2.2. The level density parameter a

The formulae described above may suggest a nuclide-specific constant value for the level density parameter a, and the first level density analyses spanning an entire range of nuclides [3,4,14] indeed treated a as a parameter independent of energy. Later, Ignatyuk et al. [15] recognized the correlation between the parameter a and the shell correction term of the liquid-drop component of the mass formula. They argued that a more realistic level density is obtained by assuming that the Fermi gas formulae outlined above are still valid, but that energy-dependent shell effects should be effectively included through an energy-dependent expression for a. This expression takes into account the presence of shell effects at low energy and their disappearance at high energy in a phenomenological manner. It reads

$$a = a(E_x) = \tilde{a}\left(1 + \delta W \frac{1-\exp[-\gamma U]}{U}\right). \tag{15}$$

Here, $\tilde{a}$ is the asymptotic level density value one would obtain when all shell effects are damped, i.e. $\tilde{a} = a(E_x \to \infty)$ in general, but also $\tilde{a} = a(E_x)$ for all E_x if $\delta W = 0$. The damping parameter γ determines how rapidly $a(E_x)$ approaches $\tilde{a}$. Finally, δW is the shell correction energy. The absolute magnitude of δW determines how much $a(E_x)$ differs from $\tilde{a}$ at low energies, while the sign of δW determines whether $a(E_x)$ decreases or increases to $\tilde{a}$ as a function of E_x.

The asymptotic value $\tilde{a}$ is given by the smooth form

$$\tilde{a} = \alpha A + \beta A^{2/3}, \tag{16}$$

where A is the mass number, while the following systematical formula for the damping parameter is used,

$$\gamma = \frac{\gamma_1}{A^{\frac{1}{3}}}. \tag{17}$$

In Eqs. (16)–(17), α, β and γ_1 are global parameters that need to be determined to give the best average level density description over a whole range of nuclides. We define δW as the difference

between the mass of the nucleus $M_{\rm exp}$ and its mass according to the spherical liquid-drop model mass $M_{\rm LDM}$ (all expressed in MeV),

$$\delta W = M - M_{\rm LDM}. \tag{18}$$

For the mass we take the value from the Audi–Wapstra mass compilation [16]. Following Mengoni and Nakajima [17], we take the formula by Myers and Swiatecki [18] for $M_{\rm LDM}$,

$$\begin{aligned}
&M_{\rm LDM} = M_n N + M_H Z + E_{\rm vol} + E_{\rm sur} + E_{\rm coul} + \delta,\\
&M_n = 8.07144\ \text{MeV},\\
&M_H = 7.28899\ \text{MeV},\\
&E_{\rm vol} = -c_1 A,\\
&E_{\rm sur} = c_2 A^{2/3},\\
&E_{\rm coul} = c_3 \frac{Z^2}{A^{1/3}} - c_4 \frac{Z^2}{A},\\
&c_i = a_i \left[1 - \kappa \left(\frac{N-Z}{A}\right)^2\right], \quad i = 1, 2,\\
&a_1 = 15.677\ \text{MeV},\\
&a_2 = 18.56\ \text{MeV},\\
&\kappa = 1.79,\\
&c_3 = 0.717\ \text{MeV},\\
&c_4 = 1.21129\ \text{MeV},\\
&\delta = -\frac{11}{\sqrt{A}} \quad \text{even–even},\\
&\quad = 0 \quad \text{odd},\\
&\quad = \frac{11}{\sqrt{A}} \quad \text{odd–odd}.
\end{aligned} \tag{19}$$

Eq. (15) should in principle be applied at all excitation energies, unless a different level density prescription is used at low energies, as e.g. for the CTM. Therefore, a helpful extra note for practical calculations is that for small excitation energies the limiting value of Eq. (15) is given by its first order Taylor expansion

$$\lim_{U \to 0} a(E_x) = \tilde{a}[1 + \gamma \delta W], \tag{20}$$

which is computationally convenient if $E_x \leqslant \Delta$.

The level density parameter a is thus determined by a further 4 parameters, α, β, γ_1 and δW. As we will outline in more detail in Section 5, for a global prediction of a we will derive values for α, β, and γ_1 through adjustment to all available experimental mean resonance spacings and the cumulative number of discrete levels simultaneously, with δW given by Eq. (18). On the other hand, when we wish to have the optimal level density parameters for a single nucleus, we need to adjust a parameter of Eq. (15).

Even though the values for δW depend strongly on the particular theoretical mass model and are merely adopted to reproduce the global trend of shell effects for various regions of the nuclide chart, we do not alter them when going from a global to a local model. Likewise, we feel that it is

dangerous to adjust γ_1 merely on the basis of discrete level information and the mean resonance spacing at the neutron separation energy, since its presence in the exponent of Eq. (15) may lead to level density values that deviate strongly from the global average at high energy. This leaves us to adjust $\tilde{a}$ per nucleus, and we must, and will, verify that the obtained values do not deviate too much from the smooth global trend given by Eq. (16).

From now on, wherever the level density parameter a appears in the formalism, we implicitly assume the form (15) for $a(E_x)$.

2.3. The spin cut-off parameter

The spin cut-off parameter σ^2 represents the width of the angular momentum distribution of the level density. The general expression for the continuum is based on the observation that a nucleus possesses collective rotational energy that cannot be used to excite the individual nucleons. In this picture, one can relate σ^2 to the (undeformed) moment of inertia of the nucleus I_0 and the thermodynamic temperature t. Indeed, an often used expression is $\sigma^2 = \sigma_\parallel^2 = I_0 t$, where the symbol $\sigma_\parallel^2$ designates the parallel spin cut-off parameter, obtained from the projection of the angular momentum of the single-particle states on the symmetry axis. However, it has been observed from microscopic level density studies that the quantity σ^2/t is not constant [19,20], but instead shows marked shell effects, similar to the level density parameter a. To take that effect into account we follow Refs. [19,21] and adopt the following expression for the Fermi gas spin cut-off parameter,

$$\sigma^2 = \sigma_\parallel^2 = \sigma_F^2(E_x) = I_0 \frac{a}{\tilde{a}} t, \tag{21}$$

with $\tilde{a}$ from Eq. (16) and where t is given by Eq. (10), and

$$I_0 = \frac{\frac{2}{5} m_0 R^2 A}{(\hbar c)^2}, \tag{22}$$

where $R = 1.2A^{1/3}$ is the radius, and m_0 the neutron mass in amu. This gives

$$\sigma_F^2(E_x) = 0.01389 \frac{A^{5/3}}{\tilde{a}} \sqrt{aU}. \tag{23}$$

On average, the $\sqrt{aU}/\tilde{a}$ term has the same energy- and mass-dependent behaviour as the temperature $\sqrt{U/a}$. Marked differences between these two terms occur however in the regions with large shell effects. We note that a $\sqrt{aU}$ dependence for σ^2 was already adopted by Gilbert and Cameron [3], although here the mass dependence, both through shell effects present in a and the form for $\tilde{a}$, is different.

Analogous to the level density parameter, we have to account for low excitation energies for which Eq. (23) is not defined ($E_x \leqslant \Delta$) or less appropriate. This leads us to an alternative method to determine the spin cut-off parameter, namely from the spins of the low-lying discrete levels. Suppose we want to determine this discrete spin cut-off parameter σ_d^2 in the energy range where the total level density agrees well with the discrete level sequence, i.e. from a lower discrete level N_L with energy E_L to an upper level N_U with energy E_U. In Appendix A, it is derived that the discrete spin cut-off parameter is

$$\sigma_d^2 = \frac{1}{3\sum_{i=N_L}^{N_U}(2J_i+1)} \sum_{i=N_L}^{N_U} J_i(J_i+1)(2J_i+1), \tag{24}$$

where J_i is the spin of discrete level i. Reading these spins from the discrete level file readily gives the value for σ_d^2. As we will discuss in Section 6, σ_d^2 can be determined on a nucleus-by-nucleus basis, when discrete levels are known, or from global systematics.

Finally, the functional form that we use for $\sigma^2(E_x)$ is a combination of Eqs. (23) and (24). Defining $E_d = \frac{1}{2}(E_L + E_U)$ as the energy in the middle of the N_L–N_U region, we assume σ_d^2 is constant up to this energy and can then be linearly interpolated to the expression given by Eq. (23). We choose the matching point to be the neutron separation energy S_n of the nucleus under consideration, i.e.

$$\begin{aligned}\sigma^2(E_x) &= \sigma_d^2 && \text{for } 0 \leqslant E_x \leqslant E_d,\\ &= \sigma_d^2 + \frac{E_x - E_d}{S_n - E_d}\big(\sigma_F^2(E_x) - \sigma_d^2\big) && \text{for } E_d \leqslant E_x \leqslant S_n,\\ &= \sigma_F^2(E_x) && \text{for } E_x \geqslant S_n. \end{aligned} \tag{25}$$

When no discrete levels are available, we adopt a systematical formula, see Eq. (80) for σ_d^2, while we take E_d equal to zero.

Analogous to the level density parameter a, from now on we implicitly assume the energy dependence for $\sigma^2(E_x)$ whenever σ^2 appears in the formalism.

2.4. Collective effects in the level density

The level density model described so far does not explicitly account for collective effects, whereas it is well known that generally various levels, especially at low energy, are constructed from a coherent excitation of the fermions it contains. Nevertheless, the model presented so far, often called the effective level density, can still be applied successfully in most cases since it incorporates collectivity in the level density in an effective way through a proper choice of the energy-dependent level density parameter a, even though this energy dependence is in principle only designed to handle shell effects. Comparisons with discrete levels and mean resonance spacings and application in nuclear reaction calculations suggest that such an effective approach indeed works surprisingly well.

Sometimes, in nuclear reaction calculations one would like to model the collective effects in more detail. This is the case for strongly deformed nuclei and when the disappearance of collective effects with excitation energy plays an important role, as in the case of fission reactions. While collective effects may naturally appear in microscopic level density calculations, it is also possible [5,22] to account for the collective effects in a phenomenological way by explicitly introducing collective enhancement factors for an intrinsic Fermi gas level density $\rho_{F,\mathrm{int}}(E_x, J, \Pi)$. Then the deformed Fermi gas level density $\rho_{F,\mathrm{def}}(E_x, J, \Pi)$ reads

$$\rho_{F,\mathrm{def}}(E_x, J, \Pi) = K_{\mathrm{rot}}(E_x) K_{\mathrm{vib}}(E_x) \rho_{F,\mathrm{int}}(E_x, J, \Pi), \tag{26}$$

while the total level densities $\rho_{F,\mathrm{def}}^{\mathrm{tot}}$ and $\rho_{F,\mathrm{int}}^{\mathrm{tot}}$ are related in the same way. K_{rot} and K_{vib} are called the rotational and vibrational enhancement factors, respectively. If K_{rot} and K_{vib} are explicitly accounted for, $\rho_{F,\mathrm{int}}(E_x, J, \Pi)$ should describe purely single-particle excitations, and is given again by the Fermi gas formula, but now with a level density parameter a that is obviously different (smaller) from that of the effective level density described before.

The vibrational enhancement of the level density is approximated [6] by

$$K_{\mathrm{vib}}(E_x) = \exp\big[\delta S - (\delta U/t)\big], \tag{27}$$

where δS and δU are changes in the entropy and excitation energy, respectively, resulting from the vibrational modes and t is again the nuclear temperature given by Eq. (10). These changes are described by the Bose gas relationships, i.e.,

$$\delta S = \sum_i (2\lambda_i + 1)\big[(1+n_i)\ln(1+n_i) - n_i \ln n_i\big],$$
$$\delta U = \sum_i (2\lambda_i + 1)\omega_i n_i, \tag{28}$$

where ω_i are the energies, λ_i the multipolarities, and n_i the occupation numbers for vibrational excitations at a given temperature. The disappearance of vibrational enhancement of the level density at high temperatures can be taken into account by defining the occupation numbers in terms of the equation

$$n_i = \frac{\exp(-\gamma_i/2\omega_i)}{\exp(\omega_i/t) - 1}, \tag{29}$$

where γ_i are the spreading widths of the vibrational excitations. This spreading of collective excitations in nuclei should be similar to the zero-sound damping in a Fermi liquid, and the corresponding width can be written as

$$\gamma_i = C\big(\omega_i^2 + 4\pi^2 t^2\big). \tag{30}$$

The value of $C = 0.0075A^{1/3}$ was obtained from the systematics of the neutron resonance densities of medium-weight nuclei [23]. For ω_2 and ω_3 we use a modified systematics [6] which includes shell effects to estimate the phonon energies (in MeV), namely

$$\omega_2 = 65A^{-5/6}/(1 + 0.05\delta W), \tag{31}$$

for the quadrupole vibrations and

$$\omega_3 = 100A^{-5/6}/(1 + 0.05\delta W), \tag{32}$$

for the octupole excitations.

A more important contribution to the collective enhancement of the level density originates from rotational excitations. Its effect is not only much stronger, but the form for the rotational enhancement depends on the nuclear shape as well. This makes it crucial, among others, for the description of fission cross sections.

The expression for the rotational enhancement factor $\kappa_{\rm rot}$ depends on the deformation [6,24]. For purely deformed cases, $\kappa_{\rm rot}$ is equal to the perpendicular spin cut-off parameter $\sigma_\perp^2$,

$$\kappa_{\rm rot}(E_x) = \sigma_\perp^2 = I_\perp t, \tag{33}$$

with the rigid-body moment of inertia perpendicular to the symmetry axis given by

$$I_\perp = I_0\left(1 + \frac{\beta_2}{3}\right) = 0.01389A^{5/3}\left(1 + \frac{\beta_2}{3}\right), \tag{34}$$

where β_2 is the ground-state quadrupole deformation, which we take from the RIPL-2 database. Hence,

$$\kappa_{\rm rot} = 0.01389A^{5/3}\left(1 + \frac{\beta_2}{3}\right)\sqrt{\frac{U}{a}}. \tag{35}$$

Note the difference with the parallel spin cut-off parameter of Eq. (23).

The damping of vibrational enhancement was already mentioned above. At high excitation energies, it is known that the rotational behavior also vanishes. To take this into account, it is customary to introduce a phenomenological damping function $f(E_x)$ which is equal to 1 for the purely rotational case and 0 for the non-rotational (spherical) case. The final expression for the level density is then

$$\begin{aligned}\rho(E_x, J, \Pi) &= \big[1 - f(E_x)\big]K_{\rm vib}(E_x)\rho_{F,\rm int}(E_x, J, \Pi) \\ &\quad + f(E_x)\kappa_{\rm rot}(E_x)K_{\rm vib}(E_x)\rho_{F,\rm int}(E_x, J, \Pi) \\ &= K_{\rm rot}(E_x)K_{\rm vib}(E_x)\rho_{F,\rm int}(E_x, J, \Pi),\end{aligned} \tag{36}$$

where

$$K_{\rm rot}(E_x) = \max\big(\big[\kappa_{\rm rot}(E_x) - 1\big]f(E_x) + 1, 1\big). \tag{37}$$

The function $f(E_x)$ is taken as a combination of Fermi functions,

$$f(E_x) = \frac{1}{1 + \exp\big(\frac{E_x - E_{\rm col}^{\rm g.s.}}{d_{\rm col}^{\rm g.s.}}\big)}, \tag{38}$$

which yields the desired property of $K_{\rm rot}$ going to 1 for high excitation energy. Little is known about the parameters that govern this damping, although attempts have been made (see e.g. [25]). We arbitrarily take $E_{\rm col}^{\rm g.s.} = 30$ MeV, $d_{\rm col}^{\rm g.s.} = 5$ MeV.

3. Observables

Before we discuss the various different models that are based on the formalism given above, we first describe our experimental database. This is more logical since some of the level density models (notably the CTM) depend directly on the available data. Our level density parameterizations are based only on model-independent observables, namely mean resonance spacings and discrete levels. However, as an extra validation step, our resulting level densities they will directly be tested with cross section calculations.

3.1. Mean resonance spacing

Parameters of level density models can be determined by relating the level density with D_0, the mean s-wave neutron level spacing at the neutron separation energy S_n of the compound nucleus, which can be obtained from the available experimental set of s-wave resonances. For any level density model, the following equation should hold:

$$\frac{1}{D_0} = \sum_{J=|I-\frac{1}{2}|}^{J=I+\frac{1}{2}} \rho(S_n, J, \Pi), \tag{39}$$

where I is the spin of the target nucleus. From this equation, parameters such as the level density parameter a or, if appropriate, the empirical pairing correction Δ can be extracted by an iterative search procedure.

Various compilations of D_0 values exist. Not seldom, values obtained from different experiments are discrepant, with error bars that are wide apart. A careful examination of all existing values has been performed by Ignatyuk for the RIPL-2 database. It contains data for 295 nuclides. In spite of this effort, one has to remain careful with this database, as advocated by its

compiler. Cases exist where only a small number of resonances were available, making a statistical analysis of such data doubtful. According to Ref. [6] there are 45 of such cases, which are nevertheless included in the compilation. A more extensive description of the methods used to obtain this compilation is given in Ref. [6]. We have adopted the RIPL-2 database, but removed the 6 nuclides ^{97}Zr, ^{135,136}Cs, ^{232,234}Pa and ^{253}Cf for this work, since their discrete level scheme was incomplete or of insufficient quality to be used in our global optimization scheme. Hence, we base our analysis on 289 nuclides for which we have D_0 values and also a well-known low-energy level scheme. The D_0 values are given in Tables 1–3.

3.2. Discrete levels

At low energies, a proper level density should reproduce the experimental discrete levels, and adjustable level density parameters should be adjusted such that both the discrete level range and the aforementioned mean resonance spacing are well reproduced. For the discrete level sequence, this condition can be fulfilled by requiring that the total level density ρ^{tot} describes the discrete level scheme from a lower level N_L with energy E_L to an upper level N_U with energy E_U, i.e.

$$N_U = N_L + \int_{E_L}^{E_U} dE_x\, \rho^{\mathrm{tot}}(E_x). \tag{40}$$

Then, the cumulative number of levels up to an energy E is given by

$$N_{\mathrm{cum}}(E) = N_L + \int_{E_L}^{E} dE_x\, \rho^{\mathrm{tot}}(E_x), \tag{41}$$

and this value can be compared with the experimental discrete level scheme, by simply counting the levels. The discrete levels have been taken from the RIPL-2 database. This collection has been obtained from the Evaluated Nuclear Structure Data File (ENSDF) by T. Belgya. ENSDF is a database whose application goes far beyond the mere listing of discrete levels with their basic quantum numbers. Therefore, considerable effort had to be invested to translate ENSDF information into a discrete level database. Not surprisingly, the degree of knowledge of the experimentally determined discrete level schemes varies widely throughout the nuclide chart. A more extensive description of the procedure that resulted in the RIPL-2 discrete level database is given in Ref. [6]. We found that for 1135 nuclides the discrete level range is of sufficient completeness and quality to be used in our analysis. The criterion for inclusion was a simple χ^2 estimator of the CTM model: we insisted that a minimum number of levels (15) exists and that the lowest levels are reasonably described by a constant temperature model. The nuclides which made it through this selection process are given in Table 4.

3.3. Nuclear reaction calculations

For the correct theoretical description of nuclear reactions from threshold up to hundreds of MeV, besides the obviously required implementation of the reaction mechanisms, three ingredients are crucial in general: the optical model potential (OMP), the pre-equilibrium strength and the level density. For capture reactions, gamma-ray strength functions and for fission, barrier parameters can be added to this. For nuclear reaction calculations on non-fissile nuclides, improved

Table 1
Experimental D_0 values from the RIPL-2 database and N_L–N_U pairs for discrete level fitting

Nuc	D_0 (eV)	N_L–N_U	Nuc	D_0 (eV)	N_L–N_U
^{24}Na	95000. (30000.)	8–16	^{71}Zn	7200. (800.)	8–15
^{25}Mg	470000. (140000.)	7–16	^{70}Ga	350. (60.)	4–29
^{26}Mg	43000. (17000.)	7–25	^{72}Ga	380. (60.)	8–16
^{27}Mg	260000. (50000.)	8–29	^{71}Ge	890. (210.)	2–17
^{28}Al	45000. (15000.)	6–20	^{73}Ge	1500. (300.)	6–20
^{29}Si	200000. (60000.)	5–24	^{74}Ge	62. (15.)	6–19
^{30}Si	350000. (160000.)	4–19	^{75}Ge	3000. (1000.)	6–24
^{32}P	75000. (20000.)	8–15	^{77}Ge	4500. (1500.)	8–15
^{33}S	150000. (35000.)	2–25	^{76}As	77. (8.)	6–27
^{34}S	27000. (10000.)	8–15	^{75}Se	340. (80.)	8–25
^{35}S	200000. (70000.)	6–17	^{77}Se	650. (100.)	5–16
^{36}Cl	23000. (6000.)	8–17	^{78}Se	110. (30.)	4–16
^{38}Cl	15000. (4000.)	2–15	^{79}Se	2000. (500.)	4–15
^{41}Ar	70200. (17000.)	7–15	^{81}Se	2000. (800.)	7–19
^{40}K	15000. (5000.)	8–19	^{83}Se	5000. (2500.)	8–15
^{42}K	15000. (5000.)	8–16	^{80}Br	47. (5.)	3–15
^{41}Ca	32600. (4300.)	6–16	^{82}Br	105. (15.)	6–29
^{43}Ca	20000. (5000.)	3–29	^{79}Kr	250. (80.)	3–28
^{44}Ca	1800. (300.)	8–27	^{81}Kr	280. (60.)	2–15
^{45}Ca	24100. (3200.)	8–23	^{84}Kr	200. (100.)	4–26
^{46}Sc	1300. (100.)	6–15	^{85}Kr	1000. (100.)	7–19
^{47}Ti	25000. (4400.)	3–15	^{86}Rb	170. (30.)	5–16
^{48}Ti	1750. (250.)	2–15	^{88}Rb	1800. (300.)	8–15
^{49}Ti	18300. (2900.)	8–16	^{85}Sr	320. (120.)	7–22
^{50}Ti	4000. (800.)	5–15	^{87}Sr	2600. (800.)	7–18
^{51}Ti	125000. (70000.)	3–16	^{88}Sr	290. (80.)	4–26
^{51}V	2300. (600.)	2–15	^{89}Sr	23700. (2900.)	7–15
^{52}V	4100. (600.)	4–15	^{90}Y	3700. (400.)	3–16
^{51}Cr	13300. (1300.)	6–15	^{91}Zr	6000. (1400.)	3–17
^{53}Cr	43400. (4370.)	5–25	^{92}Zr	550. (100.)	3–16
^{54}Cr	7800. (800.)	4–15	^{93}Zr	3500. (800.)	8–18
^{55}Cr	62000. (8000.)	8–24	^{94}Zr	160. (15.)	4–16
^{56}Mn	2300. (400.)	6–16	^{95}Zr	3200. (800.)	3–18
^{55}Fe	18000. (2400.)	3–15	^{94}Nb	80. (10.)	8–19
^{57}Fe	25400. (2200.)	8–15	^{93}Mo	2700. (500.)	8–16
^{58}Fe	6500. (1000.)	2–22	^{95}Mo	1320. (180.)	8–20
^{59}Fe	25400. (4900.)	6–16	^{96}Mo	105. (10.)	6–15
^{60}Co	1250. (150.)	7–15	^{97}Mo	1050. (200.)	6–20
^{59}Ni	13400. (900.)	2–23	^{98}Mo	75. (20.)	4–18
^{60}Ni	2000. (700.)	7–32	^{99}Mo	1000. (200.)	3–15
^{61}Ni	13800. (900.)	8–15	^{101}Mo	800. (150.)	2–22
^{62}Ni	2100. (150.)	6–18	^{100}Tc	12. (1.30)	8–17
^{63}Ni	16000. (3000.)	8–18	^{100}Ru	25. (4.)	6–28
^{65}Ni	19600. (3000.)	7–17	^{102}Ru	18. (3.)	7–19
^{64}Cu	950. (90.)	4–29	^{103}Ru	550. (150.)	7–16
^{66}Cu	1300. (110.)	5–16	^{105}Ru	300. (75.)	8–21
^{65}Zn	3590. (160.)	7–18	^{104}Rh	32. (4.)	8–15
^{67}Zn	4620. (550.)	2–19	^{105}Pd	240. (30.)	4–17
^{68}Zn	400. (60.)	8–15	^{106}Pd	10.30 (0.50)	6–28
^{69}Zn	5560. (430.)	2–25	^{107}Pd	270. (90.)	8–19

Table 2
Experimental D_0 values from the RIPL-2 database and N_L–N_U pairs for discrete level fitting

Nuc	D_0 (eV)	N_L–N_U	Nuc	D_0 (eV)	N_L–N_U
^{108}Pd	11. (0.90)	8–22	^{140}La	220. (40.)	8–25
^{109}Pd	182. (33.)	8–16	^{137}Ce	50. (20.)	8–17
^{111}Pd	150. (50.)	7–15	^{141}Ce	3100. (500.)	6–19
^{108}Ag	22. (4.)	3–28	^{142}Ce	65. (20.)	2–21
^{110}Ag	15.10 (1.40)	6–18	^{143}Ce	1100. (500.)	2–17
^{107}Cd	135. (35.)	6–16	^{142}Pr	110. (20.)	8–24
^{109}Cd	120. (30.)	5–17	^{143}Nd	860. (80.)	8–23
^{111}Cd	155. (20.)	4–27	^{144}Nd	35. (5.)	8–29
^{112}Cd	20. (4.)	6–27	^{145}Nd	450. (50.)	8–21
^{113}Cd	190. (25.)	6–15	^{146}Nd	17. (3.)	6–15
^{114}Cd	24.80 (2.60)	6–23	^{147}Nd	290. (50.)	4–20
^{115}Cd	235. (35.)	8–16	^{148}Nd	3.50 (1.70)	5–17
^{117}Cd	390. (90.)	6–15	^{149}Nd	155. (20.)	2–15
^{114}In	13. (3.)	6–15	^{151}Nd	165. (15.)	8–28
^{116}In	9.50 (0.50)	8–15	^{148}Pm	5.20 (1.20)	8–18
^{113}Sn	157. (52.)	4–17	^{145}Sm	670. (60.)	4–17
^{115}Sn	286. (106.)	4–21	^{148}Sm	5.10 (0.50)	8–29
^{117}Sn	380. (130.)	7–15	^{149}Sm	100. (20.)	7–19
^{118}Sn	55. (5.)	2–15	^{150}Sm	2.10 (0.30)	3–21
^{119}Sn	480. (90.)	8–15	^{151}Sm	46. (8.)	5–16
^{120}Sn	90. (20.)	6–21	^{152}Sm	1.04 (0.15)	5–17
^{121}Sn	1640. (200.)	3–19	^{153}Sm	48. (5.)	4–17
^{125}Sn	5000. (1200.)	8–16	^{155}Sm	114. (15.)	7–15
^{122}Sb	13. (2.)	2–17	^{152}Eu	0.73 (0.07)	2–17
^{124}Sb	24. (3.)	8–15	^{153}Eu	0.56 (0.10)	6–15
^{123}Te	132. (15.)	7–16	^{154}Eu	1.10 (0.20)	8–19
^{124}Te	17. (3.)	7–15	^{155}Eu	0.92 (0.12)	8–16
^{125}Te	190. (20.)	2–15	^{156}Eu	4.30 (1.50)	2–15
^{126}Te	38. (5.)	3–16	^{153}Gd	14. (3.)	6–19
^{127}Te	550. (100.)	2–16	^{155}Gd	14.50 (1.50)	8–16
^{129}Te	740. (150.)	3–16	^{156}Gd	1.70 (0.20)	4–16
^{131}Te	1500. (500.)	7–16	^{157}Gd	30. (6.)	5–15
^{128}I	15. (3.)	8–18	^{158}Gd	4.90 (0.50)	2–17
^{130}I	30. (3.)	8–22	^{159}Gd	82. (6.)	8–19
^{129}Xe	250. (100.)	5–21	^{161}Gd	200. (20.)	8–23
^{130}Xe	38. (5.)	8–21	^{160}Tb	4.20 (0.30)	4–22
^{131}Xe	230. (60.)	5–17	^{157}Dy	4.80 (1.60)	8–16
^{132}Xe	49. (15.)	5–17	^{159}Dy	22. (11.)	6–27
^{133}Xe	750. (236.)	8–16	^{161}Dy	27. (5.)	8–20
^{135}Xe	1600. (600.)	8–17	^{162}Dy	2.40 (0.20)	3–18
^{137}Xe	13000. (6000.)	6–15	^{163}Dy	62. (5.)	3–16
^{134}Cs	21. (2.)	8–15	^{164}Dy	6.80 (0.60)	3–15
^{131}Ba	58. (10.)	6–18	^{165}Dy	150. (10.)	6–19
^{133}Ba	110. (35.)	4–17	^{166}Ho	4.20 (0.50)	2–16
^{135}Ba	371. (36.)	2–15	^{163}Er	8. (2.)	8–18
^{136}Ba	40. (6.)	4–19	^{165}Er	21. (4.)	3–19
^{137}Ba	1210. (119.)	7–15	^{167}Er	38. (3.)	6–28
^{138}Ba	260. (50.)	8–21	^{168}Er	4.20 (0.30)	3–15
^{139}Ba	18700. (2900.)	5–15	^{169}Er	100. (10.)	8–16
^{139}La	32. (6.)	4–21	^{171}Er	147. (20.)	8–19

Table 3
Experimental D_0 values from the RIPL-2 database and N_L–N_U pairs for discrete level fitting

Nuc	D_0 (eV)	N_L–N_U	Nuc	D_0 (eV)	N_L–N_U
^{170}Tm	8.50 (0.70)	2–21	^{201}Hg	650. (150.)	3–15
^{171}Tm	3.90 (1.)	7–15	^{202}Hg	90. (30.)	8–24
^{169}Yb	8. (3.)	8–25	^{204}Tl	280. (50.)	8–26
^{170}Yb	1.60 (0.40)	6–19	^{206}Tl	5500. (1500.)	2–15
^{171}Yb	33. (6.)	8–15	^{205}Pb	2000. (500.)	8–17
^{172}Yb	5.80 (0.50)	5–16	^{207}Pb	32000. (6000.)	3–15
^{173}Yb	70. (3.)	2–16	^{208}Pb	38000. (8000.)	2–15
^{174}Yb	7.80 (0.90)	8–15	^{209}Pb	400000. (80000.)	2–33
^{175}Yb	162. (18.)	3–15	^{210}Bi	4000. (700.)	8–21
^{177}Yb	185. (20.)	3–16	^{227}Ra	31. (6.)	8–17
^{176}Lu	3. (0.40)	7–20	^{229}Th	5. (3.)	8–22
^{177}Lu	2.75 (0.85)	7–20	^{230}Th	0.62 (0.12)	3–15
^{175}Hf	18. (5.)	6–15	^{231}Th	9.60 (1.50)	3–16
^{177}Hf	30. (7.)	3–23	^{233}Th	16.60 (0.60)	7–16
^{178}Hf	2.40 (0.30)	7–18	^{233}Pa	0.75 (0.15)	7–20
^{179}Hf	57. (6.)	3–21	^{233}U	4.60 (0.70)	5–15
^{180}Hf	4.60 (0.30)	6–19	^{234}U	0.55 (0.05)	3–15
^{181}Hf	94. (15.)	8–15	^{235}U	12. (0.80)	4–16
^{181}Ta	1.20 (0.20)	8–20	^{236}U	0.43 (0.02)	4–17
^{182}Ta	4.20 (0.30)	5–17	^{237}U	15. (1.)	7–21
^{183}Ta	3.50 (0.70)	2–15	^{238}U	3.50 (0.80)	3–18
^{181}W	20. (7.)	2–18	^{239}U	20.80 (0.30)	8–34
^{183}W	60. (6.)	7–16	^{237}Np	0.60 (0.06)	8–18
^{184}W	12. (1.)	8–24	^{238}Np	0.57 (0.03)	2–15
^{185}W	70. (7.)	8–29	^{239}Np	0.41 (0.10)	3–18
^{187}W	85. (8.)	8–20	^{239}Pu	9. (1.)	4–15
^{186}Re	3.10 (0.30)	2–26	^{240}Pu	2.20 (0.05)	6–23
^{188}Re	4.10 (0.30)	2–20	^{241}Pu	12.40 (0.70)	6–17
^{187}Os	29. (3.)	7–16	^{242}Pu	0.73 (0.08)	8–15
^{188}Os	4. (0.60)	8–29	^{243}Pu	13.50 (1.50)	2–18
^{189}Os	47. (6.)	8–25	^{245}Pu	19. (3.)	7–15
^{190}Os	3.40 (0.40)	8–25	^{242}Am	0.58 (0.04)	8–16
^{191}Os	70. (10.)	2–15	^{243}Am	0.40 (0.08)	7–18
^{193}Os	115. (10.)	8–15	^{244}Am	0.73 (0.06)	7–15
^{192}Ir	2.50 (0.50)	5–25	^{243}Cm	14. (3.)	8–24
^{193}Ir	0.70 (0.20)	5–17	^{244}Cm	0.75 (0.15)	3–12
^{194}Ir	7. (2.)	8–27	^{245}Cm	11.80 (1.20)	3–27
^{193}Pt	22. (8.)	8–19	^{246}Cm	1.30 (0.20)	6–16
^{195}Pt	200. (80.)	8–20	^{247}Cm	30. (5.)	5–18
^{196}Pt	18. (3.)	3–16	^{248}Cm	1.40 (0.30)	4–15
^{197}Pt	350. (100.)	7–15	^{249}Cm	28. (5.)	8–21
^{199}Pt	340. (90.)	5–19	^{250}Bk	1.10 (0.10)	7–18
^{198}Au	16.50 (0.90)	3–17	^{250}Cf	0.70 (0.10)	4–16
^{199}Hg	105. (35.)	2–16	^{251}Cf	12. (2.)	7–19
^{200}Hg	80. (30.)	5–16			

global OMPs [7] and pre-equilibrium models [8] have already helped to reduce the uncertainty of our cross section predictions considerably. With the OMP and pre-equilibrium components

Table 4
The 1135 isotopes for which sufficient discrete level information is available

Nuc	Range	Exceptions	Nuc	Range	Exceptions	Nuc	Range	Exceptions
F	16–21		Zr	86–102	97	Lu	169–179	
Ne	18–23		Nb	87–103	98	Hf	166–182	
Na	20–26		Mo	90–105		Ta	175–185	
Mg	22–28		Tc	92–105		W	173–188	
Al	24–29		Ru	94–111		Re	177–191	182
Si	26–32		Rh	96–111	98	Os	174–194	
P	28–33		Pd	97–111		Ir	181–197	186
S	31–37		Ag	100–113		Pt	179–199	
Cl	31–38		Cd	103–123		Au	184–201	188
Ar	34–42		In	104–125	118 122	Hg	185–204	187
K	37–44		Sn	110–128		Tl	195–206	196 200 202
Ca	38–48		Sb	113–131	115	Pb	194–210	200
Sc	41–49		Te	116–136		Bi	203–211	
Ti	42–52		I	120–133		Po	203–215	
V	46–54		Xe	117–139		At	207–217	
Cr	47–56		Cs	122–143	135 136	Rn	214–214	
Mn	51–58		Ba	121–147		Fr	216–225	217
Fe	52–60		La	130–148		Ra	218–231	220
Co	54–63		Ce	127–149	132	Ac	219–231	223
Ni	56–68		Pr	132–147		Th	227–234	
Cu	58–66		Nd	132–152		Pa	231–237	232 234
Zn	60–71		Pm	139–155	152	U	232–240	
Ga	64–73		Sm	138–157	140	Np	235–239	
Ge	66–81		Eu	139–159	148	Pu	237–246	
As	68–81		Gd	141–162	145 147	Am	240–245	
Se	69–84		Tb	147–161	148 150 152	Cm	243–249	
Br	72–83		Dy	153–166		Bk	247–251	
Kr	75–90		Ho	155–169	160 162	Cf	248–251	
Rb	77–91		Er	155–172		Es	251–251	
Sr	79–98	91	Tm	157–175	160 162 172	Fm	256–256	
Y	80–101	92 94 95	Yb	162–178				

under relatively good control, the experimental cross sections and spectra can now be used as a probe for the quality of level densities. With our TALYS nuclear reaction code [26], we are able to perform such a large global validation. We have retrieved data from the EXFOR database of experimental nuclear reaction data [27], for all nuclides studied in this paper. This retrieval was done automatically, resulting in a large, though definitely not complete, set of data for all partial reaction channels. We have compared these data with *global* TALYS nuclear reaction calculations, i.e. without parameter adjustment, in an automatic way, to see to what extent our level density models give reasonable results and to determine the dispersion when using different level density models. The results will be given in Section 6.

4. The level density models

4.1. The Back-shifted Fermi gas model

In the Back-shifted Fermi gas model (BFM) [4], the pairing energy is treated as an adjustable parameter and the Fermi gas expression is used to describe the level density at all energies. Hence,

for the total level density we use Eq. (14) and for the level density Eq. (11). These expressions, as well as the energy-dependent expressions for a and σ^2, contain the effective excitation energy $U = E_x - \Delta^{\mathrm{BFM}}$, where the energy shift is given by

$$\Delta^{\mathrm{BFM}} = \chi \frac{12}{\sqrt{A}} + \delta, \tag{42}$$

with

$$\begin{aligned} \chi &= -1, \quad \text{for odd–odd,} \\ &= 0, \quad \text{for odd,} \\ &= 1, \quad \text{for even–even,} \end{aligned} \tag{43}$$

and δ an adjustable parameter to fit experimental data per nucleus.

A problem of the original BFM, which may have hampered its use as the default level density option in nuclear model analyses, is the divergence of Eq. (14) when U goes to zero. A solution to this problem has been provided by Grossjean and Feldmeier [28], and was transformed into a practical form by Demetriou and Goriely [1], which is adopted in this paper. The expression for the total BFM level density is

$$\rho^{\mathrm{tot}}_{\mathrm{BFM}}(E_x) = \left[\frac{1}{\rho^{\mathrm{tot}}_F(E_x)} + \frac{1}{\rho_0(t)} \right]^{-1}, \tag{44}$$

where ρ_0 is given by

$$\rho_0(t) = \frac{\exp(1)}{24\sigma} \frac{(a_n + a_p)^2}{\sqrt{a_n a_p}} \exp\bigl(4 a_n a_p t^2\bigr), \tag{45}$$

where $a_n = a_p = a/2$ and t is given by Eq. (10). Fig. 1 displays a typical case of the behaviour at low energies of the uncorrected formula (14) and the corrected formula (44). It is clearly seen that the difference between the two formulae disappears typically after a few hundreds of keV.

With the usual spin distribution, the level density $\rho_{\mathrm{BFM}}(E_x, J, \Pi)$ can be obtained from Eqs. (3) and (12). Optionally, the BFM can also be extended with explicit collective enhancement, i.e.

$$\rho^{\mathrm{tot}}_{\mathrm{BFM}}(E_x) = K_{\mathrm{rot}}(E_x) K_{\mathrm{vib}}(E_x) \left[\frac{1}{\rho^{\mathrm{tot}}_{F,\mathrm{int}}(E_x)} + \frac{1}{\rho_0(t)} \right]^{-1}, \tag{46}$$

and similarly for the level density ρ_{BFM}. In sum, there are two adjustable parameters for the BFM, a and δ.

4.2. Constant temperature model

In the Constant Temperature Model (CTM), as introduced by Gilbert and Cameron [3], the excitation energy range is divided into a low energy part from 0 MeV up to a matching energy E_M, where the so-called constant temperature law applies and a high energy part above E_M, where the Fermi gas model applies. Hence, for the total level density we have

$$\begin{aligned} \rho^{\mathrm{tot}}_{\mathrm{CTM}}(E_x) &= \rho^{\mathrm{tot}}_T(E_x), \quad \text{if } E_x \leqslant E_M, \\ &= \rho^{\mathrm{tot}}_F(E_x), \quad \text{if } E_x > E_M, \end{aligned} \tag{47}$$

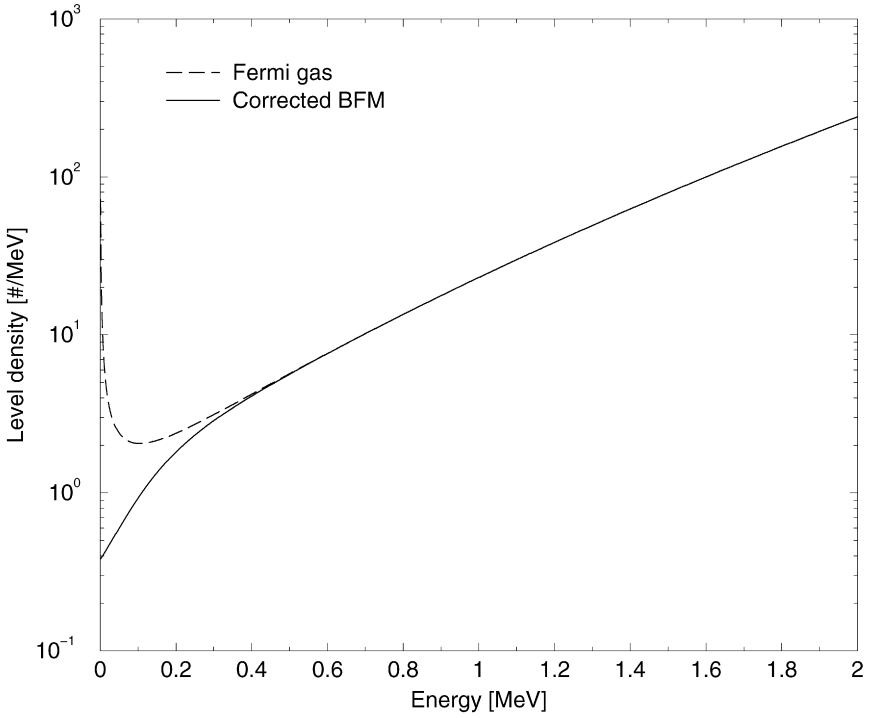

Fig. 1. Grossjean–Feldmeier correction of the Fermi gas formula at low energies for a medium mass nuclide with $a = 15\ \mathrm{MeV}^{-1}$.

and for the level density

$$\begin{aligned}\rho_{\mathrm{CTM}}(E_x, J, \Pi) &= \frac{1}{2} R_F(E_x, J)\rho_T^{\mathrm{tot}}(E_x), \quad \text{if } E_x \leqslant E_M, \\ &= \rho_F(E_x, J, \Pi), \quad \text{if } E_x > E_M. \end{aligned} \tag{48}$$

Note that the spin distribution of Eq. (12) is also used in the constant temperature region, including the low-energy behaviour for the spin cut-off parameter as expressed by Eq. (25).

For the Fermi gas expression, we use the effective excitation energy $U = E_x - \Delta^{\mathrm{CTM}}$, where the energy shift is now given by

$$\Delta^{\mathrm{CTM}} = \chi \frac{12}{\sqrt{A}}, \tag{49}$$

with

$$\begin{aligned}\chi &= 0, \quad \text{for odd–odd,} \\ &= 1, \quad \text{for odd,} \\ &= 2, \quad \text{for even–even.} \end{aligned} \tag{50}$$

Note that, unlike the BFM, no adjustable pairing shift parameter is used, and that the definition of χ is different from that of Eq. (43).

For low excitation energy, the CTM is based on the experimental evidence that the cumulated histogram $N(E_x)$ of the first discrete levels can be well reproduced by an exponential law of the type

$$N(E_x) = \exp\left(\frac{E_x - E_0}{T}\right), \tag{51}$$

which is called the constant temperature law. The nuclear temperature T and E_0 are parameters that serve to adjust the formula to the experimental discrete levels. Accordingly, the constant temperature part of the total level density reads

$$\rho_T^{\text{tot}}(E_x) = \frac{dN(E_x)}{dE_x} = \frac{1}{T}\exp\left(\frac{E_x - E_0}{T}\right). \tag{52}$$

At higher energies, the Fermi gas model is more suitable and the total level density is given by Eq. (13). The expressions for ρ_T^{tot} and ρ_F^{tot} have to be matched at a matching energy E_M where their values, and their derivatives, are identical. This directly leads to the conditions

$$E_0 = E_M - T\ln\left[T\rho_F^{\text{tot}}(E_M)\right], \tag{53}$$

and

$$\frac{1}{T} = \frac{d\ln\rho_F^{\text{tot}}}{dE_x}(E_M). \tag{54}$$

In principle, for all Fermi gas type expressions, including the energy dependent expressions for a, σ^2, K_{rot}, etc., Eq. (54) could be elaborated analytically, but in practice we use a numerical approach to allow any level density model to be used in the matching problem. Hence, we determine the inverse temperature of Eq. (54) numerically by calculating ρ_F^{tot} on a sufficiently dense energy grid.

The matching problem gives us two conditions, given by Eqs. (53) and (54), with three unknowns: T, E_0 and E_M. Hence, we need another constraint. This is obtained by demanding that in the discrete level region the constant temperature law reproduces the experimental discrete levels, i.e. ρ_T^{tot} needs to obey Eq. (40), or, after inserting Eq. (52) in that equation,

$$N_U = N_L + \left(\exp\left[\frac{E_U}{T}\right] - \exp\left[\frac{E_L}{T}\right]\right)\exp\left[\frac{-E_0}{T}\right]. \tag{55}$$

The combination of Eqs. (53), (54) and (55) determines T, E_0 and E_M. Inserting Eq. (53) in Eq. (55) yields:

$$T\rho_F^{\text{tot}}(E_M)\exp\left[\frac{-E_M}{T}\right]\left(\exp\left[\frac{E_U}{T}\right] - \exp\left[\frac{E_L}{T}\right]\right) + N_L - N_U = 0, \tag{56}$$

from which E_M can be solved by an iterative procedure with the simultaneous use of the tabulated values given by Eq. (54). The levels N_L and N_U should be chosen such that $\rho_T(E_x)$ gives the best description of the observed discrete states. This procedure is described in Section 5.

The CTM formalism can also be extended with explicit collective enhancement, see Eq. (26). Note however that the collective enhancement is not applied to the constant temperature region, since collectivity is assumed to be already implicitly included in the discrete levels. The solution of the matching problem proceeds completely analogous to that described above, although the resulting parameters E_M, E_0 and T will of course be different.

4.3. The generalized superfluid model

The Generalized Superfluid Model (GSM) takes superconductive pairing correlations into account according to the Bardeen–Cooper–Schrieffer theory. The phenomenological version of the model [5,29] is characterized by a phase transition from a superfluid behaviour at low energy, where pairing correlations strongly influence the level density, to a high energy region which is described by the FGM. The GSM thus resembles the CTM to the extent that it distinguishes between a low energy and a high energy region, although for the GSM this distinction follows naturally from the theory and does not depend on specific discrete levels that determine a matching energy, as in the CTM. Instead, the model automatically provides a constant temperature-like behaviour at low energies. For the level density expressions, it is first useful to recall the general formula (14) for the total level density, which for the GSM has two forms: one below and one above the so-called critical energy U_c.

For energies below U_c, the level density is described in terms of thermodynamical functions defined *at* U_c, which is given by

$$U_c = a_c T_c^2 + E_{\mathrm{cond}}. \tag{57}$$

Here, the critical temperature T_c is

$$T_c = 0.567 \Delta_0, \tag{58}$$

where the pairing correlation function is given by

$$\Delta_0 = \frac{12}{\sqrt{A}}. \tag{59}$$

This correlation function determines the condensation energy E_{cond}, which characterizes the decrease of the superfluid phase relative to the Fermi gas phase. It is given by the expression

$$E_{\mathrm{cond}} = \frac{3}{2\pi^2} a_c \Delta_0^2, \tag{60}$$

where the critical level density parameter a_c is given by the iterative equation

$$a_c = \tilde{a}\left[1 + \delta W \frac{1 - \exp(-\gamma a_c T_c^2)}{a_c T_c^2}\right], \tag{61}$$

which is easily obtained once $\tilde{a}$, δW and γ are given. Eq. (61) indicates that shell effects are again appropriately taken into account.

For the determination of the level density we also invoke the expression for the critical entropy S_c,

$$S_c = 2 a_c T_c, \tag{62}$$

the critical determinant D_c,

$$D_c = \frac{144}{\pi} a_c^3 T_c^5, \tag{63}$$

and the critical spin cut-off parameter σ_c^2,

$$\sigma_c^2 = 0.01389 A^{5/3} \frac{a_c}{\tilde{a}} T_c. \tag{64}$$

Now that everything is specified at U_c, we can use the superfluid Equation Of State (EOS) to define the level density below U_c. For this, we define an effective excitation energy

$$U' = E_x + \chi \Delta_0 + \delta, \tag{65}$$

where

$$\begin{aligned} \chi &= 2, \quad \text{for odd–odd,} \\ &= 1, \quad \text{for odd,} \\ &= 0, \quad \text{for even–even,} \end{aligned} \tag{66}$$

and δ is an adjustable shift parameter to obtain the best description of experimental data per nucleus. Note that the convention for χ is again different from that of the BFM or the CTM. Defining

$$\varphi^2 = 1 - \frac{U'}{U_c}, \tag{67}$$

then for $U' \leqslant U_c$ the quantities φ and T obey the superfluid EOS [5],

$$\varphi = \tanh\left(\frac{T_c}{T}\varphi\right), \tag{68}$$

which is equivalent to

$$T = 2T_c\varphi\left[\ln\frac{1+\varphi}{1-\varphi}\right]^{-1}. \tag{69}$$

The other functions for $U' \leqslant U_c$ are the entropy S,

$$S = S_c\frac{T_c}{T}\left(1-\varphi^2\right) = S_c\frac{T_c}{T}\frac{U'}{U_c}, \tag{70}$$

the determinant D,

$$D = D_c\left(1-\varphi^2\right)\left(1+\varphi^2\right)^2 = D_c\frac{U'}{U_c}\left(2-\frac{U'}{U_c}\right)^2, \tag{71}$$

and the spin cut-off parameter

$$\sigma^2 = \sigma_c^2\left(1-\varphi^2\right) = \sigma_c^2\frac{U'}{U_c}. \tag{72}$$

However, since we wish to make optimal use of discrete level spin information, we replace the formula for the spin cut-off parameter by $\sigma^2 = \sigma^2(E_x)$, where $\sigma^2(E_x)$ is given by Eq. (25), with the only difference that for the GSM we replace S_n by U_c. Note that the linear decrease of σ^2 below U_c of Eq. (72) is retained by Eq. (25).

In sum, the level density can now be specified for the entire energy range. For $U' \leqslant U_c$, the total level density is given by Eq. (14) with all ingredients given by Eqs. (70)–(72) and similarly for the level density ρ_{GSM}.

For $U' > U_c$ the FGM applies, though with an energy shift that is different from the pairing correction of the CTM and BFM, i.e. the effective excitation energy is defined by $U = E_x - \Delta^{\mathrm{GSM}}$, with

$$\Delta^{\mathrm{GSM}} = E_{\mathrm{cond}} - \chi\Delta_0 - \delta. \tag{73}$$

At the matching energy, i.e., for $E'_x = U_c - \chi\,\Delta_0 - \delta$, it is easy to verify that the two prescriptions match so that the total level density is perfectly continuous. In sum, there are two adjustable parameters for the GSM, a and δ.

Finally, the GSM can be extended with collective enhancement, i.e.

$$\rho^{\rm tot}_{\rm GSM}(E_x) = K_{\rm rot}(E_x) K_{\rm vib}(E_x) \rho^{\rm tot}_{\rm GSM,int}(E_x) \tag{74}$$

and similarly for the level density $\rho_{\rm GSM}(E_x, J, \Pi)$. We note that originally the term "generalized" in the GSM was in fact added to denote the inclusion of explicit collective enhancement.

4.4. Skyrme–Hartree–Fock–Bogolyubov combinatorial model

Besides the phenomenological models, we also include a microscopic approach, HFM (Hartree–Fock Model), in our analysis. New energy-, spin- and parity-dependent nuclear level densities based on the microscopic combinatorial model have been proposed [2]. The combinatorial model includes a detailed microscopic calculation of the intrinsic state density and collective enhancement. The only phenomenological aspect of the model consists of a simple damping function for the rotational effects, see also Eq. (36). For the rest, the calculations make coherent use of nuclear structure properties determined within the deformed Skyrme–Hartree–Fock–Bogolyubov framework. Level densities for more than 8500 nuclei are available in tabular format [30], for excitation energies up to 200 MeV and for spin values up to $J = 49$. Since these microscopical level densities, which we will call $\rho_{\rm HFM}$, have not been adjusted to experimental data, we add adjustment flexibility through a scaling function, i.e.

$$\rho(E_x, J, \pi) = \exp\bigl(c\sqrt{E_x - p}\bigr)\rho_{\rm HFM}(E_x - p, J, \pi) \tag{75}$$

where by default $c = 0$ and $p = 0$ (i.e. unaltered values from the tables). The "pairing shift" p simply means obtaining the level density from the table at a different energy. The constant c plays a role similar to that of the level density parameter a of phenomenological models. Adjusting p and c together gives adjustment flexibility at both low and higher energies, so that e.g. both discrete levels and experimental mean resonance spacings can be reproduced as good as possible.

5. Optimization procedure

We have given an outline of three different phenomenological level density prescriptions, BFM, CTM and GSM, and each of them can be used either as an effective model, with collective effects hidden in the Fermi gas level density parameter a, or as an intrinsic model with explicit collective enhancement through the functions $K_{\rm rot}$ and $K_{\rm vib}$. We thus have a total of six phenomenological level density models. Moreover, for each of these models one can construct a global parameterization, describing the level density as good as possible for the entire periodic table with a few systematic A-dependent formulae for the parameters, and a local parametrization, where the parameters for each nucleus are adjusted to optimal values that reproduce the experimental data for that nucleus.

We note that the phenomenological nature of the analytical models entails that there is no such thing as a universal level density parameter a, since a is completely model dependent. Hence, in practice adoption of the level density parameter a, from e.g. published values, in level density models is useless without specifying the pairing energy correction, the spin cut-off parameter,

and when the full energy dependence is requested, the shell correction and damping parameter. Moreover, the level density parameter a depends on the choice whether to include explicit collective enhancement or not.

The results of this paper are collected in various tables and figures. The final parameterizations are obtained by iterating between the global and the local optimization, for each of the level density models. To describe the optimization procedure in some detail, we first take the BFM as example. Next, we describe the particular optimization aspects of the CTM, GSM, and HFM as far as they differ from the BFM.

The first step is to determine an initial set of global level density parameters α, β, γ_1 and δ (which we call $\delta_{\rm global}$ for the global case), as defined in Eqs. (16), (17), and (42). For this, we select the $N = 289$ nuclides for which both an experimental D_0 value and a discrete level scheme exists and calculate all theoretical values with the global parameters. For the optimization, we adopt the following goodness-of-fit estimator for the mean resonance spacings,

$$\chi^2_{D,i} = \left(\frac{D^{\rm theo}_{0,i} - D^{\rm exp}_{0,i}}{\Delta D^{\rm exp}_{0,i}} \right)^2, \tag{76}$$

which corresponds to the normal χ^2 quantity to compare theoretical and experimental values, $D^{\rm theo}_{0,i}$ and $D^{\rm exp}_{0,i}$ respectively. The index i has been added to denote the nucleus and the theoretical mean level spacing $D^{\rm theo}_{0,i}$ is directly obtained from Eq. (39). For discrete levels, such an estimator is more ambiguous, since there is no true measure for the uncertainty in the cumulative level scheme. We follow Ignatyuk et al. [29] by giving more weight to the correct description of the lower-lying levels, while including higher-lying levels if their description by a level density model is still reasonably good. The goodness-of-fit estimator that provides this is

$$\chi^2_{{\rm lev},i} = \sum_{k=N^i_L}^{N^i_U} \frac{(N^i_{\rm cum}(E_k) - k)^2}{k}, \tag{77}$$

where k runs over the discrete levels and the theoretical number of cumulative levels $N^i_{\rm cum}$ is calculated from Eq. (41). We also performed tests with the denominator k of Eq. (77) replaced by $(N^i_U - N^i_L)$ to put equal weight on all levels, and insisting less on a very good fit of the low-lying levels. The results are not very different. The total goodness-of-fit estimator for the global level density model is thus

$$\chi^2_{\rm global} = \sum_{i=1}^{N} \chi^2_{D,i} + \chi^2_{{\rm lev},i}. \tag{78}$$

In the first iteration for the global parameters, we have no a priori knowledge of the discrete level values N_L and N_U. For all nuclides our *initial* values are $N_L = 5$ and $N_U = 20$, which we think is a reasonable starting point for nuclides for which D_0 values exist. In the next iteration of optimizing the global parameters however, these values will be replaced by the N_L, N_U points obtained from the optimization of the local parameters. To determine the parameters α, β, γ_1 and $\delta_{\rm global}$ for which $\chi^2_{\rm global}$ has the minimal value, we use the method of simulated annealing, which we already have successfully used in optical model parameter searches [7]. In short, simulated annealing is a global optimization method that distinguishes between different local optima and uses Monte Carlo criteria for convergence to the optimum. Our simulated annealing program drives the TALYS nuclear model code, which automatically produces level density tables on the

basis of input level density parameters. In the process, we thus make entirely sure that the results of this work are indeed used in future reaction calculations by TALYS.

Next, we search for the best level density parameters for each nucleus separately. The initial set of global parameters α, β, γ_1 and δ_{global} that we obtained above provides the starting values for a and δ. The optimization of the local level density parameters now consists of adjusting the 4 parameters N_L, N_U, $\tilde{a}$ (and thereby automatically the corresponding value for $a(S_n)$), and δ to give simultaneously the optimal description of the cumulated discrete levels between N_L and N_U and the D_0 value at S_n for each nucleus. As an extra condition we impose $2 \leqslant N_L \leqslant 8$ and $N_U \geqslant 15$. In previous level density parameter studies, $N_L = 1$ or $N_L = 2$ was often used as lower limit for the discrete level matching. The extended range that we allow for N_L has two reasons: (a) this should avoid collective effects for the lowest levels to incorrectly influence the level density description, (b) in statistical model calculations, the first few levels are taken into account explicitly in a Hauser–Feshbach model anyway, so that a good fit by a level density model is irrelevant for these levels in an actual nuclear reaction calculation. Our goodness-of-fit estimator for the local level density model for one nuclide is

$$\chi^2 = \chi^2_{D,i} + \chi^2_{\text{lev},i}. \tag{79}$$

Throughout the search, the energy dependence of a is always consistently taken into account, which is necessary since we optimize the description of the cumulated discrete levels and D_0 simultaneously. Apart from the optimal parameters N_L, N_U and δ, the search thus also produces an *adjusted* $\tilde{a}$ value, and related $a(S_n)$ value, for each nucleus separately (see the discussion in Section 2.2 for the justification of this strategy).

Eq. (79) is used for the 289 nuclides for which both an experimental D_0 value and a discrete level sequence exists. For 846 nuclides we only have an experimental discrete level range, and then the first term of Eq. (79) is obviously absent, and we fix a at the global value obtained from α, β, and γ_1, and only vary δ to obtain the best description of these levels. For the discrete level range, δ is the most sensitive parameter and optimizing a on the basis of the discrete level range only may lead to unrealistic values of the level density at S_n and beyond.

As mentioned before, we next return to the optimization of the global parameters α, β, γ_1 and δ_{global}, but now using the discrete level values N_L and N_U as obtained from the local analysis. This alters the global parameters slightly. Finally, we again repeat the optimization of the local parameters, but now with the final global parameters as starting values for the parameter search. This last step gives practically no differences in the results. Hence, convergence is reached in two iterations.

This procedure of iterating between a global and a local approach is also followed for the other level density models, and there are only small differences with the procedure for the BFM. For the GSM the same procedure is followed, but now the pairing parameter to be optimized is that of Eq. (65). For the CTM, δ is not a free parameter, and $a(S_n)$ is adjusted to reproduce the experimental D_0, again yielding a global and a local parameterization. The discrete levels N_L and N_U are adjusted such that the constant temperature expression gives the best description of the discrete levels between N_L and N_U, resulting in the optimal values for E_0 and T. For each set of a, N_L and N_U values, Eq. (56) is solved, which eventually yields the optimal set of parameters for the CTM. In general, the constant temperature description gives the best description of the low-lying levels, although exceptions exist (especially for deformed nuclides). We found that the N_L, N_U values for the other level density models were equal or very close to those of the CTM. Therefore, we adopt the N_L, N_U set of the effective CTM for all level density models. We do not give all 1135 N_L, N_U values here, but those for the cases where also

Table 5
Global level density parameters for the phenomenological and microscopical models

Model	α	β	γ_1	δ_{global}	f_{rms}	f_{lev}
BFM effective	0.0722396	0.195267	0.410289	0.173015	1.68	28.5
BFM collective	0.0381563	0.105378	0.546474	0.743229	1.71	35.3
CTM effective	0.0692559	0.282769	0.433090	0.	1.76	24.2
CTM collective	0.0207305	0.229537	0.473625	0.	1.77	47.8
GSM effective	0.110575	0.0313662	0.648723	1.13208	1.78	28.0
GSM collective	0.0357750	0.135307	0.699663	−0.149106	1.94	47.4
HFM			$c = 0$	$p = 0$	2.35	46.8

an experimental D_0 values exists are given in Tables 1–3. The optimization approach for the various analytical level density models is essentially the same when explicit collective enhancement is taken into account, since the expressions for the rotational and vibrational enhancement are not treated as adjustable. Of course, for the HFM the global results are directly available from the original tables. The determination of c and p for individual nuclides proceeds analogous to that of the BFM.

6. Results

6.1. Level density parameters

This study has resulted in a large collection of level density parameters for different models. There are local parameterizations for cases where experimental mean resonance spacing and discrete level data are available and global parameterizations which are supposed to reliably predict level densities in the absence of such experimental data. We have tried to order the presentation of our results in the most logical way in tables, formulae and figures, and we will now discuss them in some detail.

Table 5 summarizes the *global* level density parameters α, β, γ_1 and δ_{global} for the various models. The differences in the parameters, which are also reflected by the trends in Figs. 2 and 3, can easily be associated with the obvious differences in the various analytical formulae. Since both the vibrational and rotational collective enhancement, K_{vib} and K_{rot} generally exceed unity, the obtained $a(S_n)$ parameters are lower for the collective cases than for the effective cases. Also, the pairing conventions which are different for the CTM, BFM and GSM, entail that the $a(S_n)$ values are somewhat larger for the CTM than for the BFM. Note that for some of the global models, the pairing correction δ_{global} deviates from 0. This is a reflection of the fact that at low energies the pairing correlation is more complicated than the simple energy shift that we adopt in our models and that therefore $\delta_{\text{global}} = 0$ cannot generally be expected. The energy-dependent description of $a(E_x)$ is completely driven by the α and β parameters of Eq. (16). Nevertheless, it may be interesting to relate the values of Table 5 to the simple law $a = A/k$ which has been used a lot in the past. Fitting this linear law to Eq. (16) gives for the various effective models $k = 9.4$ (BFM), $k = 8.4$ (CTM), $k = 8.6$ (GSM) and for the collective models $k = 17.6$ (BFM), $k = 16.3$ (CTM), and $k = 16.8$ (GSM).

Tables 6–17 give the *local* level density parameters for the nuclides for which both an experimental D_0 value and discrete level information are available, for the CTM, BFM and GSM, respectively. For each nuclide, we give the fitted values $a(S_n)$ and δ, with the global value of $a(S_n)$ from Eqs. (15)–(17) between brackets for comparison. For each model, this is given for

Table 6
Local level density parameters $a(S_n)$, T, E_0 and E_M for CTM. For comparison, the values between brackets come from the global systematics

CTM	Effective model				Collective model			
Nuc	$a(S_n)$	T	E_0	E_M	$a(S_n)$	T	E_0	E_M
^{24}Na	3.47 (3.76)	2.01 (1.95)	−1.72 (−2.18)	7.65 (8.27)	2.26 (2.25)	1.28 (1.82)	0.56 (−1.30)	2.73 (7.00)
^{25}Mg	3.67 (3.56)	2.11 (2.03)	−0.99 (0.09)	16.26 (14.32)	2.31 (2.11)	1.97 (1.91)	−0.44 (0.80)	12.97 (12.25)
^{26}Mg	4.43 (4.06)	1.86 (1.84)	1.44 (2.61)	15.28 (14.00)	2.56 (2.41)	1.96 (1.71)	1.11 (3.35)	15.46 (11.38)
^{27}Mg	4.73 (4.17)	1.07 (1.79)	2.54 (0.16)	3.94 (10.04)	2.85 (2.47)	1.60 (1.67)	0.61 (1.08)	9.63 (8.88)
^{28}Al	3.83 (3.77)	1.95 (2.03)	−2.46 (−2.83)	11.45 (12.42)	2.33 (2.21)	1.84 (1.92)	−1.94 (−2.10)	9.20 (9.66)
^{29}Si	3.94 (3.04)	1.52 (2.50)	2.03 (−4.40)	12.83 (26.78)	2.53 (1.74)	1.37 (2.45)	2.55 (−3.17)	8.37 (19.62)
^{30}Si	2.67 (3.85)	3.14 (1.97)	−3.05 (1.49)	29.00 (17.08)	2.12 (2.24)	2.12 (1.87)	0.80 (2.29)	16.97 (14.15)
^{32}P	3.75 (3.92)	1.89 (2.02)	−1.65 (−3.49)	11.41 (15.30)	2.21 (2.27)	1.70 (1.93)	−0.84 (−2.66)	6.77 (11.41)
^{33}S	4.20 (4.08)	1.86 (1.91)	−0.89 (−0.96)	15.09 (15.45)	2.48 (2.35)	1.82 (1.82)	−0.70 (−0.23)	12.99 (12.18)
^{34}S	4.39 (4.70)	2.01 (1.68)	−0.24 (1.77)	17.95 (13.37)	2.60 (2.73)	1.89 (1.58)	0.32 (2.40)	15.37 (11.51)
^{35}S	4.08 (5.14)	2.41 (1.54)	−4.74 (−0.13)	19.44 (9.54)	2.97 (2.99)	1.74 (1.44)	−1.79 (0.51)	12.30 (8.28)
^{36}Cl	4.27 (4.86)	1.91 (1.67)	−2.90 (−2.44)	11.72 (9.85)	2.40 (2.81)	1.82 (1.57)	−2.56 (−1.86)	9.44 (7.72)
^{38}Cl	6.09 (6.28)	1.32 (1.32)	−1.82 (−2.06)	5.51 (5.83)	3.42 (3.66)	1.00 (1.22)	0.32 (−1.40)	5.64 (5.14)
^{41}Ar	7.78 (8.10)	1.07 (1.10)	0.26 (−0.19)	6.08 (6.65)	4.89 (4.75)	0.98 (1.01)	0.62 (0.53)	6.13 (6.32)
^{40}K	5.17 (6.15)	1.75 (1.35)	−3.53 (−2.08)	9.79 (6.41)	2.87 (3.56)	1.61 (1.25)	−2.84 (−1.52)	8.12 (5.47)
^{42}K	5.78 (7.46)	1.96 (1.14)	−6.57 (−2.05)	12.13 (5.08)	2.96 (4.33)	1.89 (1.05)	−6.03 (−1.39)	10.67 (4.62)
^{41}Ca	6.23 (6.12)	1.37 (1.36)	−0.51 (−0.23)	9.04 (8.57)	3.72 (3.53)	1.29 (1.26)	−0.19 (0.32)	8.39 (7.51)
^{43}Ca	7.31 (7.56)	1.37 (1.14)	−1.77 (−0.22)	9.35 (7.00)	5.12 (4.39)	1.09 (1.05)	−0.65 (0.41)	7.93 (6.49)
^{44}Ca	7.47 (7.71)	1.40 (1.12)	−0.54 (1.57)	11.78 (8.72)	4.25 (4.46)	1.36 (1.03)	−0.34 (2.19)	11.73 (8.23)
^{45}Ca	7.66 (7.88)	1.23 (1.11)	−0.92 (−0.24)	8.00 (7.57)	4.54 (4.56)	1.15 (1.02)	−0.58 (0.35)	7.85 (6.42)
^{46}Sc	6.92 (7.56)	1.37 (1.14)	−3.16 (−2.02)	7.39 (6.06)	3.79 (4.35)	1.31 (1.05)	−2.82 (−1.49)	6.99 (4.76)
^{47}Ti	6.35 (7.34)	1.61 (1.18)	−2.66 (−0.30)	11.90 (7.56)	3.55 (4.21)	1.47 (1.09)	−1.96 (0.20)	10.24 (6.74)
^{48}Ti	6.99 (7.42)	1.47 (1.17)	−0.80 (1.41)	13.08 (9.29)	3.93 (4.24)	1.40 (1.08)	−0.40 (1.90)	12.01 (8.46)
^{49}Ti	7.57 (7.32)	1.30 (1.19)	−1.56 (−0.18)	10.75 (8.60)	4.24 (4.18)	1.25 (1.10)	−1.15 (0.15)	8.94 (7.60)
^{50}Ti	6.63 (7.04)	1.46 (1.23)	−0.17 (1.28)	13.09 (10.14)	3.61 (3.99)	1.43 (1.15)	−0.02 (1.69)	11.91 (8.91)
^{51}Ti	7.26 (7.21)	1.06 (1.21)	0.76 (−0.32)	7.01 (9.06)	3.44 (4.09)	1.21 (1.12)	0.15 (−0.01)	6.96 (7.27)

Table 6 (*continued*)

CTM	Effective model				Collective model			
Nuc	$a(S_n)$	T	E_0	E_M	$a(S_n)$	T	E_0	E_M
^{51}V	6.67 (7.08)	1.26 (1.24)	−0.12 (−0.45)	8.20 (8.60)	3.57 (4.01)	1.17 (1.15)	0.33 (−0.06)	6.59 (7.29)
^{52}V	6.87 (7.18)	1.17 (1.22)	−1.43 (−2.12)	5.63 (6.85)	3.71 (4.06)	1.10 (1.14)	−1.12 (−1.74)	4.27 (5.54)
^{51}Cr	6.86 (6.79)	1.30 (1.28)	−0.76 (−0.44)	10.70 (10.13)	3.79 (3.84)	1.24 (1.20)	−0.47 (−0.18)	8.23 (7.64)
^{53}Cr	6.45 (6.95)	1.45 (1.25)	−1.67 (−0.53)	11.74 (9.12)	3.58 (3.91)	1.37 (1.17)	−1.30 (−0.19)	9.69 (7.55)
^{54}Cr	6.87 (7.59)	1.48 (1.16)	−0.82 (1.18)	13.69 (9.73)	3.77 (4.28)	1.38 (1.08)	−0.31 (1.49)	11.61 (8.55)
^{55}Cr	7.81 (8.19)	1.18 (1.09)	−0.82 (−0.43)	8.30 (7.47)	4.39 (4.64)	1.08 (1.02)	−0.37 (−0.08)	7.10 (6.53)
^{56}Mn	7.47 (7.62)	1.31 (1.17)	−3.31 (−2.11)	9.04 (6.73)	4.10 (4.28)	1.27 (1.09)	−3.12 (−1.84)	7.66 (5.42)
^{55}Fe	6.10 (6.11)	1.52 (1.44)	−2.06 (−1.22)	15.34 (13.48)	3.54 (3.39)	1.40 (1.38)	−1.41 (−0.87)	11.14 (10.11)
^{57}Fe	7.16 (7.27)	1.31 (1.21)	−1.42 (−0.60)	10.83 (9.12)	4.06 (4.06)	1.21 (1.14)	−0.98 (−0.36)	8.63 (7.46)
^{58}Fe	7.47 (7.91)	1.36 (1.13)	−0.60 (1.06)	12.93 (9.70)	4.18 (4.44)	1.27 (1.06)	−0.24 (1.33)	11.08 (8.43)
^{59}Fe	8.51 (8.57)	1.14 (1.06)	−1.12 (−0.48)	8.55 (7.42)	4.80 (4.82)	1.08 (0.98)	−1.00 (−0.18)	7.79 (6.43)
^{60}Co	8.08 (8.10)	1.12 (1.11)	−2.11 (−2.09)	6.60 (6.56)	4.37 (4.53)	1.07 (1.04)	−1.86 (−1.83)	5.35 (5.26)
^{59}Ni	6.61 (6.42)	1.42 (1.39)	−1.97 (−1.24)	14.63 (13.23)	3.96 (3.54)	1.30 (1.33)	−1.42 (−0.92)	10.69 (9.84)
^{60}Ni	6.69 (7.11)	1.55 (1.27)	−1.90 (0.72)	17.83 (12.16)	4.14 (3.95)	1.37 (1.20)	−1.06 (0.97)	13.33 (9.81)
^{61}Ni	7.97 (7.75)	1.18 (1.16)	−1.13 (−0.62)	9.68 (8.79)	4.48 (4.31)	1.09 (1.09)	−0.62 (−0.38)	7.60 (7.18)
^{62}Ni	7.39 (8.23)	1.50 (1.10)	−2.20 (0.95)	15.79 (9.69)	4.09 (4.59)	1.40 (1.03)	−1.63 (1.22)	12.77 (8.33)
^{63}Ni	9.08 (8.96)	1.00 (1.02)	−0.38 (−0.52)	7.07 (7.36)	5.09 (5.01)	0.94 (0.95)	−0.17 (−0.22)	6.21 (6.33)
^{65}Ni	10.00 (10.02)	0.90 (0.94)	−0.15 (−0.50)	6.15 (6.72)	5.64 (5.62)	0.83 (0.87)	0.11 (−0.16)	5.46 (5.92)
^{64}Cu	8.39 (8.79)	1.13 (1.04)	−2.50 (−2.05)	7.11 (6.13)	4.59 (4.90)	1.03 (0.97)	−1.95 (−1.79)	5.32 (4.96)
^{66}Cu	8.97 (9.82)	1.03 (0.95)	−2.04 (−2.00)	5.69 (5.36)	4.78 (5.49)	0.95 (0.88)	−1.69 (−1.69)	4.62 (4.50)
^{65}Zn	9.67 (9.45)	1.10 (0.98)	−1.86 (−0.52)	9.15 (7.06)	5.44 (5.28)	1.04 (0.91)	−1.61 (−0.26)	8.15 (6.12)
^{67}Zn	10.74 (10.69)	0.98 (0.89)	−1.37 (−0.51)	7.68 (6.42)	6.04 (5.99)	0.92 (0.82)	−1.14 (−0.18)	7.11 (5.72)
^{68}Zn	9.95 (10.78)	1.04 (0.88)	−0.04 (0.94)	9.45 (7.81)	5.31 (6.03)	0.98 (0.81)	0.29 (1.28)	8.66 (7.13)
^{69}Zn	11.51 (11.60)	0.89 (0.84)	−1.02 (−0.51)	6.86 (6.12)	6.45 (6.52)	0.85 (0.77)	−0.88 (−0.16)	6.54 (5.52)

Table 7
Local level density parameters $a(S_n)$, T, E_0 and E_M for CTM. For comparison, the values between brackets come from the global systematics

CTM	Effective model				Collective model			
Nuc	$a(S_n)$	T	E_0	E_M	$a(S_n)$	T	E_0	E_M
^{71}Zn	12.40 (12.44)	0.71 (0.79)	0.17 (−0.52)	4.90 (5.91)	7.07 (7.00)	0.67 (0.73)	0.36 (−0.14)	4.58 (5.37)
^{70}Ga	10.11 (11.28)	1.03 (0.84)	−2.99 (−1.96)	6.50 (4.75)	5.38 (6.30)	0.95 (0.78)	−2.54 (−1.63)	5.54 (4.11)
^{72}Ga	11.48 (12.43)	0.98 (0.78)	−3.39 (−1.94)	6.52 (4.44)	6.15 (6.96)	0.92 (0.72)	−2.99 (−1.59)	5.80 (3.92)
^{71}Ge	12.73 (12.21)	0.87 (0.80)	−1.56 (−0.52)	7.24 (5.93)	7.32 (6.85)	0.82 (0.73)	−1.26 (−0.18)	6.76 (5.38)
^{73}Ge	13.10 (12.98)	0.92 (0.76)	−2.33 (−0.53)	8.03 (5.76)	7.39 (7.28)	0.87 (0.70)	−2.04 (−0.18)	7.50 (5.26)
^{74}Ge	12.25 (12.46)	0.86 (0.78)	0.16 (0.86)	8.25 (7.25)	6.59 (6.95)	0.83 (0.72)	0.37 (1.19)	7.84 (6.70)
^{75}Ge	12.55 (12.99)	0.91 (0.76)	−1.76 (−0.54)	7.50 (5.80)	7.21 (7.27)	0.83 (0.70)	−1.42 (−0.18)	6.87 (5.26)
^{77}Ge	12.75 (12.66)	0.82 (0.78)	−1.00 (−0.55)	6.57 (5.95)	7.12 (7.05)	0.79 (0.72)	−0.90 (−0.24)	6.24 (5.32)
^{76}As	12.61 (13.09)	0.92 (0.75)	−3.45 (−1.91)	6.40 (4.33)	6.83 (7.30)	0.87 (0.69)	−3.19 (−1.59)	5.83 (3.81)
^{75}Se	13.28 (13.05)	0.91 (0.75)	−2.36 (−0.53)	8.03 (5.73)	7.42 (7.29)	0.87 (0.69)	−2.14 (−0.20)	7.53 (5.21)
^{77}Se	13.41 (13.44)	0.84 (0.74)	−1.53 (−0.54)	6.99 (5.68)	7.41 (7.50)	0.79 (0.68)	−1.29 (−0.22)	6.53 (5.16)
^{78}Se	12.37 (12.92)	0.85 (0.75)	0.14 (0.81)	8.15 (7.14)	6.77 (7.18)	0.79 (0.69)	0.42 (1.13)	7.58 (6.57)
^{79}Se	12.39 (13.35)	0.97 (0.75)	−2.47 (−0.55)	8.43 (5.75)	6.76 (7.43)	0.91 (0.69)	−2.17 (−0.23)	7.63 (5.18)
^{81}Se	12.90 (12.59)	0.72 (0.78)	−0.16 (−0.58)	5.35 (6.04)	7.02 (6.97)	0.69 (0.73)	−0.06 (−0.30)	4.92 (5.31)
^{83}Se	13.02 (11.84)	0.70 (0.83)	−0.01 (−0.61)	5.20 (6.42)	7.34 (6.51)	0.67 (0.77)	0.07 (−0.36)	4.65 (5.50)
^{80}Br	12.60 (13.33)	0.96 (0.74)	−3.99 (−1.89)	7.19 (4.35)	6.79 (7.39)	0.91 (0.68)	−3.62 (−1.57)	6.35 (3.79)
^{82}Br	11.94 (12.63)	0.82 (0.77)	−1.96 (−1.90)	4.87 (4.66)	6.43 (6.97)	0.75 (0.72)	−1.62 (−1.62)	4.01 (3.95)
^{79}Kr	13.32 (13.43)	0.90 (0.73)	−2.26 (−0.55)	7.91 (5.68)	7.41 (7.47)	0.85 (0.68)	−2.00 (−0.24)	7.29 (5.14)
^{81}Kr	13.90 (13.55)	0.80 (0.73)	−1.45 (−0.56)	6.85 (5.69)	8.29 (7.52)	0.71 (0.68)	−0.96 (−0.23)	6.03 (5.12)
^{84}Kr	10.35 (12.19)	0.97 (0.80)	0.21 (0.71)	8.75 (7.54)	5.32 (6.69)	0.89 (0.74)	0.62 (0.97)	7.43 (6.69)
^{85}Kr	13.11 (11.96)	0.67 (0.82)	0.19 (−0.62)	4.83 (6.41)	7.44 (6.55)	0.60 (0.76)	0.50 (−0.37)	3.71 (5.46)
^{86}Rb	9.92 (11.47)	0.96 (0.85)	−1.96 (−1.94)	5.90 (5.43)	5.08 (6.26)	0.86 (0.79)	−1.51 (−1.72)	4.11 (4.33)
^{88}Rb	10.22 (11.31)	0.88 (0.86)	−1.48 (−1.95)	5.08 (5.64)	5.23 (6.15)	0.80 (0.81)	−1.15 (−1.76)	3.34 (4.42)
^{85}Sr	12.70 (12.84)	0.84 (0.77)	−1.25 (−0.59)	7.00 (5.99)	7.08 (7.06)	0.78 (0.71)	−0.97 (−0.31)	6.20 (5.24)
^{87}Sr	10.14 (11.55)	0.86 (0.85)	0.01 (−0.65)	5.89 (6.71)	5.25 (6.30)	0.72 (0.79)	0.57 (−0.43)	3.56 (5.60)

Table 7 (*continued*)

CTM	Effective model				Collective model			
Nuc	$a(S_n)$	T	E_0	E_M	$a(S_n)$	T	E_0	E_M
^{88}Sr	9.24 (10.52)	0.94 (0.93)	1.34 (0.52)	7.81 (9.03)	4.75 (5.69)	0.74 (0.87)	2.15 (0.69)	5.65 (7.42)
^{89}Sr	9.78 (10.94)	0.61 (0.88)	1.49 (−0.71)	1.63 (7.24)	4.87 (5.92)	0.72 (0.83)	1.19 (−0.53)	6.44 (5.85)
^{90}Y	9.23 (10.83)	0.86 (0.90)	−0.71 (−2.00)	4.05 (6.20)	4.60 (5.85)	0.75 (0.85)	−0.33 (−1.84)	3.96 (4.69)
^{91}Zr	10.48 (10.94)	0.86 (0.89)	−0.22 (−0.74)	6.50 (7.38)	5.54 (5.90)	0.77 (0.84)	0.16 (−0.57)	4.40 (5.90)
^{92}Zr	11.50 (12.13)	0.86 (0.81)	0.52 (0.59)	8.08 (7.81)	6.03 (6.58)	0.80 (0.76)	0.75 (0.80)	6.86 (6.71)
^{93}Zr	12.15 (12.68)	0.75 (0.78)	−0.09 (−0.65)	5.47 (6.31)	6.42 (6.89)	0.68 (0.73)	0.23 (−0.43)	4.15 (5.31)
^{94}Zr	14.09 (13.64)	0.67 (0.74)	1.04 (0.62)	6.43 (7.17)	7.69 (7.44)	0.63 (0.69)	1.20 (0.86)	5.75 (6.34)
^{95}Zr	12.94 (13.88)	0.64 (0.73)	0.48 (−0.62)	4.18 (5.88)	6.63 (7.57)	0.58 (0.68)	0.65 (−0.40)	3.07 (5.06)
^{94}Nb	12.42 (12.85)	0.72 (0.77)	−1.21 (−1.88)	3.93 (5.00)	6.51 (6.98)	0.65 (0.72)	−0.91 (−1.66)	2.65 (4.02)
^{93}Mo	10.40 (10.66)	0.93 (0.92)	−0.77 (−0.80)	7.90 (7.86)	5.49 (5.72)	0.85 (0.86)	−0.37 (−0.66)	5.58 (6.12)
^{95}Mo	12.51 (12.55)	0.82 (0.79)	−0.92 (−0.66)	6.88 (6.43)	6.74 (6.80)	0.77 (0.74)	−0.68 (−0.46)	5.73 (5.35)
^{96}Mo	13.09 (13.48)	0.78 (0.74)	0.38 (0.59)	7.65 (7.25)	6.96 (7.32)	0.72 (0.69)	0.69 (0.81)	6.58 (6.35)
^{97}Mo	14.03 (14.27)	0.78 (0.71)	−1.26 (−0.62)	6.77 (5.78)	7.53 (7.77)	0.73 (0.66)	−1.00 (−0.40)	5.89 (4.98)
^{98}Mo	14.59 (15.03)	0.75 (0.68)	0.08 (0.61)	7.59 (6.77)	7.83 (8.20)	0.69 (0.63)	0.37 (0.84)	6.77 (6.06)
^{99}Mo	16.32 (16.21)	0.70 (0.64)	−1.26 (−0.58)	6.25 (5.33)	8.92 (8.87)	0.66 (0.59)	−1.05 (−0.34)	5.66 (4.72)
^{101}Mo	18.26 (17.85)	0.70 (0.60)	−1.86 (−0.56)	6.68 (5.06)	12.93 (9.81)	0.55 (0.55)	−1.25 (−0.32)	5.52 (4.54)
^{100}Tc	16.16 (15.74)	0.66 (0.65)	−2.00 (−1.79)	4.44 (4.19)	8.69 (8.58)	0.62 (0.60)	−1.82 (−1.55)	3.90 (3.54)
^{100}Ru	14.31 (14.16)	0.79 (0.71)	−0.40 (0.57)	8.48 (7.05)	7.75 (7.67)	0.76 (0.66)	−0.20 (0.77)	7.58 (6.19)
^{102}Ru	15.70 (15.64)	0.68 (0.65)	0.32 (0.59)	7.01 (6.62)	8.45 (8.50)	0.64 (0.61)	0.49 (0.81)	6.39 (5.93)
^{103}Ru	16.66 (16.84)	0.75 (0.62)	−2.02 (−0.58)	7.15 (5.22)	8.99 (9.19)	0.71 (0.57)	−1.76 (−0.35)	6.38 (4.62)
^{105}Ru	18.88 (17.85)	0.64 (0.59)	−1.45 (−0.57)	6.12 (5.06)	10.40 (9.76)	0.61 (0.55)	−1.28 (−0.34)	5.65 (4.51)
^{104}Rh	16.04 (16.17)	0.66 (0.64)	−2.01 (−1.77)	4.50 (4.15)	8.63 (8.79)	0.61 (0.59)	−1.70 (−1.55)	3.72 (3.49)
^{105}Pd	16.01 (15.55)	0.74 (0.66)	−1.64 (−0.61)	6.94 (5.52)	8.71 (8.42)	0.70 (0.61)	−1.47 (−0.40)	6.19 (4.76)
^{106}Pd	15.90 (15.82)	0.68 (0.65)	0.20 (0.56)	7.11 (6.60)	8.62 (8.56)	0.63 (0.60)	0.47 (0.77)	6.29 (5.87)
^{107}Pd	17.29 (16.96)	0.67 (0.62)	−1.33 (−0.59)	6.21 (5.22)	9.37 (9.21)	0.64 (0.57)	−1.13 (−0.37)	5.59 (4.58)

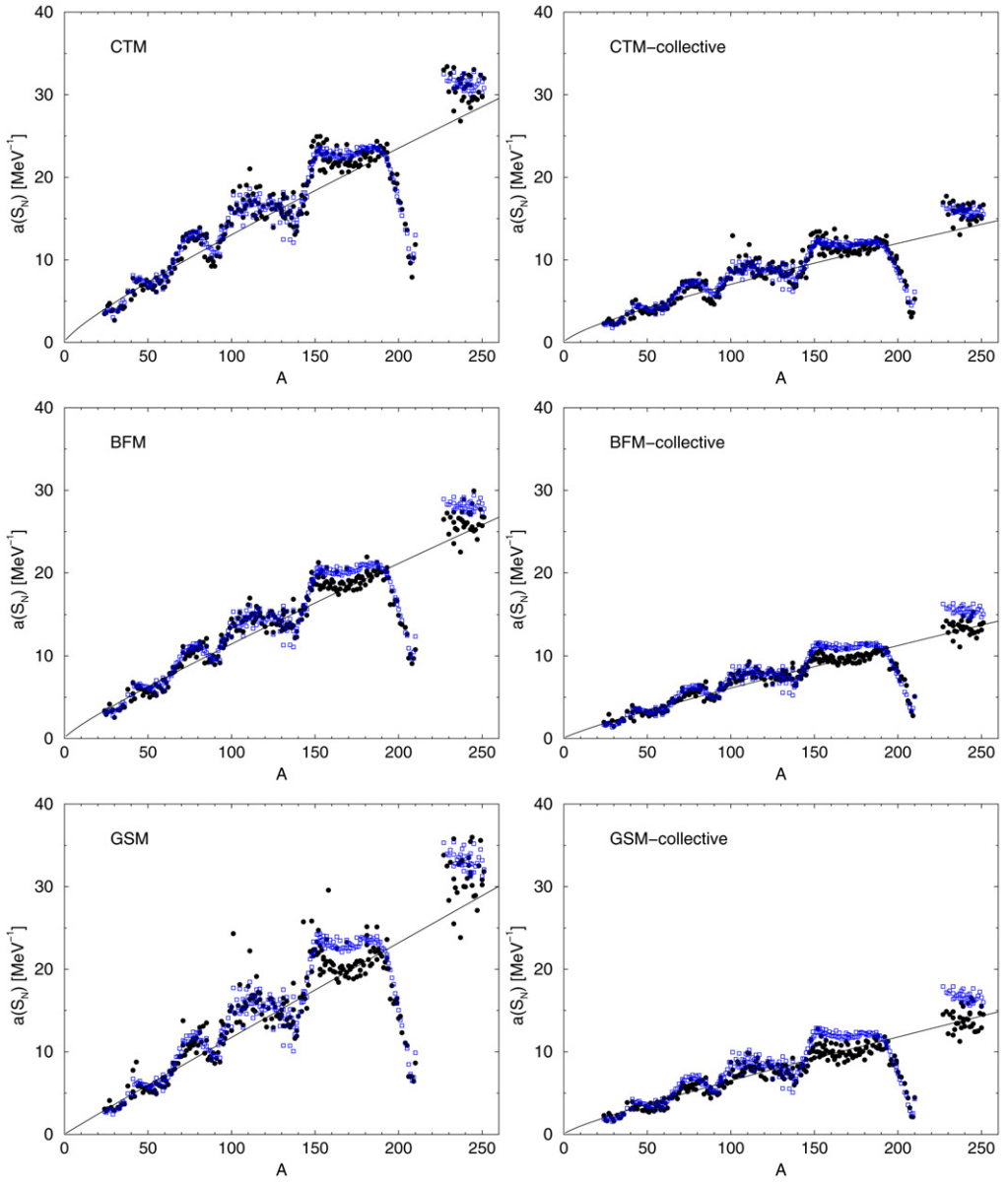

Fig. 2. Level density parameters a at the neutron separation energy S_n, for the CTM, BFM and GSM without and with explicit collective enhancement. The closed circles represent the values adjusted to experimental data per nucleus. The open squares represent the values from the global systematics. The solid line represents the global value for $\tilde{a}$, the asymptotic limit for a. Only values for which an experimental D_0 value exists are plotted.

the effective case and for the case with explicit collective enhancement. For the CTM, where the adjustable δ is not used, we give T, E_0 and E_M for both the local and global case. The HFM values for c and p are given in Tables 18–19.

Table 8
Local level density parameters $a(S_n)$, T, E_0 and E_M for CTM. For comparison, the values between brackets come from the global systematics

CTM	Effective model				Collective model			
Nuc	$a(S_n)$	T	E_0	E_M	$a(S_n)$	T	E_0	E_M
^{108}Pd	16.52 (16.87)	0.63 (0.61)	0.55 (0.57)	6.42 (6.36)	8.78 (9.15)	0.59 (0.57)	0.69 (0.79)	5.88 (5.72)
^{109}Pd	19.04 (17.91)	0.69 (0.59)	−2.16 (−0.57)	7.02 (5.07)	10.54 (9.74)	0.66 (0.55)	−2.02 (−0.35)	6.43 (4.48)
^{111}Pd	21.02 (18.57)	0.57 (0.58)	−1.08 (−0.57)	5.47 (4.97)	11.84 (10.10)	0.54 (0.53)	−0.89 (−0.35)	5.02 (4.41)
^{108}Ag	16.17 (16.22)	0.68 (0.64)	−2.24 (−1.76)	4.89 (4.20)	9.16 (8.77)	0.60 (0.59)	−1.82 (−1.54)	3.86 (3.49)
^{110}Ag	17.78 (17.33)	0.61 (0.60)	−1.96 (−1.73)	4.27 (3.99)	9.69 (9.38)	0.57 (0.56)	−1.75 (−1.51)	3.68 (3.36)
^{107}Cd	15.12 (14.11)	0.74 (0.72)	−1.37 (−0.67)	6.98 (6.03)	8.36 (7.58)	0.70 (0.67)	−1.17 (−0.50)	5.97 (5.01)
^{109}Cd	16.64 (15.55)	0.64 (0.66)	−0.79 (−0.63)	5.68 (5.57)	9.21 (8.38)	0.60 (0.62)	−0.61 (−0.43)	4.96 (4.75)
^{111}Cd	17.16 (16.59)	0.66 (0.63)	−1.20 (−0.61)	6.12 (5.33)	9.65 (8.96)	0.61 (0.58)	−0.93 (−0.40)	5.30 (4.60)
^{112}Cd	16.68 (16.62)	0.63 (0.62)	0.46 (0.53)	6.53 (6.44)	9.20 (8.96)	0.57 (0.58)	0.76 (0.74)	5.67 (5.71)
^{113}Cd	17.99 (17.44)	0.63 (0.60)	−1.07 (−0.59)	5.79 (5.17)	9.75 (9.43)	0.60 (0.56)	−0.90 (−0.38)	5.19 (4.50)
^{114}Cd	17.10 (17.21)	0.61 (0.61)	0.55 (0.53)	6.30 (6.32)	9.18 (9.28)	0.57 (0.56)	0.70 (0.73)	5.69 (5.63)
^{115}Cd	18.76 (17.93)	0.58 (0.59)	−0.69 (−0.59)	5.18 (5.10)	10.18 (9.69)	0.55 (0.55)	−0.57 (−0.39)	4.66 (4.44)
^{117}Cd	18.90 (18.02)	0.62 (0.59)	−1.19 (−0.59)	5.86 (5.11)	10.23 (9.72)	0.60 (0.55)	−1.09 (−0.40)	5.32 (4.43)
^{114}In	15.37 (16.69)	0.65 (0.62)	−1.58 (−1.73)	4.11 (4.18)	7.89 (8.98)	0.58 (0.58)	−1.22 (−1.52)	3.03 (3.44)
^{116}In	16.81 (17.31)	0.58 (0.60)	−1.32 (−1.71)	3.54 (4.08)	8.81 (9.31)	0.53 (0.56)	−1.12 (−1.50)	2.80 (3.37)
^{113}Sn	15.41 (15.17)	0.64 (0.68)	−0.30 (−0.65)	5.14 (5.75)	8.39 (8.12)	0.58 (0.63)	−0.06 (−0.46)	4.10 (4.80)
^{115}Sn	14.97 (15.65)	0.57 (0.66)	0.37 (−0.65)	3.99 (5.63)	8.04 (8.38)	0.44 (0.62)	0.82 (−0.45)	2.28 (4.72)
^{117}Sn	15.80 (16.35)	0.63 (0.64)	−0.35 (−0.63)	5.09 (5.46)	8.36 (8.76)	0.55 (0.59)	0.10 (−0.43)	3.73 (4.61)
^{118}Sn	15.28 (16.13)	0.65 (0.64)	0.69 (0.46)	6.38 (6.62)	8.07 (8.62)	0.59 (0.60)	0.95 (0.67)	5.30 (5.74)
^{119}Sn	16.47 (16.63)	0.61 (0.63)	−0.42 (−0.63)	5.10 (5.42)	8.77 (8.90)	0.57 (0.59)	−0.20 (−0.42)	4.22 (4.57)
^{120}Sn	14.94 (16.07)	0.68 (0.65)	0.51 (0.45)	6.72 (6.67)	7.79 (8.57)	0.62 (0.60)	0.74 (0.64)	5.63 (5.74)
^{121}Sn	15.12 (16.34)	0.69 (0.64)	−0.75 (−0.65)	5.86 (5.52)	7.75 (8.72)	0.65 (0.60)	−0.61 (−0.45)	4.92 (4.61)
^{125}Sn	13.91 (14.11)	0.59 (0.73)	0.48 (−0.76)	4.03 (6.46)	7.14 (7.41)	0.41 (0.68)	0.96 (−0.62)	2.03 (5.03)
^{122}Sb	16.71 (17.10)	0.67 (0.61)	−2.27 (−1.71)	5.10 (4.22)	8.84 (9.14)	0.63 (0.57)	−2.02 (−1.52)	4.14 (3.40)
^{124}Sb	16.13 (16.41)	0.71 (0.64)	−2.48 (−1.73)	5.66 (4.45)	8.46 (8.73)	0.67 (0.60)	−2.24 (−1.56)	4.53 (3.51)

(*continued on next page*)

Table 8 (*continued*)

CTM	Effective model				Collective model			
Nuc	$a(S_n)$	T	E_0	E_M	$a(S_n)$	T	E_0	E_M
^{123}Te	17.75 (17.62)	0.63 (0.60)	−1.04 (−0.61)	5.83 (5.21)	9.49 (9.42)	0.59 (0.56)	−0.77 (−0.43)	4.93 (4.43)
^{124}Te	16.88 (16.93)	0.62 (0.62)	0.43 (0.45)	6.47 (6.45)	9.07 (9.02)	0.57 (0.58)	0.66 (0.62)	5.51 (5.58)
^{125}Te	17.94 (17.08)	0.63 (0.62)	−1.09 (−0.63)	5.97 (5.37)	9.73 (9.10)	0.60 (0.58)	−0.94 (−0.46)	5.16 (4.49)
^{126}Te	16.17 (16.21)	0.62 (0.64)	0.64 (0.40)	6.31 (6.69)	8.68 (8.59)	0.56 (0.60)	0.92 (0.56)	5.05 (5.68)
^{127}Te	16.65 (16.05)	0.66 (0.65)	−0.94 (−0.67)	6.05 (5.70)	8.93 (8.50)	0.63 (0.61)	−0.84 (−0.53)	5.12 (4.64)
^{129}Te	16.35 (14.51)	0.67 (0.71)	−1.03 (−0.76)	6.54 (6.37)	9.03 (7.60)	0.64 (0.67)	−0.91 (−0.63)	5.33 (4.95)
^{131}Te	15.20 (12.46)	0.64 (0.81)	−0.29 (−0.97)	5.81 (8.00)	8.05 (6.42)	0.61 (0.78)	−0.20 (−0.87)	4.06 (5.71)
^{128}I	16.49 (16.71)	0.71 (0.63)	−2.57 (−1.71)	5.80 (4.43)	8.71 (8.86)	0.66 (0.59)	−2.31 (−1.56)	4.59 (3.47)
^{130}I	15.69 (15.53)	0.76 (0.67)	−2.90 (−1.76)	6.78 (4.89)	8.27 (8.18)	0.72 (0.63)	−2.67 (−1.63)	5.29 (3.68)
^{129}Xe	16.73 (17.20)	0.69 (0.61)	−1.40 (−0.64)	6.60 (5.38)	8.80 (9.13)	0.66 (0.57)	−1.23 (−0.48)	5.58 (4.46)
^{130}Xe	15.95 (16.42)	0.68 (0.64)	0.09 (0.38)	7.22 (6.67)	8.42 (8.67)	0.63 (0.60)	0.33 (0.53)	5.96 (5.63)
^{131}Xe	17.43 (16.17)	0.62 (0.65)	−0.78 (−0.68)	5.72 (5.72)	9.49 (8.52)	0.58 (0.61)	−0.60 (−0.55)	4.65 (4.62)
^{132}Xe	15.06 (15.25)	0.71 (0.68)	0.11 (0.31)	7.56 (7.17)	7.98 (8.00)	0.66 (0.65)	0.31 (0.45)	6.09 (5.85)
^{133}Xe	15.62 (14.58)	0.63 (0.71)	−0.33 (−0.77)	5.41 (6.45)	8.37 (7.61)	0.59 (0.67)	−0.20 (−0.66)	4.00 (4.95)
^{135}Xe	14.21 (12.45)	0.58 (0.82)	0.51 (−1.03)	4.18 (8.33)	7.29 (6.39)	0.55 (0.78)	0.64 (−0.94)	4.66 (5.82)
^{137}Xe	16.46 (12.08)	0.52 (0.81)	0.27 (−1.04)	4.27 (8.37)	8.70 (6.14)	0.43 (0.78)	0.61 (−0.95)	2.19 (5.82)
^{134}Cs	15.57 (15.73)	0.76 (0.67)	−2.77 (−1.75)	6.69 (4.92)	8.17 (8.25)	0.72 (0.63)	−2.63 (−1.63)	5.24 (3.67)
^{131}Ba	17.95 (18.18)	0.62 (0.58)	−1.00 (−0.61)	5.76 (5.15)	9.52 (9.66)	0.58 (0.54)	−0.78 (−0.45)	4.83 (4.33)
^{133}Ba	17.51 (17.46)	0.62 (0.61)	−0.80 (−0.64)	5.59 (5.35)	9.44 (9.24)	0.57 (0.57)	−0.56 (−0.49)	4.52 (4.42)
^{135}Ba	15.88 (16.27)	0.65 (0.65)	−0.64 (−0.69)	5.71 (5.75)	8.28 (8.54)	0.60 (0.61)	−0.43 (−0.57)	4.38 (4.59)
^{136}Ba	15.08 (15.39)	0.72 (0.68)	−0.04 (0.28)	7.83 (7.19)	8.39 (8.05)	0.63 (0.64)	0.38 (0.41)	5.84 (5.81)
^{137}Ba	13.97 (14.47)	0.58 (0.72)	0.56 (−0.81)	3.86 (6.65)	7.03 (7.52)	0.54 (0.68)	0.75 (−0.71)	4.75 (5.00)
^{138}Ba	13.05 (13.65)	0.73 (0.76)	0.73 (0.12)	7.25 (8.41)	6.69 (7.05)	0.63 (0.73)	1.12 (0.21)	4.15 (6.36)
^{139}Ba	14.07 (14.46)	0.65 (0.71)	−0.08 (−0.80)	5.21 (6.59)	7.01 (7.48)	0.55 (0.67)	0.36 (−0.70)	2.34 (4.95)
^{139}La	13.44 (14.86)	0.77 (0.71)	−0.78 (−0.80)	6.86 (6.58)	6.80 (7.72)	0.69 (0.67)	−0.46 (−0.69)	4.55 (4.95)

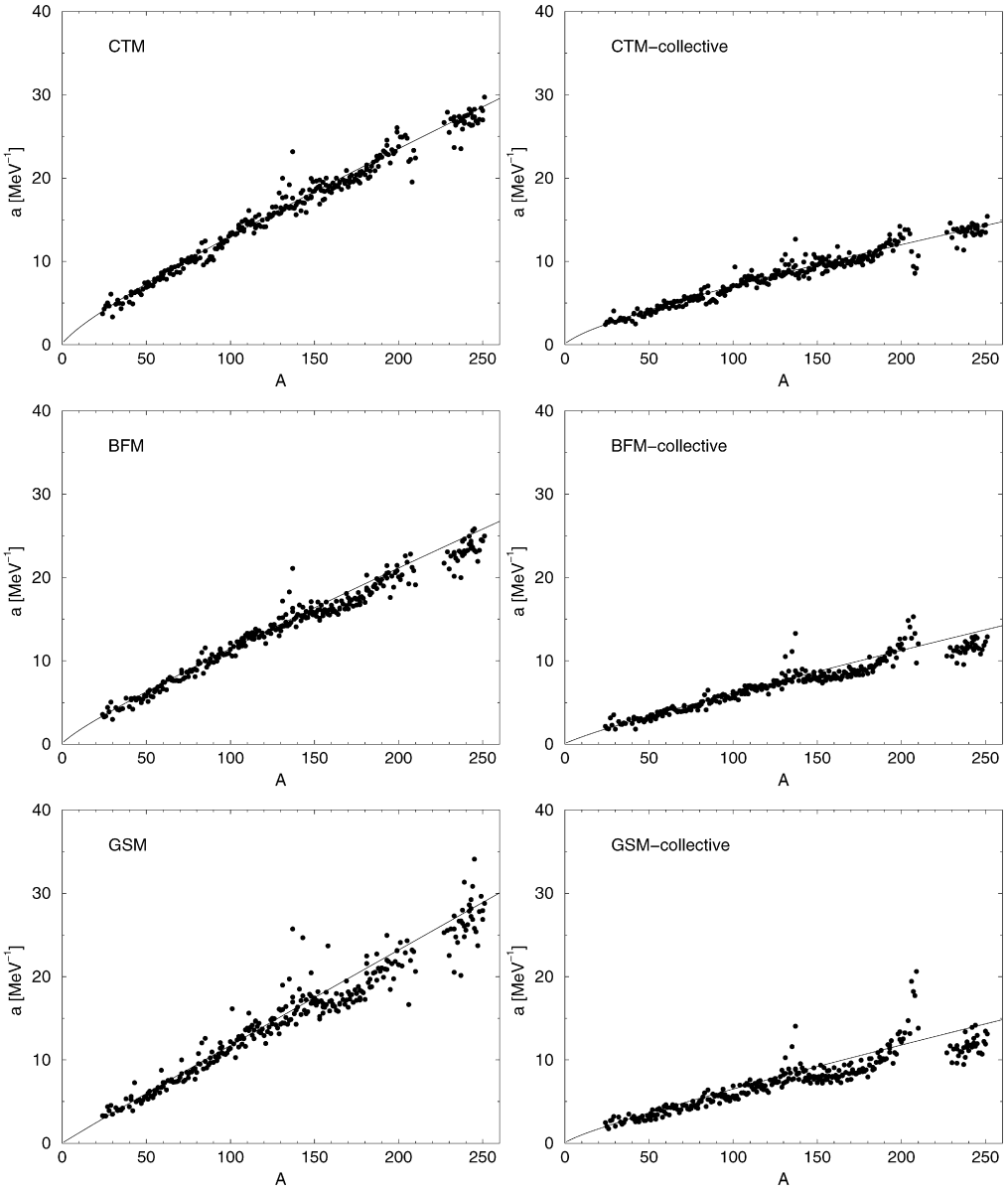

Fig. 3. Level density parameters $\tilde{a}$, for the CTM, BFM and GSM without and with explicit collective enhancement. The closed circles represent the values adjusted to experimental data per nucleus. The solid line represents the global value for $\tilde{a}$, the asymptotic limit for a. Only values for which an experimental D_0 value exists are plotted.

Fig. 2 displays the level density parameter at the neutron separation energy, $a(S_n)$, against A, for the CTM, BFM and GSM. The shell structure around the magic numbers is clearly visible, and we observe the required condition that the scattered local and global sets more or less overlap for all of the models. For comparison, we have plotted the curve of the asymptotic value $\tilde{a}$ of Eq. (16)

for the α and β values given in Table 5. Remind that this curve represents the asymptotic value for the global data set of $a(S_n)$ values.

In Fig. 3 we display the asymptotic level density parameter $\tilde{a}$, against A, for the CTM, BFM and GSM. As expected, the asymptotic values of the local models are grouped around the global curves given by Eq. (16). The deviation from the global value is a measure for the difference of an adjusted and a global level density model. Note that there are a few cases for which this difference is non-negligible, especially for the shell closures around $A = 140$ and $A = 208$, and to a lesser extent $A = 90$. Here, some differences can be expected when applying different (local or global) level density models.

The top panels of Fig. 4 display for all 1135 nuclides the total pairing correction for the BFM, for the effective and the collective case, that produces the best description of experimental data for each individual nuclide. The main trend for the pairing energies indeed follows Eq. (43) for the even, odd, and odd–odd nuclides, although there is clearly quite some scattering around the main trend. Fig. 4 also displays the adjustable pairing shift parameters δ for the BFM and GSM, respectively. This concerns the extra correction on top of the global A-dependent pairing term $12/\sqrt{A}$ that is necessary to optimally describe each individual nucleus. Since the global A-dependent trends are supposed to be covered by the total pairing correction term, these plots represent a correction on a correction and are expected to merely present noise. Note however, that some shell effects can be observed.

In Fig. 5, the spin cut-off parameter for the discrete level region and at the neutron separation energy is plotted for all level density models. The values for the discrete level region are simply obtained by using Eq. (24) and reading the discrete level database. The collection of discrete level values has been fitted with the equation

$$\sigma^2_{d,\mathrm{global}} = \left(0.83A^{0.26}\right)^2 \tag{80}$$

which we use in case the discrete level energies are not or insufficiently known, i.e. for nuclides not in Table 4. The values at the separation energies are directly obtained by inserting $a(S_n)$ into Eq. (23), and Eq. (25) is used to interpolate between the two sets of values. At low energies, there is generally a strong pairing effect and it plays a role in the actual value of σ^2_d. Around the separation energy, the shell correction dominates, as is clearly visible in the figures.

In Fig. 6, we plot the parameters T, E_0 and E_M, for the CTM and the cases without and with explicit collective enhancement. For nuclides for which no, or not enough, discrete levels are known we rely on empirical formulae for the temperature. From Fig. 6 it is clear that shell effects are present in the A-dependent plot of the temperature. To take this into account in the low-energy region, we fit the independent nucleus values by a formula that is inspired by Eq. (10) and the low-energy limit of $a(E_x)$, see Eq. (20). For the effective model,

$$T = -0.22 + \frac{9.4}{\sqrt{A(1+\gamma\delta W)}}, \tag{81}$$

and for the collective model

$$T = -0.25 + \frac{10.2}{\sqrt{A(1+\gamma\delta W)}}, \tag{82}$$

where γ is taken from Eq. (17) and Table 5. Next, we directly obtain E_M from Eq. (54) and E_0 from Eq. (53). Again, Eqs. (81) and (82) were obtained by fitting all individual values of the nuclides for which sufficient discrete level information exists. In a few cases, the global

Table 9
Local level density parameters $a(S_n)$, T, E_0 and E_M for CTM. For comparison, the values between brackets come from the global systematics

CTM	Effective model				Collective model			
Nuc	$a(S_n)$	T	E_0	E_M	$a(S_n)$	T	E_0	E_M
^{140}La	15.47 (15.66)	0.62 (0.67)	−1.18 (−1.75)	4.01 (5.06)	7.91 (8.15)	0.55 (0.63)	−0.92 (−1.64)	2.23 (3.69)
^{137}Ce	18.16 (17.56)	0.54 (0.60)	−0.13 (−0.65)	4.44 (5.37)	9.83 (9.25)	0.48 (0.57)	0.09 (−0.51)	3.31 (4.39)
^{141}Ce	15.88 (16.12)	0.53 (0.65)	0.46 (−0.72)	3.68 (5.89)	8.12 (8.40)	0.44 (0.61)	0.80 (−0.59)	3.36 (4.61)
^{142}Ce	17.81 (17.16)	0.57 (0.62)	0.62 (0.33)	5.98 (6.56)	9.68 (8.98)	0.52 (0.58)	0.80 (0.47)	4.83 (5.45)
^{143}Ce	19.03 (18.14)	0.52 (0.59)	−0.16 (−0.65)	4.39 (5.29)	11.15 (9.53)	0.44 (0.55)	0.08 (−0.51)	3.19 (4.30)
^{142}Pr	15.59 (17.03)	0.58 (0.62)	−0.89 (−1.69)	3.34 (4.59)	7.95 (8.91)	0.47 (0.59)	−0.51 (−1.55)	1.17 (3.45)
^{143}Nd	16.56 (17.14)	0.54 (0.62)	0.24 (−0.68)	3.98 (5.57)	8.41 (8.96)	0.44 (0.58)	0.65 (−0.55)	2.94 (4.44)
^{144}Nd	17.36 (18.14)	0.60 (0.59)	0.40 (0.35)	6.30 (6.29)	8.92 (9.51)	0.56 (0.55)	0.59 (0.51)	5.20 (5.30)
^{145}Nd	19.03 (19.20)	0.55 (0.56)	−0.42 (−0.62)	4.77 (5.06)	9.90 (10.10)	0.51 (0.52)	−0.24 (−0.47)	3.81 (4.18)
^{146}Nd	19.45 (19.94)	0.58 (0.54)	0.11 (0.40)	6.38 (5.90)	10.05 (10.51)	0.54 (0.51)	0.29 (0.54)	5.48 (5.08)
^{147}Nd	21.79 (21.16)	0.51 (0.52)	−0.58 (−0.57)	4.69 (4.72)	11.54 (11.19)	0.48 (0.48)	−0.46 (−0.42)	4.04 (3.99)
^{148}Nd	23.73 (21.61)	0.49 (0.50)	0.21 (0.43)	5.80 (5.62)	13.04 (11.42)	0.46 (0.47)	0.33 (0.58)	5.22 (4.92)
^{149}Nd	24.36 (22.74)	0.53 (0.49)	−1.46 (−0.53)	5.67 (4.50)	13.20 (12.06)	0.51 (0.45)	−1.37 (−0.38)	5.09 (3.86)
^{151}Nd	23.10 (22.78)	0.52 (0.48)	−1.04 (−0.53)	5.18 (4.49)	12.11 (12.06)	0.50 (0.45)	−0.90 (−0.39)	4.54 (3.84)
^{148}Pm	20.90 (21.54)	0.50 (0.50)	−1.33 (−1.54)	3.39 (3.64)	10.83 (11.38)	0.45 (0.47)	−1.11 (−1.39)	2.55 (2.95)
^{145}Sm	15.64 (17.58)	0.60 (0.60)	−0.07 (−0.67)	4.66 (5.46)	7.81 (9.19)	0.50 (0.57)	0.36 (−0.53)	2.59 (4.37)
^{148}Sm	20.10 (20.54)	0.53 (0.53)	0.43 (0.41)	5.79 (5.78)	10.47 (10.82)	0.49 (0.49)	0.61 (0.55)	4.94 (5.01)
^{149}Sm	22.00 (21.84)	0.53 (0.50)	−0.97 (−0.55)	5.21 (4.61)	11.57 (11.54)	0.50 (0.47)	−0.81 (−0.40)	4.49 (3.92)
^{150}Sm	22.29 (22.21)	0.51 (0.49)	0.22 (0.44)	5.83 (5.51)	11.70 (11.74)	0.48 (0.46)	0.32 (0.59)	5.24 (4.85)
^{151}Sm	24.92 (23.45)	0.53 (0.47)	−1.57 (−0.51)	5.73 (4.40)	13.40 (12.43)	0.51 (0.44)	−1.43 (−0.36)	5.10 (3.79)
^{152}Sm	23.21 (22.86)	0.53 (0.48)	−0.26 (0.45)	6.38 (5.41)	12.33 (12.07)	0.50 (0.44)	−0.10 (0.60)	5.69 (4.78)
^{153}Sm	23.70 (23.28)	0.57 (0.47)	−1.89 (−0.52)	6.23 (4.42)	12.52 (12.31)	0.55 (0.44)	−1.76 (−0.38)	5.50 (3.79)
^{155}Sm	22.09 (22.60)	0.52 (0.49)	−0.82 (−0.54)	4.96 (4.52)	11.40 (11.91)	0.49 (0.45)	−0.68 (−0.40)	4.24 (3.83)
^{152}Eu	23.95 (23.55)	0.52 (0.46)	−2.25 (−1.48)	4.40 (3.37)	12.74 (12.46)	0.48 (0.43)	−2.01 (−1.32)	3.66 (2.79)
^{153}Eu	20.82 (23.07)	0.58 (0.47)	−1.34 (−0.51)	5.69 (4.38)	10.63 (12.17)	0.54 (0.44)	−1.17 (−0.37)	4.87 (3.77)

(*continued on next page*)

Table 9 (*continued*)

CTM	Effective model				Collective model			
Nuc	$a(S_n)$	T	E_0	E_M	$a(S_n)$	T	E_0	E_M
^{154}Eu	22.78 (23.14)	0.53 (0.47)	−2.14 (−1.48)	4.37 (3.44)	11.94 (12.21)	0.49 (0.44)	−1.91 (−1.34)	3.58 (2.81)
^{155}Eu	20.92 (22.74)	0.55 (0.48)	−0.96 (−0.52)	5.20 (4.45)	10.70 (11.97)	0.51 (0.44)	−0.80 (−0.39)	4.41 (3.79)
^{156}Eu	20.58 (22.38)	0.54 (0.49)	−1.74 (−1.50)	4.05 (3.56)	10.50 (11.77)	0.49 (0.45)	−1.48 (−1.37)	3.08 (2.87)
^{153}Gd	24.94 (23.58)	0.54 (0.47)	−1.71 (−0.51)	5.90 (4.37)	13.42 (12.48)	0.51 (0.43)	−1.58 (−0.36)	5.25 (3.76)
^{155}Gd	24.18 (23.46)	0.55 (0.47)	−1.75 (−0.51)	6.02 (4.38)	12.86 (12.39)	0.53 (0.44)	−1.65 (−0.37)	5.34 (3.76)
^{156}Gd	22.13 (22.87)	0.56 (0.48)	−0.38 (0.44)	6.60 (5.40)	11.55 (12.04)	0.52 (0.44)	−0.18 (0.57)	5.76 (4.75)
^{157}Gd	22.93 (22.90)	0.53 (0.48)	−1.20 (−0.53)	5.42 (4.47)	12.02 (12.05)	0.50 (0.45)	−1.06 (−0.40)	4.68 (3.79)
^{158}Gd	21.87 (22.64)	0.55 (0.48)	−0.18 (0.42)	6.38 (5.45)	11.34 (11.90)	0.51 (0.45)	0.03 (0.55)	5.49 (4.76)
^{159}Gd	22.32 (22.66)	0.52 (0.49)	−0.93 (−0.54)	5.11 (4.52)	11.54 (11.90)	0.49 (0.45)	−0.79 (−0.41)	4.35 (3.81)
^{161}Gd	21.56 (22.43)	0.52 (0.49)	−0.76 (−0.55)	4.94 (4.56)	10.97 (11.76)	0.49 (0.46)	−0.62 (−0.43)	4.13 (3.82)
^{160}Tb	21.20 (22.55)	0.55 (0.48)	−1.96 (−1.49)	4.35 (3.56)	10.88 (11.83)	0.51 (0.45)	−1.73 (−1.36)	3.40 (2.85)
^{157}Dy	24.57 (23.49)	0.52 (0.47)	−1.34 (−0.51)	5.46 (4.37)	13.21 (12.38)	0.49 (0.43)	−1.20 (−0.37)	4.79 (3.74)
^{159}Dy	22.07 (23.20)	0.57 (0.47)	−1.49 (−0.52)	5.86 (4.42)	11.47 (12.20)	0.53 (0.44)	−1.27 (−0.39)	4.94 (3.76)
^{161}Dy	22.86 (23.00)	0.54 (0.48)	−1.29 (−0.53)	5.55 (4.46)	11.94 (12.07)	0.51 (0.45)	−1.15 (−0.41)	4.78 (3.76)
^{162}Dy	21.79 (22.64)	0.55 (0.48)	−0.23 (0.40)	6.44 (5.45)	13.72 (11.86)	0.45 (0.45)	0.14 (0.52)	5.20 (4.72)
^{163}Dy	21.78 (22.49)	0.58 (0.49)	−1.56 (−0.55)	6.07 (4.55)	11.20 (11.77)	0.55 (0.46)	−1.44 (−0.43)	5.17 (3.80)
^{164}Dy	21.39 (22.37)	0.56 (0.49)	−0.31 (0.39)	6.61 (5.50)	10.95 (11.69)	0.54 (0.46)	−0.20 (0.50)	5.73 (4.73)
^{165}Dy	21.88 (22.44)	0.55 (0.49)	−1.15 (−0.55)	5.50 (4.57)	11.21 (11.72)	0.52 (0.46)	−0.97 (−0.44)	4.56 (3.80)
^{166}Ho	20.61 (22.18)	0.51 (0.49)	−1.37 (−1.49)	3.61 (3.67)	10.43 (11.56)	0.46 (0.46)	−1.11 (−1.38)	2.48 (2.87)
^{163}Er	23.83 (23.52)	0.52 (0.47)	−1.20 (−0.52)	5.34 (4.39)	12.62 (12.33)	0.49 (0.43)	−1.04 (−0.39)	4.57 (3.71)
^{165}Er	22.76 (23.19)	0.55 (0.47)	−1.44 (−0.53)	5.78 (4.44)	11.84 (12.13)	0.52 (0.44)	−1.28 (−0.41)	4.91 (3.73)
^{167}Er	22.23 (22.61)	0.55 (0.49)	−1.23 (−0.55)	5.58 (4.54)	11.53 (11.79)	0.51 (0.45)	−1.04 (−0.44)	4.62 (3.77)
^{168}Er	21.58 (22.59)	0.55 (0.49)	−0.22 (0.38)	6.44 (5.47)	11.02 (11.77)	0.52 (0.45)	−0.03 (0.48)	5.45 (4.69)
^{169}Er	21.75 (22.53)	0.53 (0.49)	−0.95 (−0.55)	5.22 (4.57)	11.10 (11.73)	0.50 (0.46)	−0.79 (−0.45)	4.29 (3.77)
^{171}Er	22.10 (22.59)	0.52 (0.49)	−0.89 (−0.55)	5.11 (4.57)	11.29 (11.75)	0.50 (0.46)	−0.77 (−0.46)	4.24 (3.76)

Table 10
Local level density parameters $a(S_n)$, T, E_0 and E_M for CTM. For comparison, the values between brackets come from the global systematics

CTM	Effective model				Collective model			
Nuc	$a(S_n)$	T	E_0	E_M	$a(S_n)$	T	E_0	E_M
^{170}Tm	20.67 (22.35)	0.52 (0.49)	−1.51 (−1.48)	3.84 (3.66)	10.54 (11.62)	0.47 (0.46)	−1.25 (−1.38)	2.69 (2.85)
^{171}Tm	21.43 (22.62)	0.54 (0.48)	−0.94 (−0.55)	5.22 (4.54)	11.05 (11.76)	0.49 (0.45)	−0.67 (−0.45)	4.09 (3.74)
^{169}Yb	23.95 (23.32)	0.49 (0.47)	−0.93 (−0.53)	4.98 (4.43)	12.75 (12.17)	0.46 (0.44)	−0.77 (−0.42)	4.18 (3.70)
^{170}Yb	21.42 (23.09)	0.58 (0.47)	−0.58 (0.39)	6.92 (5.38)	10.91 (12.03)	0.55 (0.44)	−0.41 (0.49)	5.90 (4.63)
^{171}Yb	22.02 (23.00)	0.54 (0.48)	−1.04 (−0.54)	5.32 (4.49)	11.29 (11.97)	0.50 (0.45)	−0.86 (−0.44)	4.35 (3.72)
^{172}Yb	22.51 (22.89)	0.54 (0.48)	−0.35 (0.37)	6.53 (5.42)	11.75 (11.90)	0.51 (0.45)	−0.18 (0.47)	5.56 (4.63)
^{173}Yb	21.31 (22.61)	0.56 (0.49)	−1.11 (−0.55)	5.52 (4.57)	10.81 (11.74)	0.52 (0.46)	−0.90 (−0.46)	4.43 (3.74)
^{174}Yb	21.72 (22.78)	0.53 (0.48)	0.08 (0.36)	5.96 (5.45)	11.06 (11.82)	0.49 (0.45)	0.27 (0.46)	4.94 (4.63)
^{175}Yb	21.45 (22.74)	0.53 (0.48)	−0.87 (−0.55)	5.15 (4.56)	10.80 (11.79)	0.50 (0.45)	−0.76 (−0.46)	4.21 (3.73)
^{177}Yb	22.13 (23.08)	0.54 (0.48)	−1.04 (−0.55)	5.33 (4.51)	11.19 (11.96)	0.51 (0.45)	−0.93 (−0.45)	4.42 (3.69)
^{176}Lu	21.26 (22.85)	0.50 (0.48)	−1.39 (−1.45)	3.64 (3.62)	10.78 (11.84)	0.45 (0.45)	−1.11 (−1.36)	2.44 (2.80)
^{177}Lu	21.47 (23.44)	0.54 (0.47)	−0.96 (−0.53)	5.23 (4.44)	10.65 (12.16)	0.50 (0.44)	−0.76 (−0.43)	4.19 (3.66)
^{175}Hf	22.98 (23.62)	0.53 (0.47)	−1.19 (−0.53)	5.44 (4.41)	11.88 (12.28)	0.50 (0.44)	−1.05 (−0.42)	4.54 (3.65)
^{177}Hf	23.02 (23.52)	0.53 (0.47)	−1.14 (−0.53)	5.38 (4.44)	11.93 (12.20)	0.49 (0.44)	−0.99 (−0.43)	4.46 (3.65)
^{178}Hf	23.15 (23.70)	0.54 (0.47)	−0.40 (0.37)	6.49 (5.31)	11.93 (12.29)	0.51 (0.44)	−0.24 (0.47)	5.54 (4.53)
^{179}Hf	22.73 (23.57)	0.52 (0.47)	−1.05 (−0.53)	5.27 (4.44)	11.63 (12.21)	0.49 (0.44)	−0.86 (−0.44)	4.28 (3.64)
^{180}Hf	22.41 (23.60)	0.56 (0.47)	−0.60 (0.36)	6.84 (5.33)	11.31 (12.22)	0.54 (0.44)	−0.46 (0.46)	5.83 (4.53)
^{181}Hf	23.15 (23.56)	0.46 (0.47)	−0.36 (−0.54)	4.21 (4.45)	11.87 (12.19)	0.43 (0.44)	−0.28 (−0.44)	3.39 (3.64)
^{181}Ta	23.41 (23.43)	0.36 (0.47)	0.46 (−0.54)	2.79 (4.45)	12.14 (12.11)	0.30 (0.44)	0.62 (−0.44)	1.83 (3.64)
^{182}Ta	21.39 (23.25)	0.50 (0.47)	−1.33 (−1.43)	3.57 (3.60)	10.76 (12.00)	0.44 (0.44)	−1.08 (−1.34)	2.37 (2.76)
^{183}Ta	22.01 (23.81)	0.47 (0.46)	−0.24 (−0.53)	4.08 (4.41)	11.10 (12.31)	0.42 (0.43)	−0.11 (−0.43)	3.12 (3.60)
^{181}W	22.87 (23.48)	0.52 (0.47)	−1.09 (−0.54)	5.33 (4.45)	12.01 (12.14)	0.49 (0.44)	−0.92 (−0.44)	4.34 (3.64)
^{183}W	22.30 (23.31)	0.52 (0.47)	−0.92 (−0.55)	5.15 (4.49)	11.37 (12.03)	0.48 (0.44)	−0.74 (−0.45)	4.10 (3.65)
^{184}W	23.05 (23.56)	0.53 (0.47)	−0.34 (0.35)	6.41 (5.34)	11.93 (12.16)	0.50 (0.44)	−0.21 (0.44)	5.45 (4.51)
^{185}W	23.59 (23.70)	0.48 (0.47)	−0.71 (−0.54)	4.72 (4.44)	12.18 (12.23)	0.45 (0.44)	−0.56 (−0.44)	3.79 (3.61)

(*continued on next page*)

Table 10 (*continued*)

CTM	Effective model				Collective model			
Nuc	$a(S_n)$	T	E_0	E_M	$a(S_n)$	T	E_0	E_M
^{187}W	24.33 (23.88)	0.45 (0.46)	−0.46 (−0.53)	4.27 (4.42)	12.66 (12.31)	0.42 (0.44)	−0.30 (−0.44)	3.36 (3.59)
^{186}Re	22.06 (23.34)	0.48 (0.47)	−1.32 (−1.43)	3.54 (3.61)	11.29 (12.02)	0.43 (0.44)	−1.08 (−1.33)	2.35 (2.75)
^{188}Re	22.48 (23.44)	0.49 (0.47)	−1.50 (−1.42)	3.80 (3.61)	11.54 (12.06)	0.44 (0.44)	−1.25 (−1.33)	2.62 (2.74)
^{187}Os	23.47 (23.56)	0.52 (0.47)	−1.15 (−0.54)	5.41 (4.46)	12.21 (12.13)	0.49 (0.44)	−0.98 (−0.45)	4.39 (3.61)
^{188}Os	23.29 (23.25)	0.49 (0.47)	0.09 (0.32)	5.75 (5.39)	12.30 (11.95)	0.46 (0.45)	0.25 (0.42)	4.75 (4.50)
^{189}Os	23.78 (23.41)	0.51 (0.47)	−1.14 (−0.55)	5.39 (4.50)	12.44 (12.04)	0.48 (0.44)	−0.99 (−0.45)	4.40 (3.61)
^{190}Os	22.91 (22.92)	0.51 (0.48)	−0.08 (0.31)	6.07 (5.45)	12.04 (11.75)	0.48 (0.45)	0.09 (0.40)	4.98 (4.52)
^{191}Os	23.48 (22.84)	0.53 (0.48)	−1.30 (−0.57)	5.71 (4.61)	12.30 (11.70)	0.50 (0.46)	−1.16 (−0.48)	4.65 (3.65)
^{193}Os	22.98 (21.92)	0.43 (0.50)	−0.04 (−0.60)	3.74 (4.79)	12.08 (11.18)	0.39 (0.47)	0.05 (−0.52)	2.64 (3.72)
^{192}Ir	23.04 (22.67)	0.53 (0.49)	−2.10 (−1.44)	4.80 (3.77)	12.23 (11.60)	0.49 (0.46)	−1.88 (−1.35)	3.59 (2.80)
^{193}Ir	22.22 (22.14)	0.54 (0.50)	−1.16 (−0.60)	5.67 (4.75)	11.73 (11.30)	0.50 (0.47)	−0.97 (−0.51)	4.42 (3.71)
^{194}Ir	21.41 (21.52)	0.53 (0.51)	−1.72 (−1.48)	4.44 (4.03)	11.21 (10.95)	0.49 (0.48)	−1.48 (−1.40)	3.03 (2.90)
^{193}Pt	24.00 (22.32)	0.51 (0.49)	−1.12 (−0.59)	5.44 (4.71)	12.90 (11.40)	0.48 (0.47)	−1.00 (−0.50)	4.41 (3.69)
^{195}Pt	19.83 (20.94)	0.63 (0.52)	−1.81 (−0.64)	7.14 (5.03)	10.18 (10.62)	0.61 (0.50)	−1.70 (−0.57)	5.59 (3.81)
^{196}Pt	20.38 (20.15)	0.55 (0.55)	0.02 (0.18)	6.39 (6.14)	10.77 (10.18)	0.51 (0.52)	0.20 (0.24)	4.81 (4.77)
^{197}Pt	19.37 (19.61)	0.62 (0.56)	−1.49 (−0.70)	6.89 (5.42)	10.00 (9.88)	0.58 (0.53)	−1.24 (−0.65)	4.99 (3.96)
^{199}Pt	20.34 (18.30)	0.52 (0.59)	−0.51 (−0.78)	5.12 (5.92)	10.12 (9.14)	0.52 (0.57)	−0.53 (−0.73)	3.71 (4.16)
^{198}Au	18.51 (18.62)	0.62 (0.59)	−2.00 (−1.63)	5.80 (5.05)	9.67 (9.33)	0.57 (0.57)	−1.77 (−1.58)	3.64 (3.30)
^{199}Hg	19.22 (17.65)	0.59 (0.62)	−0.98 (−0.84)	6.39 (6.35)	10.44 (8.79)	0.54 (0.60)	−0.74 (−0.80)	4.16 (4.33)
^{200}Hg	17.14 (16.96)	0.68 (0.64)	−0.63 (−0.07)	8.93 (7.75)	9.00 (8.41)	0.65 (0.63)	−0.49 (−0.04)	6.32 (5.40)
^{201}Hg	16.92 (16.04)	0.61 (0.67)	−0.63 (−1.01)	6.39 (7.51)	8.37 (7.89)	0.61 (0.65)	−0.76 (−0.97)	4.29 (4.79)
^{202}Hg	16.11 (15.36)	0.70 (0.71)	−0.60 (−0.33)	9.86 (9.38)	8.57 (7.52)	0.67 (0.70)	−0.43 (−0.25)	6.45 (6.06)
^{204}Tl	14.32 (13.63)	0.68 (0.81)	−1.13 (−1.62)	6.78 (3.57)	7.43 (6.57)	0.60 (0.81)	−0.86 (−2.42)	3.78 (6.38)
^{206}Tl	10.35 (11.35)	0.84 (0.98)	−0.31 (−1.64)	3.56 (3.56)	4.84 (5.31)	0.76 (1.04)	−0.71 (−3.08)	3.90 (3.90)
^{205}Pb	13.61 (13.19)	0.69 (0.82)	−0.28 (−0.78)	7.93 (4.40)	6.86 (6.31)	0.64 (0.83)	−0.03 (−1.65)	5.89 (7.56)

Table 11
Local level density parameters $a(S_n)$, T, E_0 and E_M for CTM. For comparison, the values between brackets come from the global systematics

CTM	Effective model				Collective model			
Nuc	$a(S_n)$	T	E_0	E_M	$a(S_n)$	T	E_0	E_M
^{207}Pb	9.60 (10.47)	0.75 (1.04)	1.48 (−0.81)	1.32 (4.39)	3.66 (4.81)	0.63 (1.13)	1.59 (−2.60)	4.73 (4.73)
^{208}Pb	7.90 (9.84)	0.92 (1.11)	1.37 (0.01)	14.34 (5.21)	3.09 (4.46)	0.68 (1.22)	2.43 (−2.16)	5.55 (5.55)
^{209}Pb	10.22 (10.70)	0.62 (0.91)	1.40 (−0.79)	1.20 (4.37)	3.59 (4.86)	0.61 (0.94)	1.36 (−2.49)	4.71 (11.20)
^{210}Bi	11.85 (12.98)	0.74 (0.80)	−0.92 (−1.61)	7.05 (3.53)	5.24 (6.14)	0.67 (0.81)	−0.64 (−2.44)	3.87 (6.50)
^{227}Ra	32.98 (32.48)	0.40 (0.35)	−1.01 (−0.34)	4.46 (3.52)	16.95 (16.65)	0.38 (0.33)	−0.93 (−0.26)	3.84 (2.95)
^{229}Th	33.40 (31.67)	0.41 (0.36)	−1.37 (−0.35)	4.95 (3.58)	17.69 (16.18)	0.40 (0.34)	−1.27 (−0.28)	4.24 (2.97)
^{230}Th	30.34 (31.63)	0.43 (0.36)	−0.32 (0.44)	5.52 (4.36)	15.50 (16.14)	0.40 (0.33)	−0.21 (0.51)	4.75 (3.75)
^{231}Th	32.56 (32.02)	0.41 (0.35)	−1.15 (−0.35)	4.68 (3.55)	16.87 (16.36)	0.39 (0.33)	−1.05 (−0.27)	3.98 (2.95)
^{233}Th	33.26 (32.70)	0.38 (0.35)	−0.82 (−0.33)	4.19 (3.50)	17.14 (16.70)	0.36 (0.33)	−0.71 (−0.26)	3.53 (2.91)
^{233}Pa	28.01 (31.78)	0.47 (0.35)	−1.42 (−0.35)	5.26 (3.55)	13.86 (16.19)	0.44 (0.33)	−1.28 (−0.28)	4.32 (2.94)
^{233}U	30.76 (30.78)	0.41 (0.37)	−0.96 (−0.38)	4.52 (3.65)	15.95 (15.66)	0.38 (0.34)	−0.79 (−0.31)	3.67 (2.99)
^{234}U	30.29 (30.99)	0.41 (0.36)	−0.06 (0.42)	5.16 (4.42)	15.77 (15.76)	0.38 (0.34)	0.09 (0.48)	4.32 (3.76)
^{235}U	30.89 (31.31)	0.42 (0.36)	−1.09 (−0.36)	4.70 (3.61)	15.81 (15.93)	0.40 (0.34)	−1.02 (−0.30)	3.96 (2.96)
^{236}U	31.87 (31.57)	0.39 (0.36)	−0.08 (0.42)	5.09 (4.36)	16.54 (16.06)	0.37 (0.34)	0.08 (0.49)	4.31 (3.72)
^{237}U	31.34 (31.76)	0.39 (0.36)	−0.68 (−0.35)	4.08 (3.57)	16.01 (16.15)	0.36 (0.34)	−0.56 (−0.29)	3.34 (2.93)
^{238}U	31.95 (32.26)	0.39 (0.35)	−0.07 (0.44)	5.06 (4.30)	16.49 (16.42)	0.36 (0.33)	0.09 (0.50)	4.27 (3.68)
^{239}U	32.52 (32.58)	0.34 (0.35)	−0.28 (−0.34)	3.42 (3.50)	16.64 (16.58)	0.31 (0.33)	−0.14 (−0.27)	2.69 (2.89)
^{237}Np	26.80 (31.06)	0.49 (0.36)	−1.43 (−0.37)	5.39 (3.62)	13.05 (15.77)	0.46 (0.34)	−1.24 (−0.30)	4.30 (2.96)
^{238}Np	29.29 (30.95)	0.37 (0.36)	−1.07 (−1.15)	2.81 (2.86)	14.91 (15.70)	0.33 (0.34)	−0.86 (−1.08)	1.84 (2.18)
^{239}Np	30.70 (31.72)	0.42 (0.36)	−1.07 (−0.35)	4.66 (3.56)	15.89 (16.11)	0.39 (0.33)	−0.94 (−0.29)	3.83 (2.92)
^{239}Pu	29.70 (30.45)	0.41 (0.37)	−0.73 (−0.39)	4.25 (3.69)	15.21 (15.42)	0.38 (0.35)	−0.60 (−0.32)	3.40 (2.98)
^{240}Pu	30.93 (31.02)	0.41 (0.36)	−0.17 (0.40)	5.26 (4.41)	16.02 (15.72)	0.38 (0.34)	−0.02 (0.47)	4.42 (3.73)
^{241}Pu	31.13 (31.25)	0.40 (0.36)	−0.90 (−0.37)	4.42 (3.62)	15.99 (15.84)	0.38 (0.34)	−0.81 (−0.31)	3.66 (2.94)
^{242}Pu	32.37 (31.76)	0.38 (0.36)	0.03 (0.42)	4.89 (4.34)	16.83 (16.11)	0.36 (0.33)	0.13 (0.48)	4.17 (3.68)
^{243}Pu	32.20 (31.95)	0.36 (0.35)	−0.49 (−0.35)	3.75 (3.56)	16.65 (16.20)	0.34 (0.33)	−0.41 (−0.29)	3.08 (2.90)

(*continued on next page*)

Table 11 (*continued*)

CTM	Effective model				Collective model			
Nuc	$a(S_n)$	T	E_0	E_M	$a(S_n)$	T	E_0	E_M
^{245}Pu	33.04 (32.78)	0.32 (0.35)	−0.07 (−0.33)	3.07 (3.48)	16.93 (16.64)	0.29 (0.33)	0.05 (−0.27)	2.32 (2.86)
^{242}Am	29.03 (30.44)	0.36 (0.37)	−0.94 (−1.16)	2.63 (2.92)	14.84 (15.39)	0.31 (0.35)	−0.69 (−1.10)	1.50 (2.20)
^{243}Am	31.13 (31.20)	0.39 (0.36)	−0.74 (−0.37)	4.17 (3.61)	16.28 (15.79)	0.36 (0.34)	−0.60 (−0.31)	3.36 (2.93)
^{244}Am	29.35 (31.13)	0.34 (0.36)	−0.73 (−1.14)	2.28 (2.85)	14.89 (15.75)	0.28 (0.34)	−0.47 (−1.08)	1.06 (2.16)
^{243}Cm	28.42 (30.06)	0.35 (0.38)	0.04 (−0.40)	3.09 (3.73)	14.27 (15.18)	0.31 (0.35)	0.15 (−0.34)	2.14 (2.99)
^{244}Cm	29.68 (30.43)	0.38 (0.37)	0.30 (0.38)	4.62 (4.46)	15.28 (15.37)	0.35 (0.35)	0.42 (0.44)	3.77 (3.73)
^{245}Cm	29.70 (30.45)	0.41 (0.37)	−0.78 (−0.39)	4.34 (3.69)	15.18 (15.37)	0.38 (0.35)	−0.66 (−0.33)	3.45 (2.96)
^{246}Cm	29.53 (30.99)	0.42 (0.36)	−0.08 (0.39)	5.19 (4.41)	14.91 (15.65)	0.39 (0.34)	0.08 (0.45)	4.25 (3.70)
^{247}Cm	29.40 (31.23)	0.44 (0.36)	−1.15 (−0.37)	4.88 (3.62)	14.68 (15.77)	0.42 (0.34)	−1.03 (−0.31)	3.95 (2.92)
^{248}Cm	30.30 (31.76)	0.38 (0.36)	0.26 (0.40)	4.62 (4.33)	15.35 (16.05)	0.35 (0.34)	0.42 (0.46)	3.73 (3.65)
^{249}Cm	32.34 (32.39)	0.36 (0.35)	−0.50 (−0.34)	3.76 (3.52)	16.44 (16.38)	0.34 (0.33)	−0.41 (−0.29)	3.04 (2.86)
^{250}Bk	29.82 (31.56)	0.41 (0.36)	−1.51 (−1.12)	3.50 (2.83)	15.01 (15.93)	0.37 (0.34)	−1.32 (−1.07)	2.53 (2.13)
^{250}Cf	29.74 (30.22)	0.39 (0.37)	0.16 (0.36)	4.82 (4.48)	15.28 (15.20)	0.36 (0.35)	0.31 (0.41)	3.86 (3.71)
^{251}Cf	31.95 (30.80)	0.39 (0.37)	−0.80 (−0.38)	4.25 (3.67)	16.64 (15.51)	0.37 (0.35)	−0.73 (−0.33)	3.49 (2.92)

Table 12
Local level density parameters $a(S_n)$, and δ for BFM. For comparison, the values between brackets come from the global systematics

BFM	Effective model		Collective model			Effective model		Collective model	
Nuc	$a(S_n)$	δ	$a(S_n)$	δ	Nuc	$a(S_n)$	δ	$a(S_n)$	δ
^{24}Na	3.34 (3.18)	1.89	1.97 (1.68)	2.47	^{71}Zn	11.13 (10.58)	0.68	6.11 (5.93)	0.97
^{25}Mg	2.89 (3.06)	−1.04	1.61 (1.59)	−0.58	^{70}Ga	8.74 (9.66)	0.21	4.70 (5.29)	0.91
^{26}Mg	3.21 (3.43)	−0.96	1.73 (1.82)	−0.81	^{72}Ga	9.63 (10.60)	−0.29	5.08 (5.90)	0.14
^{27}Mg	4.16 (3.54)	1.59	2.93 (1.87)	2.31	^{71}Ge	10.39 (10.41)	−0.49	5.70 (5.79)	−0.22
^{28}Al	3.30 (3.26)	0.06	1.89 (1.69)	0.80	^{73}Ge	10.04 (11.04)	−0.98	5.39 (6.20)	−0.73
^{29}Si	3.46 (2.75)	0.81	2.16 (1.34)	1.73	^{74}Ge	10.43 (10.66)	−0.18	5.43 (5.90)	0.09
^{30}Si	2.53 (3.36)	−2.46	1.47 (1.72)	−1.05	^{75}Ge	10.02 (11.08)	−0.45	5.28 (6.20)	−0.15
^{32}P	3.47 (3.43)	0.83	2.03 (1.75)	1.84	^{77}Ge	10.38 (10.84)	−0.21	5.59 (6.02)	0.14
^{33}S	3.41 (3.57)	−1.08	1.90 (1.82)	−0.37	^{76}As	11.02 (11.19)	0.00	5.93 (6.22)	0.41
^{34}S	3.68 (4.05)	−0.95	2.11 (2.11)	−0.21	^{75}Se	10.73 (11.14)	−0.73	5.81 (6.21)	−0.47
^{35}S	4.01 (4.39)	−0.55	2.38 (2.31)	0.31	^{77}Se	11.06 (11.47)	−0.39	5.92 (6.42)	−0.11
^{36}Cl	3.78 (4.19)	0.06	2.13 (2.18)	1.17	^{78}Se	10.74 (11.09)	−0.19	5.69 (6.12)	0.08
^{38}Cl	5.93 (5.29)	2.38	3.28 (2.86)	2.77	^{79}Se	9.84 (11.43)	−0.87	5.14 (6.37)	−0.54
^{41}Ar	6.77 (6.70)	0.86	3.99 (3.76)	1.18	^{81}Se	11.38 (10.85)	0.56	5.63 (5.96)	0.85
^{40}K	4.54 (5.23)	0.13	2.50 (2.79)	1.07	^{83}Se	11.64 (10.28)	0.61	6.37 (5.56)	0.95
^{42}K	4.81 (6.26)	−1.12	2.11 (3.43)	−1.36	^{80}Br	10.73 (11.44)	−0.45	5.73 (6.33)	−0.06
^{41}Ca	5.41 (5.22)	0.33	3.17 (2.78)	0.90	^{82}Br	11.01 (10.90)	0.47	5.95 (5.96)	1.01
^{43}Ca	6.35 (6.35)	−0.18	3.60 (3.48)	0.07	^{79}Kr	11.03 (11.50)	−0.77	5.92 (6.39)	−0.51
^{44}Ca	6.07 (6.48)	−0.46	3.26 (3.54)	−0.26	^{81}Kr	11.70 (11.62)	−0.39	6.40 (6.45)	−0.13
^{45}Ca	6.37 (6.62)	0.07	3.64 (3.64)	0.49	^{84}Kr	9.14 (10.58)	−0.05	4.49 (5.72)	0.50
^{46}Sc	5.98 (6.40)	−0.03	3.20 (3.47)	0.39	^{85}Kr	12.11 (10.40)	0.63	6.87 (5.60)	1.07
^{47}Ti	5.21 (6.25)	−0.89	2.81 (3.37)	−0.35	^{86}Rb	9.24 (10.02)	0.44	4.87 (5.34)	1.22
^{48}Ti	5.62 (6.32)	−1.13	3.04 (3.40)	−0.74	^{88}Rb	9.54 (9.92)	0.66	5.06 (5.24)	1.45
^{49}Ti	5.92 (6.27)	−0.65	3.31 (3.35)	−0.11	^{85}Sr	11.17 (11.11)	−0.05	6.09 (6.06)	0.37
^{50}Ti	5.57 (6.06)	−0.37	2.98 (3.21)	0.25	^{87}Sr	9.56 (10.10)	0.65	5.01 (5.38)	1.35

(*continued on next page*)

Table 12 (*continued*)

BFM	Effective model		Collective model			Effective model		Collective model	
Nuc	$a(S_n)$	δ	$a(S_n)$	δ	Nuc	$a(S_n)$	δ	$a(S_n)$	δ
^{51}Ti	4.99 (6.21)	−0.31	2.70 (3.29)	0.64	^{88}Sr	9.25 (9.28)	0.94	4.72 (4.83)	1.71
^{51}V	6.00 (6.10)	0.43	3.00 (3.23)	0.88	^{89}Sr	9.98 (9.63)	1.42	5.15 (5.03)	2.05
^{52}V	6.19 (6.20)	0.59	3.33 (3.27)	1.20	^{90}Y	8.94 (9.55)	0.97	4.60 (4.97)	1.81
^{51}Cr	5.70 (5.89)	−0.41	3.20 (3.08)	0.29	^{91}Zr	9.58 (9.65)	0.41	5.14 (5.02)	1.15
^{53}Cr	5.27 (6.03)	−0.83	2.89 (3.15)	0.04	^{92}Zr	9.95 (10.62)	−0.04	5.00 (5.66)	0.40
^{54}Cr	5.52 (6.54)	−1.15	2.94 (3.47)	−0.44	^{93}Zr	11.08 (11.08)	0.51	5.92 (5.95)	1.07
^{55}Cr	6.47 (7.03)	−0.04	3.55 (3.78)	0.63	^{94}Zr	12.52 (11.86)	0.29	6.67 (6.46)	0.60
^{56}Mn	6.27 (6.59)	−0.45	3.41 (3.48)	0.24	^{95}Zr	11.99 (12.06)	0.84	5.97 (6.58)	1.29
^{55}Fe	5.21 (5.41)	−1.15	2.94 (2.73)	−0.22	^{94}Nb	11.71 (11.23)	0.69	6.23 (6.03)	1.22
^{57}Fe	6.22 (6.33)	−0.23	3.43 (3.29)	0.47	^{93}Mo	9.15 (9.45)	−0.10	4.96 (4.87)	0.73
^{58}Fe	6.02 (6.85)	−1.11	3.22 (3.62)	−0.46	^{95}Mo	10.96 (11.00)	0.02	5.93 (5.87)	0.56
^{59}Fe	7.09 (7.38)	−0.19	3.86 (3.95)	0.32	^{96}Mo	11.41 (11.76)	−0.08	6.02 (6.35)	0.32
^{60}Co	7.16 (7.02)	0.26	3.90 (3.71)	0.93	^{97}Mo	11.96 (12.40)	−0.13	6.36 (6.78)	0.30
^{59}Ni	5.64 (5.69)	−1.15	3.07 (2.86)	−0.35	^{98}Mo	12.52 (13.04)	−0.19	6.52 (7.18)	0.16
^{60}Ni	5.72 (6.24)	−1.42	3.15 (3.21)	−0.58	^{99}Mo	13.39 (13.99)	−0.27	7.08 (7.83)	0.04
^{61}Ni	6.77 (6.76)	−0.27	3.76 (3.52)	0.39	^{101}Mo	13.93 (15.34)	−0.73	7.70 (8.73)	−0.42
^{62}Ni	6.20 (7.15)	−1.30	3.33 (3.76)	−0.59	^{100}Tc	14.46 (13.64)	0.22	7.80 (7.55)	0.63
^{63}Ni	7.87 (7.73)	0.28	4.35 (4.13)	0.82	^{100}Ru	12.27 (12.35)	−0.34	6.60 (6.69)	0.09
^{65}Ni	8.64 (8.59)	0.38	4.79 (4.68)	0.87	^{102}Ru	13.66 (13.58)	−0.11	7.28 (7.48)	0.22
^{64}Cu	7.87 (7.62)	0.60	4.42 (4.04)	1.28	^{103}Ru	13.03 (14.55)	−0.81	6.81 (8.15)	−0.48
^{66}Cu	8.10 (8.45)	0.41	4.34 (4.56)	1.04	^{105}Ru	15.23 (15.40)	−0.37	8.13 (8.70)	−0.10
^{65}Zn	7.96 (8.15)	−0.59	4.39 (4.38)	−0.09	^{104}Rh	14.58 (14.04)	0.28	7.91 (7.76)	0.71
^{67}Zn	8.60 (9.15)	−0.50	4.48 (5.01)	−0.16	^{105}Pd	13.10 (13.54)	−0.60	7.04 (7.43)	−0.23
^{68}Zn	8.65 (9.24)	−0.01	4.56 (5.05)	0.44	^{106}Pd	14.09 (13.78)	−0.01	7.56 (7.55)	0.34
^{69}Zn	9.04 (9.89)	−0.30	4.81 (5.49)	0.10	^{107}Pd	14.22 (14.71)	−0.41	7.57 (8.19)	−0.08

Table 13
Local level density parameters $a(S_n)$, and δ for BFM. For comparison, the values between brackets come from the global systematics

BFM	Effective model		Collective model			Effective model		Collective model	
Nuc	$a(S_n)$	δ	$a(S_n)$	δ	Nuc	$a(S_n)$	δ	$a(S_n)$	δ
^{108}Pd	14.66 (14.66)	0.05	7.73 (8.12)	0.37	^{140}La	14.17 (14.01)	0.38	7.41 (7.25)	0.97
^{109}Pd	14.68 (15.50)	−0.91	7.85 (8.71)	−0.64	^{137}Ce	16.80 (15.54)	0.33	9.13 (8.33)	0.74
^{111}Pd	16.95 (16.06)	−0.34	9.29 (9.07)	−0.10	^{141}Ce	15.48 (14.40)	0.84	8.16 (7.50)	1.38
^{108}Ag	14.59 (14.13)	0.10	7.95 (7.76)	0.55	^{142}Ce	15.09 (15.26)	0.02	7.58 (8.08)	0.43
^{110}Ag	16.12 (15.05)	0.26	8.84 (8.35)	0.65	^{143}Ce	15.64 (16.09)	0.13	7.75 (8.62)	0.50
^{107}Cd	12.95 (12.40)	−0.35	7.16 (6.63)	0.09	^{142}Pr	14.40 (15.16)	0.43	7.22 (8.01)	1.01
^{109}Cd	14.38 (13.59)	−0.12	7.86 (7.41)	0.24	^{143}Nd	15.97 (15.26)	0.75	8.50 (8.06)	1.31
^{111}Cd	14.67 (14.46)	−0.23	7.90 (7.96)	0.12	^{144}Nd	15.74 (16.10)	0.26	8.23 (8.61)	0.77
^{112}Cd	15.06 (14.50)	0.10	7.96 (7.96)	0.42	^{145}Nd	17.05 (16.98)	0.26	8.98 (9.20)	0.70
^{113}Cd	14.99 (15.18)	−0.31	8.03 (8.42)	0.03	^{146}Nd	16.72 (17.60)	−0.17	8.64 (9.60)	0.21
^{114}Cd	15.13 (15.01)	0.08	7.87 (8.27)	0.38	^{147}Nd	18.18 (18.62)	−0.11	9.37 (10.30)	0.22
^{115}Cd	15.95 (15.59)	−0.06	8.53 (8.68)	0.25	^{148}Nd	20.05 (19.01)	−0.19	10.51 (10.53)	0.05
^{117}Cd	15.22 (15.69)	−0.42	8.09 (8.73)	−0.08	^{149}Nd	18.94 (19.94)	−0.62	10.01 (11.18)	−0.32
^{114}In	14.32 (14.59)	0.47	7.51 (7.99)	1.00	^{151}Nd	18.58 (20.00)	−0.44	9.63 (11.19)	−0.10
^{116}In	15.73 (15.11)	0.54	8.36 (8.32)	0.99	^{148}Pm	19.21 (18.95)	0.34	10.14 (10.48)	0.78
^{113}Sn	13.99 (13.33)	0.33	7.38 (7.17)	0.72	^{145}Sm	14.91 (15.65)	0.62	7.69 (8.30)	1.22
^{115}Sn	14.68 (13.74)	0.79	7.38 (7.42)	1.19	^{148}Sm	17.91 (18.12)	0.06	9.36 (9.92)	0.44
^{117}Sn	14.88 (14.33)	0.60	7.95 (7.80)	1.05	^{149}Sm	18.66 (19.20)	−0.16	9.79 (10.66)	0.20
^{118}Sn	13.92 (14.17)	0.19	7.38 (7.67)	0.62	^{150}Sm	18.63 (19.53)	−0.24	9.54 (10.84)	0.05
^{119}Sn	14.59 (14.59)	0.17	7.82 (7.94)	0.62	^{151}Sm	19.67 (20.56)	−0.64	10.40 (11.56)	−0.35
^{120}Sn	13.53 (14.14)	0.19	7.13 (7.62)	0.71	^{152}Sm	19.45 (20.09)	−0.54	10.26 (11.18)	−0.26
^{121}Sn	12.81 (14.37)	−0.15	6.47 (7.77)	0.35	^{153}Sm	18.43 (20.44)	−0.88	9.58 (11.44)	−0.57
^{125}Sn	12.85 (12.59)	0.54	6.66 (6.50)	1.09	^{155}Sm	18.46 (19.90)	−0.29	9.48 (11.05)	0.06
^{122}Sb	14.76 (15.01)	−0.07	7.88 (8.17)	0.40	^{152}Eu	21.26 (20.67)	−0.01	11.41 (11.57)	0.35
^{124}Sb	13.85 (14.46)	−0.29	7.35 (7.78)	0.22	^{153}Eu	18.02 (20.29)	−0.47	9.24 (11.27)	−0.14

(*continued on next page*)

Table 13 (*continued*)

BFM	Effective model		Collective model			Effective model		Collective model	
Nuc	$a(S_n)$	δ	$a(S_n)$	δ	Nuc	$a(S_n)$	δ	$a(S_n)$	δ
^{123}Te	15.26 (15.44)	−0.18	8.13 (8.46)	0.20	^{154}Eu	20.22 (20.35)	−0.04	10.73 (11.32)	0.36
^{124}Te	15.40 (14.90)	0.19	8.34 (8.07)	0.60	^{155}Eu	18.26 (20.03)	−0.32	9.40 (11.08)	0.03
^{125}Te	14.95 (15.02)	−0.40	8.04 (8.15)	−0.03	^{156}Eu	18.80 (19.74)	0.19	9.71 (10.89)	0.64
^{126}Te	14.67 (14.32)	0.12	7.79 (7.66)	0.50	^{153}Gd	19.95 (20.70)	−0.71	10.59 (11.60)	−0.44
^{127}Te	13.79 (14.20)	−0.37	7.15 (7.57)	0.05	^{155}Gd	19.48 (20.62)	−0.73	10.27 (11.52)	−0.43
^{129}Te	13.73 (12.96)	−0.30	7.49 (6.70)	0.15	^{156}Gd	18.80 (20.15)	−0.51	9.81 (11.16)	−0.19
^{131}Te	13.37 (11.29)	0.12	7.54 (5.54)	0.69	^{157}Gd	18.94 (20.18)	−0.51	9.89 (11.19)	−0.17
^{128}I	14.36 (14.75)	−0.24	7.70 (7.92)	0.28	^{158}Gd	18.12 (19.98)	−0.64	9.31 (11.03)	−0.33
^{130}I	13.04 (13.80)	−0.54	6.99 (7.27)	0.06	^{159}Gd	18.65 (19.99)	−0.33	9.63 (11.05)	0.03
^{129}Xe	13.75 (15.17)	−0.52	7.10 (8.19)	−0.06	^{161}Gd	18.05 (19.83)	−0.26	9.23 (10.91)	0.16
^{130}Xe	14.23 (14.53)	−0.07	7.63 (7.75)	0.45	^{160}Tb	19.17 (19.93)	0.10	10.02 (10.96)	0.55
^{131}Xe	14.99 (14.34)	−0.15	8.11 (7.61)	0.27	^{157}Dy	20.60 (20.67)	−0.50	11.03 (11.51)	−0.21
^{132}Xe	13.20 (13.59)	−0.22	7.09 (7.10)	0.35	^{159}Dy	18.33 (20.45)	−0.59	9.64 (11.34)	−0.22
^{133}Xe	13.80 (13.05)	0.08	7.51 (6.71)	0.62	^{161}Dy	18.86 (20.30)	−0.55	9.84 (11.22)	−0.20
^{135}Xe	13.77 (11.32)	0.77	7.62 (5.51)	1.38	^{162}Dy	18.20 (20.02)	−0.62	9.37 (11.00)	−0.29
^{137}Xe	15.35 (11.06)	0.67	8.54 (5.23)	1.16	^{163}Dy	17.78 (19.90)	−0.62	9.16 (10.92)	−0.23
^{134}Cs	13.44 (14.00)	−0.37	7.20 (7.35)	0.23	^{164}Dy	17.37 (19.81)	−0.78	8.86 (10.84)	−0.41
^{131}Ba	15.56 (16.00)	−0.24	8.25 (8.72)	0.15	^{165}Dy	18.06 (19.87)	−0.40	9.26 (10.89)	−0.01
^{133}Ba	15.36 (15.42)	−0.17	8.13 (8.31)	0.22	^{166}Ho	18.89 (19.68)	0.22	9.77 (10.72)	0.69
^{135}Ba	13.92 (14.46)	−0.09	7.23 (7.63)	0.36	^{163}Er	20.13 (20.76)	−0.45	10.64 (11.49)	−0.12
^{136}Ba	13.39 (13.75)	−0.17	7.22 (7.15)	0.43	^{165}Er	18.73 (20.51)	−0.62	9.73 (11.30)	−0.26
^{137}Ba	13.65 (13.00)	0.82	7.20 (6.63)	1.41	^{167}Er	18.67 (20.04)	−0.43	9.73 (10.96)	−0.03
^{138}Ba	12.15 (12.33)	0.35	6.43 (6.17)	1.08	^{168}Er	17.90 (20.04)	−0.62	9.10 (10.94)	−0.27
^{139}Ba	12.93 (13.02)	0.47	6.66 (6.57)	1.14	^{169}Er	18.24 (20.00)	−0.36	9.36 (10.91)	0.05
^{139}La	12.26 (13.33)	0.07	6.40 (6.85)	0.81	^{171}Er	18.59 (20.07)	−0.26	9.56 (10.93)	0.15

Table 14
Local level density parameters $a(S_n)$, and δ for BFM. For comparison, the values between brackets come from the global systematics

BFM	Effective model		Collective model			Effective model		Collective model	
Nuc	$a(S_n)$	δ	$a(S_n)$	δ	Nuc	$a(S_n)$	δ	$a(S_n)$	δ
^{170}Tm	19.09 (19.86)	0.24	9.97 (10.79)	0.73	^{200}Hg	14.93 (15.60)	−0.49	8.09 (7.51)	0.26
^{171}Tm	18.95 (20.09)	−0.17	9.89 (10.93)	0.24	^{201}Hg	13.93 (14.85)	−0.45	7.08 (6.95)	0.21
^{169}Yb	20.49 (20.66)	−0.28	10.81 (11.34)	0.07	^{202}Hg	13.79 (14.27)	−0.75	7.50 (6.57)	0.11
^{170}Yb	18.10 (20.48)	−0.60	9.27 (11.20)	−0.19	^{204}Tl	13.44 (12.82)	0.26	7.12 (5.60)	1.15
^{171}Yb	18.63 (20.41)	−0.41	9.61 (11.15)	−0.02	^{206}Tl	9.73 (10.92)	−0.02	4.55 (4.28)	1.21
^{172}Yb	18.99 (20.33)	−0.54	9.97 (11.08)	−0.15	^{205}Pb	12.63 (12.47)	0.07	6.42 (5.31)	0.95
^{173}Yb	17.89 (20.10)	−0.45	9.14 (10.92)	−0.02	^{207}Pb	10.21 (10.19)	1.31	4.20 (3.73)	2.32
^{174}Yb	18.99 (20.25)	−0.13	9.76 (11.00)	0.27	^{208}Pb	9.07 (9.67)	0.97	3.23 (3.35)	2.18
^{175}Yb	17.98 (20.23)	−0.35	9.11 (10.98)	0.09	^{209}Pb	9.67 (10.46)	0.82	2.75 (3.66)	1.74
^{177}Yb	18.09 (20.53)	−0.47	9.18 (11.16)	−0.05	^{210}Bi	10.76 (12.35)	−0.05	5.08 (5.07)	1.13
^{176}Lu	19.62 (20.34)	0.25	10.24 (11.03)	0.76	^{227}Ra	26.45 (28.93)	−0.40	13.52 (16.23)	−0.11
^{177}Lu	18.71 (20.84)	−0.21	9.36 (11.36)	0.22	^{229}Th	27.22 (28.27)	−0.60	14.23 (15.72)	−0.32
^{175}Hf	19.39 (20.97)	−0.46	10.08 (11.47)	−0.08	^{230}Th	24.68 (28.25)	−0.67	12.83 (15.67)	−0.38
^{177}Hf	19.39 (20.90)	−0.38	10.03 (11.41)	0.02	^{231}Th	26.74 (28.58)	−0.41	13.86 (15.91)	−0.11
^{178}Hf	19.52 (21.06)	−0.46	10.13 (11.50)	−0.07	^{233}Th	27.35 (29.17)	−0.32	14.06 (16.30)	−0.04
^{179}Hf	19.12 (20.96)	−0.38	9.84 (11.42)	0.03	^{233}Pa	23.53 (28.41)	−0.56	11.76 (15.72)	−0.21
^{180}Hf	18.53 (21.00)	−0.58	9.42 (11.43)	−0.17	^{233}U	26.11 (27.56)	−0.33	13.64 (15.16)	0.00
^{181}Hf	20.03 (20.98)	−0.08	10.30 (11.41)	0.28	^{234}U	25.37 (27.75)	−0.49	13.02 (15.27)	−0.22
^{181}Ta	21.92 (20.87)	0.47	11.50 (11.32)	0.85	^{235}U	25.21 (28.02)	−0.51	12.95 (15.46)	−0.18
^{182}Ta	19.72 (20.73)	0.25	10.19 (11.21)	0.74	^{236}U	26.62 (28.25)	−0.43	13.78 (15.59)	−0.17
^{183}Ta	19.78 (21.21)	0.12	9.62 (11.52)	0.46	^{237}U	26.51 (28.42)	−0.23	13.61 (15.71)	0.09
^{181}W	20.23 (20.91)	−0.34	10.14 (11.35)	0.01	^{238}U	26.35 (28.86)	−0.46	13.28 (15.99)	−0.20
^{183}W	19.06 (20.79)	−0.29	9.81 (11.25)	0.12	^{239}U	28.89 (29.13)	0.15	14.79 (16.18)	0.43
^{184}W	19.43 (21.01)	−0.46	10.14 (11.38)	−0.05	^{237}Np	22.52 (27.84)	−0.57	11.09 (15.28)	−0.17
^{185}W	20.25 (21.13)	−0.15	10.40 (11.46)	0.24	^{238}Np	27.35 (27.75)	0.30	14.25 (15.21)	0.68

(*continued on next page*)

Table 14 (*continued*)

BFM	Effective model		Collective model			Effective model		Collective model	
Nuc	$a(S_n)$	δ	$a(S_n)$	δ	Nuc	$a(S_n)$	δ	$a(S_n)$	δ
^{187}W	21.25 (21.30)	0.01	11.09 (11.55)	0.36	^{239}Np	26.11 (28.41)	−0.41	13.50 (15.65)	−0.09
^{186}Re	20.18 (20.85)	0.26	10.60 (11.24)	0.75	^{239}Pu	25.52 (27.33)	−0.23	13.15 (14.92)	0.09
^{188}Re	20.62 (20.95)	0.21	10.84 (11.28)	0.67	^{240}Pu	25.81 (27.82)	−0.47	13.44 (15.24)	−0.15
^{187}Os	19.72 (21.04)	−0.45	10.34 (11.36)	−0.05	^{241}Pu	26.05 (28.03)	−0.33	13.46 (15.38)	−0.01
^{188}Os	20.46 (20.78)	−0.17	10.67 (11.17)	0.22	^{242}Pu	27.20 (28.47)	−0.36	14.21 (15.66)	−0.06
^{189}Os	20.09 (20.93)	−0.33	10.58 (11.26)	0.06	^{243}Pu	27.27 (28.64)	−0.12	13.24 (15.78)	0.16
^{190}Os	20.08 (20.52)	−0.21	10.65 (10.97)	0.18	^{245}Pu	29.92 (29.36)	0.24	15.32 (16.25)	0.49
^{191}Os	19.14 (20.47)	−0.59	10.10 (10.91)	−0.16	^{242}Am	27.23 (27.35)	0.32	14.29 (14.88)	0.72
^{193}Os	20.64 (19.72)	0.16	10.93 (10.37)	0.52	^{243}Am	27.08 (28.01)	−0.25	14.27 (15.32)	0.06
^{192}Ir	20.16 (20.33)	−0.26	10.92 (10.81)	0.22	^{244}Am	28.38 (27.96)	0.54	14.72 (15.27)	0.90
^{193}Ir	19.37 (19.90)	−0.38	10.41 (10.51)	0.06	^{243}Cm	25.25 (27.04)	0.16	12.55 (14.67)	0.53
^{194}Ir	19.41 (19.39)	0.07	10.43 (10.15)	0.60	^{244}Cm	25.56 (27.36)	−0.30	13.07 (14.87)	−0.06
^{193}Pt	20.10 (20.05)	−0.49	10.91 (10.60)	−0.07	^{245}Cm	25.07 (27.39)	−0.28	12.76 (14.88)	0.09
^{195}Pt	16.15 (18.92)	−0.83	8.37 (9.80)	−0.24	^{246}Cm	25.21 (27.86)	−0.30	12.83 (15.18)	0.04
^{196}Pt	17.78 (18.25)	−0.32	9.42 (9.35)	0.13	^{247}Cm	24.04 (28.06)	−0.50	12.14 (15.32)	−0.11
^{197}Pt	16.17 (17.82)	−0.59	8.48 (9.02)	0.00	^{248}Cm	25.85 (28.52)	−0.27	12.94 (15.62)	0.02
^{199}Pt	16.61 (16.74)	−0.20	8.57 (8.24)	0.32	^{249}Cm	27.67 (29.06)	−0.07	13.80 (15.99)	0.22
^{198}Au	16.71 (16.98)	−0.07	9.06 (8.47)	0.59	^{250}Bk	26.78 (28.38)	0.06	13.84 (15.48)	0.48
^{199}Hg	16.59 (16.18)	−0.47	9.00 (7.90)	0.12	^{250}Cf	25.69 (27.24)	−0.24	13.13 (14.70)	0.04

Table 15
Local level density parameters $a(S_n)$, and δ for GSM. For comparison, the values between brackets come from the global systematics

GSM	Effective model		Collective model			Effective model		Collective model	
Nuc	$a(S_n)$	δ	$a(S_n)$	δ	Nuc	$a(S_n)$	δ	$a(S_n)$	δ
^{24}Na	3.06 (2.74)	−0.61	2.27 (1.86)	−2.24	^{71}Zn	13.76 (11.37)	0.79	6.24 (6.67)	0.03
^{25}Mg	2.83 (2.63)	1.34	1.70 (1.76)	−0.27	^{70}Ga	9.45 (9.95)	1.28	5.51 (5.81)	0.01
^{26}Mg	3.09 (2.99)	1.66	1.64 (2.01)	−0.57	^{72}Ga	9.59 (11.24)	2.02	5.91 (6.56)	0.77
^{27}Mg	4.09 (3.09)	0.03	2.53 (2.06)	−1.41	^{71}Ge	10.79 (11.02)	2.13	5.84 (6.45)	1.13
^{28}Al	3.24 (2.85)	0.37	2.25 (1.88)	−1.53	^{73}Ge	10.13 (11.93)	2.68	5.54 (6.97)	1.51
^{29}Si	2.96 (2.42)	0.00	1.92 (1.53)	−1.41	^{74}Ge	10.84 (11.23)	1.74	5.15 (6.52)	0.40
^{30}Si	2.84 (2.94)	1.59	1.61 (1.90)	−0.95	^{75}Ge	10.39 (11.94)	1.99	5.54 (6.95)	0.93
^{32}P	3.25 (3.05)	−0.30	2.29 (1.95)	−2.40	^{77}Ge	10.78 (11.55)	1.71	5.73 (6.69)	0.63
^{33}S	3.13 (3.15)	1.64	1.97 (2.01)	−0.39	^{76}As	11.24 (11.94)	1.81	6.67 (6.91)	0.71
^{34}S	3.56 (3.62)	1.47	1.99 (2.32)	−0.81	^{75}Se	10.97 (11.93)	2.48	5.89 (6.93)	1.39
^{35}S	3.75 (3.96)	1.66	2.31 (2.53)	0.22	^{77}Se	11.60 (12.40)	1.96	6.05 (7.18)	0.98
^{36}Cl	3.64 (3.78)	0.46	2.44 (2.40)	−1.40	^{78}Se	11.22 (11.73)	1.66	5.46 (6.76)	0.42
^{38}Cl	5.85 (4.94)	−0.60	3.85 (3.14)	−1.69	^{79}Se	9.88 (12.30)	2.38	5.41 (7.10)	1.18
^{41}Ar	7.75 (6.70)	1.00	3.93 (4.26)	0.03	^{81}Se	12.95 (11.42)	0.79	6.23 (6.55)	−0.07
^{40}K	4.43 (4.85)	0.74	3.03 (3.05)	−1.07	^{83}Se	13.09 (10.57)	0.70	6.55 (6.02)	−0.16
^{42}K	4.58 (6.02)	2.19	3.04 (3.79)	0.47	^{80}Br	10.77 (12.17)	2.21	6.36 (6.99)	1.03
^{41}Ca	5.15 (4.84)	1.15	3.18 (3.03)	−0.46	^{82}Br	11.17 (11.39)	1.13	6.55 (6.51)	0.01
^{43}Ca	8.76 (6.15)	1.61	3.49 (3.86)	0.74	^{79}Kr	11.65 (12.33)	2.39	6.10 (7.10)	1.37
^{44}Ca	5.85 (6.27)	2.21	3.05 (3.91)	0.26	^{81}Kr	12.31 (12.47)	1.93	6.49 (7.16)	1.02
^{45}Ca	6.12 (6.47)	1.71	3.65 (4.03)	0.33	^{84}Kr	9.82 (10.90)	1.26	4.86 (6.19)	−0.40
^{46}Sc	5.79 (6.14)	1.61	3.65 (3.80)	0.18	^{85}Kr	13.48 (10.67)	0.80	6.84 (6.05)	−0.13
^{47}Ti	5.05 (5.97)	2.04	2.89 (3.68)	0.40	^{86}Rb	9.04 (10.12)	0.83	5.22 (5.71)	−0.61
^{48}Ti	5.42 (6.04)	2.45	2.87 (3.71)	0.51	^{88}Rb	9.25 (9.94)	0.62	5.63 (5.58)	−0.79
^{49}Ti	5.66 (5.97)	1.99	3.40 (3.65)	0.31	^{85}Sr	11.37 (11.62)	1.58	6.09 (6.61)	0.48
^{50}Ti	5.34 (5.72)	1.51	2.82 (3.48)	−0.76	^{87}Sr	9.37 (10.21)	0.62	4.93 (5.75)	−0.79

(*continued on next page*)

Table 15 (*continued*)

GSM	Effective model		Collective model			Effective model		Collective model	
Nuc	$a(S_n)$	δ	$a(S_n)$	δ	Nuc	$a(S_n)$	δ	$a(S_n)$	δ
^{51}Ti	5.10 (5.87)	1.06	2.69 (3.56)	−0.72	^{88}Sr	8.98 (9.15)	0.25	4.37 (5.12)	−1.73
^{51}V	5.69 (5.77)	0.86	2.94 (3.50)	−0.81	^{89}Sr	9.86 (9.52)	−0.21	5.04 (5.32)	−1.55
^{52}V	5.89 (5.86)	0.73	3.78 (3.54)	−0.80	^{90}Y	8.59 (9.43)	0.16	5.05 (5.26)	−1.32
^{51}Cr	5.46 (5.52)	1.55	3.24 (3.33)	−0.25	^{91}Zr	9.20 (9.53)	0.82	5.03 (5.30)	−0.70
^{53}Cr	5.08 (5.65)	1.59	3.00 (3.39)	−0.26	^{92}Zr	9.89 (10.81)	1.23	4.76 (6.05)	−0.28
^{54}Cr	5.33 (6.24)	2.13	2.79 (3.75)	−0.12	^{93}Zr	11.18 (11.42)	0.83	5.86 (6.39)	−0.37
^{55}Cr	6.15 (6.83)	1.41	3.59 (4.11)	−0.20	^{94}Zr	13.68 (12.50)	1.01	6.31 (7.02)	−0.18
^{56}Mn	6.03 (6.28)	1.65	3.92 (3.75)	−0.06	^{95}Zr	13.32 (12.78)	0.44	6.27 (7.17)	−0.57
^{55}Fe	4.90 (4.99)	1.90	3.00 (2.94)	−0.25	^{94}Nb	11.97 (11.59)	0.68	6.84 (6.48)	−0.41
^{57}Fe	5.89 (5.96)	1.41	3.43 (3.53)	−0.28	^{93}Mo	8.76 (9.25)	1.22	4.95 (5.11)	−0.50
^{58}Fe	5.80 (6.56)	2.20	2.96 (3.90)	0.15	^{95}Mo	10.95 (11.25)	1.29	5.90 (6.27)	0.06
^{59}Fe	6.85 (7.20)	1.57	3.92 (4.29)	0.16	^{96}Mo	11.66 (12.28)	1.35	5.68 (6.86)	0.01
^{60}Co	6.89 (6.75)	1.10	4.36 (3.99)	−0.44	^{97}Mo	12.30 (13.21)	1.50	6.41 (7.39)	0.40
^{59}Ni	6.58 (5.26)	1.65	3.26 (3.06)	−0.06	^{98}Mo	13.16 (14.09)	1.54	6.18 (7.88)	0.27
^{60}Ni	5.70 (5.87)	2.37	2.92 (3.44)	0.49	^{99}Mo	14.92 (15.59)	1.64	7.33 (8.74)	0.74
^{61}Ni	6.45 (6.42)	1.49	3.76 (3.77)	−0.14	^{101}Mo	24.30 (17.71)	1.89	7.80 (9.93)	1.28
^{62}Ni	6.01 (6.87)	2.26	3.17 (4.04)	0.40	^{100}Tc	15.43 (14.89)	1.41	8.71 (8.31)	0.48
^{63}Ni	7.66 (7.58)	1.16	4.34 (4.47)	−0.19	^{100}Ru	12.55 (13.01)	1.74	6.31 (7.23)	0.32
^{65}Ni	8.60 (8.68)	1.17	4.77 (5.13)	−0.08	^{102}Ru	14.62 (14.75)	1.48	7.00 (8.20)	0.29
^{64}Cu	7.29 (7.42)	0.86	4.51 (4.36)	−0.63	^{103}Ru	13.54 (16.30)	2.27	7.01 (9.09)	1.20
^{66}Cu	7.92 (8.44)	1.06	4.90 (4.96)	−0.31	^{105}Ru	18.13 (17.60)	1.75	8.51 (9.80)	0.97
^{65}Zn	7.78 (8.07)	2.05	4.42 (4.75)	0.63	^{104}Rh	15.59 (15.36)	1.26	8.79 (8.52)	0.34
^{67}Zn	8.61 (9.37)	2.01	4.76 (5.51)	0.78	^{105}Pd	13.60 (14.64)	1.99	7.15 (8.11)	0.94
^{68}Zn	8.59 (9.43)	1.54	4.31 (5.53)	−0.17	^{106}Pd	15.03 (14.90)	1.38	7.29 (8.24)	0.18
^{69}Zn	9.39 (10.39)	1.84	5.08 (6.10)	0.66	^{107}Pd	15.36 (16.37)	1.81	7.76 (9.07)	0.87

Table 16
Local level density parameters $a(S_n)$, and δ for GSM. For comparison, the values between brackets come from the global systematics

GSM	Effective model		Collective model			Effective model		Collective model	
Nuc	$a(S_n)$	δ	$a(S_n)$	δ	Nuc	$a(S_n)$	δ	$a(S_n)$	δ
^{108}Pd	15.98 (16.17)	1.29	7.48 (8.93)	0.15	^{140}La	14.28 (14.31)	0.73	8.25 (7.52)	−0.41
^{109}Pd	15.58 (17.58)	2.45	8.12 (9.73)	1.46	^{137}Ce	18.30 (16.65)	0.84	9.23 (8.87)	−0.03
^{111}Pd	22.20 (18.45)	1.68	9.79 (10.20)	1.05	^{141}Ce	16.55 (14.82)	0.26	8.06 (7.80)	−0.78
^{108}Ag	15.22 (15.36)	1.45	8.72 (8.48)	0.47	^{142}Ce	16.62 (16.09)	1.03	7.19 (8.50)	−0.17
^{110}Ag	17.91 (16.71)	1.30	9.87 (9.21)	0.48	^{143}Ce	25.71 (17.31)	0.67	8.14 (9.18)	0.03
^{107}Cd	13.23 (12.91)	1.69	7.18 (7.09)	0.58	^{142}Pr	14.87 (15.94)	0.68	8.27 (8.42)	−0.42
^{109}Cd	15.54 (14.59)	1.44	8.03 (8.03)	0.54	^{143}Nd	17.00 (16.05)	0.41	8.38 (8.47)	−0.64
^{111}Cd	16.40 (15.84)	1.58	8.19 (8.72)	0.70	^{144}Nd	16.41 (17.28)	0.93	7.80 (9.14)	−0.44
^{112}Cd	16.79 (15.81)	1.21	7.78 (8.68)	0.11	^{145}Nd	18.97 (18.62)	0.91	9.06 (9.88)	0.00
^{113}Cd	16.44 (16.89)	1.70	8.21 (9.29)	0.78	^{146}Nd	18.06 (19.53)	1.31	8.28 (10.37)	0.18
^{114}Cd	16.79 (16.52)	1.19	7.63 (9.06)	0.11	^{147}Nd	22.12 (21.19)	1.23	9.88 (11.28)	0.47
^{115}Cd	19.10 (17.50)	1.33	8.83 (9.61)	0.57	^{148}Nd	25.82 (21.69)	1.27	10.07 (11.53)	0.52
^{117}Cd	17.09 (17.61)	1.74	8.36 (9.65)	0.84	^{149}Nd	22.35 (23.31)	1.85	10.49 (12.42)	1.05
^{114}In	14.90 (15.87)	0.97	8.16 (8.69)	−0.05	^{151}Nd	21.75 (23.30)	1.67	9.98 (12.39)	0.82
^{116}In	17.24 (16.62)	0.87	9.26 (9.09)	0.01	^{148}Pm	22.11 (21.56)	0.98	11.36 (11.46)	0.17
^{113}Sn	15.08 (14.08)	0.89	7.67 (7.69)	−0.03	^{145}Sm	15.24 (16.58)	0.50	7.58 (8.74)	−0.64
^{115}Sn	15.96 (14.63)	0.45	8.07 (7.98)	−0.44	^{148}Sm	19.67 (20.24)	1.13	9.04 (10.73)	0.01
^{117}Sn	16.33 (15.46)	0.65	7.95 (8.43)	−0.26	^{149}Sm	21.60 (22.01)	1.37	10.06 (11.70)	0.56
^{118}Sn	14.52 (15.16)	1.02	7.07 (8.24)	−0.24	^{150}Sm	22.29 (22.41)	1.34	9.26 (11.89)	0.44
^{119}Sn	15.56 (15.80)	1.14	7.84 (8.60)	0.15	^{151}Sm	23.32 (24.20)	1.89	10.86 (12.87)	1.12
^{120}Sn	13.86 (15.07)	1.08	6.82 (8.17)	−0.38	^{152}Sm	21.97 (23.21)	1.71	10.00 (12.30)	0.84
^{121}Sn	12.99 (15.42)	1.36	6.64 (8.36)	0.19	^{153}Sm	19.99 (23.89)	2.18	9.93 (12.67)	1.26
^{125}Sn	12.93 (12.68)	0.55	6.65 (6.75)	−0.63	^{155}Sm	21.18 (22.93)	1.42	9.79 (12.13)	0.59
^{122}Sb	15.24 (16.29)	1.47	8.68 (8.84)	0.42	^{152}Eu	24.71 (24.15)	1.45	12.75 (12.81)	0.71
^{124}Sb	13.98 (15.43)	1.63	8.13 (8.33)	0.45	^{153}Eu	19.31 (23.38)	1.69	9.37 (12.37)	0.81

(*continued on next page*)

Table 16 (*continued*)

GSM	Effective model		Collective model			Effective model		Collective model	
Nuc	$a(S_n)$	δ	$a(S_n)$	δ	Nuc	$a(S_n)$	δ	$a(S_n)$	δ
^{123}Te	16.38 (16.95)	1.45	8.26 (9.20)	0.52	^{154}Eu	22.31 (23.53)	1.46	11.87 (12.45)	0.62
^{124}Te	16.40 (16.05)	1.06	8.05 (8.68)	−0.13	^{155}Eu	19.66 (22.93)	1.52	9.62 (12.11)	0.64
^{125}Te	15.90 (16.26)	1.62	8.20 (8.79)	0.67	^{156}Eu	20.51 (22.51)	1.05	10.79 (11.87)	0.18
^{126}Te	15.40 (15.16)	1.02	7.51 (8.16)	−0.14	^{153}Gd	22.83 (24.27)	2.03	10.98 (12.87)	1.23
^{127}Te	14.33 (14.97)	1.50	7.45 (8.04)	0.45	^{155}Gd	21.45 (24.03)	2.05	10.58 (12.72)	1.18
^{129}Te	14.01 (13.10)	1.40	7.57 (6.95)	0.32	^{156}Gd	20.58 (23.14)	1.68	9.69 (12.21)	0.70
^{131}Te	13.12 (10.74)	0.96	6.89 (5.56)	−0.29	^{157}Gd	20.91 (23.24)	1.71	10.18 (12.27)	0.85
^{128}I	14.53 (15.74)	1.58	8.41 (8.46)	0.42	^{158}Gd	29.55 (22.83)	1.51	8.97 (12.03)	0.79
^{130}I	15.06 (14.32)	1.59	7.74 (7.64)	0.43	^{159}Gd	20.95 (22.90)	1.47	9.91 (12.07)	0.62
^{129}Xe	14.18 (16.34)	1.71	7.29 (8.79)	0.59	^{161}Gd	19.73 (22.57)	1.43	9.48 (11.87)	0.48
^{130}Xe	14.46 (15.37)	1.29	7.29 (8.23)	−0.11	^{160}Tb	20.75 (22.65)	1.17	11.05 (11.91)	0.28
^{131}Xe	15.79 (15.06)	1.30	8.24 (8.04)	0.32	^{157}Dy	23.59 (23.99)	1.76	11.38 (12.67)	1.01
^{132}Xe	13.10 (13.98)	1.36	6.70 (7.42)	−0.12	^{159}Dy	19.96 (23.57)	1.83	9.97 (12.42)	0.90
^{133}Xe	13.86 (13.15)	1.04	7.46 (6.93)	−0.13	^{161}Dy	20.51 (23.29)	1.77	10.08 (12.25)	0.87
^{135}Xe	12.96 (10.72)	0.33	7.33 (5.51)	−0.96	^{162}Dy	19.62 (22.74)	1.72	9.06 (11.94)	0.73
^{137}Xe	15.08 (10.05)	0.42	8.02 (5.07)	−0.61	^{163}Dy	18.79 (22.57)	1.81	9.44 (11.84)	0.82
^{134}Cs	13.27 (14.51)	1.58	7.79 (7.70)	0.28	^{164}Dy	18.40 (22.37)	1.85	8.47 (11.72)	0.80
^{131}Ba	16.49 (17.51)	1.46	8.37 (9.42)	0.51	^{165}Dy	19.56 (22.49)	1.51	9.49 (11.78)	0.58
^{133}Ba	16.12 (16.60)	1.35	8.31 (8.89)	0.38	^{166}Ho	20.36 (22.06)	0.96	10.77 (11.53)	0.05
^{135}Ba	14.18 (15.12)	1.17	7.32 (8.04)	0.08	^{163}Er	22.48 (23.91)	1.64	10.94 (12.56)	0.84
^{136}Ba	13.22 (14.10)	1.29	6.81 (7.45)	−0.20	^{165}Er	20.19 (23.45)	1.81	9.97 (12.29)	0.89
^{137}Ba	13.59 (12.99)	0.22	7.05 (6.81)	−0.98	^{167}Er	19.97 (22.64)	1.62	9.90 (11.83)	0.67
^{138}Ba	11.60 (12.10)	0.66	5.97 (6.29)	−1.04	^{168}Er	19.12 (22.58)	1.66	8.74 (11.79)	0.65
^{139}Ba	12.53 (12.82)	0.58	6.45 (6.67)	−0.73	^{169}Er	19.61 (22.52)	1.46	9.55 (11.75)	0.51
^{139}La	11.88 (13.49)	0.96	6.28 (7.08)	−0.49	^{171}Er	20.22 (22.57)	1.36	9.76 (11.76)	0.43

Table 17
Local level density parameters $a(S_n)$, and δ for GSM. For comparison, the values between brackets come from the global systematics

GSM	Effective model		Collective model			Effective model		Collective model	
Nuc	$a(S_n)$	δ	$a(S_n)$	δ	Nuc	$a(S_n)$	δ	$a(S_n)$	δ
^{170}Tm	20.39 (22.20)	0.94	10.86 (11.56)	0.02	^{200}Hg	14.03 (15.04)	1.39	7.53 (7.34)	−0.22
^{171}Tm	20.24 (22.53)	1.30	10.00 (11.73)	0.38	^{201}Hg	14.30 (13.83)	1.19	6.98 (6.63)	−0.22
^{169}Yb	23.26 (23.53)	1.43	11.21 (12.29)	0.64	^{202}Hg	12.29 (13.14)	1.84	6.91 (6.16)	−0.25
^{170}Yb	18.95 (23.17)	1.76	8.96 (12.08)	0.58	^{204}Tl	11.06 (11.07)	1.74	6.15 (5.08)	−0.21
^{171}Yb	19.97 (23.07)	1.52	9.79 (12.02)	0.59	^{206}Tl	6.98 (8.46)	3.27	4.38 (3.56)	−1.77
^{172}Yb	20.28 (22.88)	1.67	9.62 (11.91)	0.59	^{205}Pb	10.76 (10.40)	1.35	5.08 (4.67)	−0.17
^{173}Yb	18.83 (22.52)	1.54	9.28 (11.70)	0.55	^{207}Pb	7.03 (7.29)	1.60	3.20 (2.88)	−1.49
^{174}Yb	20.63 (22.72)	1.19	9.52 (11.80)	0.10	^{208}Pb	6.97 (6.48)	2.07	2.15 (2.41)	−1.76
^{175}Yb	19.06 (22.68)	1.42	9.49 (11.77)	0.43	^{209}Pb	6.43 (6.92)	0.92	2.12 (2.54)	−2.23
^{177}Yb	19.21 (23.10)	1.55	9.65 (11.98)	0.57	^{210}Bi	8.63 (9.87)	1.47	4.45 (4.28)	−0.83
^{176}Lu	20.93 (22.76)	0.96	11.14 (11.80)	0.01	^{227}Ra	33.80 (35.29)	1.40	14.52 (17.90)	0.77
^{177}Lu	19.88 (23.53)	1.31	9.83 (12.20)	0.36	^{229}Th	32.49 (33.94)	1.69	14.88 (17.17)	1.01
^{175}Hf	20.94 (23.82)	1.58	10.30 (12.38)	0.68	^{230}Th	28.31 (33.77)	1.61	12.17 (17.06)	0.84
^{177}Hf	21.01 (23.66)	1.51	10.31 (12.27)	0.59	^{231}Th	32.95 (34.42)	1.42	14.50 (17.40)	0.77
^{178}Hf	20.93 (23.86)	1.60	9.96 (12.37)	0.49	^{233}Th	35.78 (35.40)	1.26	14.84 (17.89)	0.68
^{179}Hf	20.49 (23.69)	1.49	10.03 (12.27)	0.54	^{233}Pa	25.50 (33.86)	1.60	12.01 (17.07)	0.75
^{180}Hf	19.45 (23.70)	1.69	9.00 (12.26)	0.52	^{233}U	30.92 (32.49)	1.32	14.11 (16.37)	0.63
^{181}Hf	22.95 (23.66)	1.09	10.59 (12.24)	0.29	^{234}U	29.83 (32.75)	1.37	12.67 (16.48)	0.68
^{181}Ta	25.13 (23.41)	0.59	11.33 (12.09)	−0.13	^{235}U	29.28 (33.25)	1.51	13.42 (16.75)	0.76
^{182}Ta	21.14 (23.17)	0.88	11.17 (11.96)	−0.04	^{236}U	32.68 (33.55)	1.34	13.44 (16.88)	0.67
^{183}Ta	22.14 (23.90)	0.85	9.93 (12.34)	0.09	^{237}U	32.91 (33.86)	1.19	14.16 (17.04)	0.53
^{181}W	24.09 (23.51)	1.39	10.48 (12.15)	0.57	^{238}U	33.01 (34.55)	1.34	12.90 (17.39)	0.66
^{183}W	20.42 (23.26)	1.33	9.97 (12.00)	0.41	^{239}U	40.06 (35.05)	0.74	15.48 (17.64)	0.28
^{184}W	20.63 (23.57)	1.57	9.83 (12.15)	0.45	^{237}Np	23.81 (32.73)	1.59	11.24 (16.44)	0.66
^{185}W	22.57 (23.76)	1.22	10.76 (12.25)	0.36	^{238}Np	33.21 (32.57)	0.69	15.91 (16.35)	0.07

(*continued on next page*)

Table 17 (*continued*)

GSM	Effective model		Collective model			Effective model		Collective model	
Nuc	$a(S_n)$	δ	$a(S_n)$	δ	Nuc	$a(S_n)$	δ	$a(S_n)$	δ
^{187}W	25.10 (23.97)	0.99	11.43 (12.34)	0.25	^{239}Np	30.02 (33.65)	1.40	13.97 (16.90)	0.69
^{186}Re	22.08 (23.22)	0.85	11.71 (11.94)	−0.03	^{239}Pu	29.98 (31.87)	1.16	13.59 (15.98)	0.47
^{188}Re	22.43 (23.32)	0.90	11.94 (11.97)	0.03	^{240}Pu	29.96 (32.65)	1.42	13.06 (16.38)	0.60
^{187}Os	21.15 (23.51)	1.51	10.53 (12.09)	0.60	^{241}Pu	30.98 (33.00)	1.29	13.95 (16.56)	0.59
^{188}Os	22.16 (23.05)	1.24	10.42 (11.83)	0.19	^{242}Pu	33.49 (33.69)	1.30	13.89 (16.90)	0.54
^{189}Os	21.86 (23.28)	1.38	10.79 (11.95)	0.50	^{243}Pu	35.44 (33.98)	1.00	14.55 (17.05)	0.44
^{190}Os	21.55 (22.58)	1.23	10.27 (11.56)	0.21	^{245}Pu	42.80 (35.17)	0.59	16.16 (17.65)	0.20
^{191}Os	20.18 (22.46)	1.63	10.27 (11.49)	0.67	^{242}Am	32.56 (31.74)	0.67	15.84 (15.88)	0.02
^{193}Os	23.58 (21.21)	0.77	11.13 (10.78)	0.01	^{243}Am	31.72 (32.80)	1.22	14.70 (16.42)	0.56
^{192}Ir	20.85 (22.22)	1.46	11.80 (11.34)	0.45	^{244}Am	35.96 (32.69)	0.36	16.52 (16.35)	−0.14
^{193}Ir	20.06 (21.53)	1.41	10.46 (10.96)	0.45	^{243}Cm	31.35 (31.21)	0.71	13.01 (15.60)	0.05
^{194}Ir	20.05 (20.71)	1.02	11.26 (10.51)	0.01	^{244}Cm	30.14 (31.69)	1.11	13.07 (15.84)	0.50
^{193}Pt	21.35 (21.75)	1.55	11.06 (11.08)	0.62	^{245}Cm	28.82 (31.73)	1.25	13.38 (15.85)	0.47
^{195}Pt	16.36 (19.92)	1.80	8.43 (10.06)	0.55	^{246}Cm	28.91 (32.46)	1.20	12.41 (16.22)	0.34
^{196}Pt	17.98 (18.94)	1.25	8.98 (9.53)	0.11	^{247}Cm	27.11 (32.81)	1.49	12.43 (16.39)	0.63
^{197}Pt	15.83 (18.18)	1.52	8.41 (9.09)	0.30	^{248}Cm	32.50 (33.53)	1.10	12.51 (16.76)	0.36
^{199}Pt	16.47 (16.48)	1.08	8.64 (8.13)	−0.05	^{249}Cm	35.59 (34.48)	0.95	14.65 (17.25)	0.37
^{198}Au	16.20 (17.06)	1.06	9.48 (8.48)	−0.22	^{250}Bk	30.82 (33.18)	0.99	15.49 (16.55)	0.23
^{199}Hg	15.95 (15.81)	1.41	8.89 (7.77)	0.14	^{250}Cf	30.21 (31.26)	1.05	12.89 (15.55)	0.37

expression for T leads to a value for E_M which is clearly off scale. In that case, we resort to empirical expressions for the matching energy. For the effective model

$$E_M = 2.33 + 253/A + \Delta^{\mathrm{CTM}}, \tag{83}$$

and for the collective model

$$E_M = 2.67 + 253/A + \Delta^{\mathrm{CTM}}, \tag{84}$$

after which we obtain T from Eq. (54).

6.2. Mean resonance spacings

The predictive power of a global level density formula can be inferred to some extent from the rms deviation factor which relates experimental and theoretical D_0 values for all N nuclides. It is defined as

$$f_{\mathrm{rms}} = \exp\left[\frac{1}{N}\sum_{i=1}^{N}\left(\ln\frac{D_{0,i}^{\mathrm{theo}}}{D_{0,i}^{\mathrm{exp}}}\right)^2\right]. \tag{85}$$

The resulting values for the various models are given in Table 5. The f_{rms} for the CTM, BFM and effective GSM are lower than those of the collective GSM and HFM.

6.3. Discrete levels

For the description of experimental discrete levels by a global model, we use the goodness-of-fit estimator

$$f_{\mathrm{lev}} = \frac{1}{N}\sum_{i=1}^{N}\sum_{k=N_L^i}^{N_U^i}\frac{(N_{\mathrm{cum}}^i(E_k)-k)^2}{k}, \tag{86}$$

where i runs over all N nuclides. The values for the various models are given in Table 5.

These global values for the description of the cumulative number of discrete levels should be reflected in the comparison for individual nuclides. To test this, we have made a visual comparison between the calculated and experimental cumulative number of levels for the entire periodic table of elements. A few examples are shown in Fig. 8, where the various level density models, with local and global parameterization, are displayed for a few nuclides in the vicinity of $A = 90$. The entire collection of graphs for all nuclides for which experimental discrete levels exist can be found at [31].

6.4. Cross section and spectrum calculations

All level density models in this paper have been adjusted in an optimal way to the same set of experimental discrete levels and mean resonance spacings. Although various level densities are thus rather close for energies where these basic observables are available, the values over a large energy range may be different. The next interesting question is then what effect such differences have on nuclear reaction calculations. It gives an indication of how much effort in precise level density determination is still required. The level density models and parameters of this paper are included in the nuclear reaction model code TALYS. This enables to directly test the effect of

Table 18
Local level density parameters c and p for HFM

Nuc	c	p	Nuc	c	p	Nuc	c	p
^{24}Na	−0.01	0.15	^{71}Zn	0.33	0.65	^{108}Pd	−0.15	0.78
^{25}Mg	0.00	0.00	^{70}Ga	0.54	1.61	^{109}Pd	−0.27	−0.98
^{26}Mg	−0.08	1.91	^{72}Ga	−0.49	−1.27	^{111}Pd	0.46	−0.36
^{27}Mg	0.01	1.94	^{71}Ge	0.12	−0.90	^{108}Ag	0.96	−0.15
^{28}Al	−0.24	−0.59	^{73}Ge	−0.49	0.00	^{110}Ag	−0.09	0.11
^{29}Si	1.01	4.15	^{74}Ge	−0.35	1.38	^{107}Cd	0.09	−0.47
^{30}Si	−0.47	0.94	^{75}Ge	−0.20	−0.10	^{109}Cd	0.29	0.08
^{32}P	0.00	0.00	^{77}Ge	0.01	−0.12	^{111}Cd	−0.06	0.44
^{33}S	−0.24	0.59	^{76}As	−0.29	−0.71	^{112}Cd	0.16	0.67
^{34}S	−0.52	−0.48	^{75}Se	0.00	−1.42	^{113}Cd	0.11	0.01
^{35}S	0.00	−0.98	^{77}Se	0.13	0.28	^{114}Cd	0.34	0.54
^{36}Cl	−0.18	0.23	^{78}Se	0.15	0.64	^{115}Cd	0.40	−0.14
^{38}Cl	0.56	1.61	^{79}Se	−0.37	−1.64	^{117}Cd	−0.23	−0.70
^{41}Ar	0.68	1.25	^{81}Se	0.70	0.17	^{114}In	−0.17	−0.52
^{40}K	−0.34	−0.58	^{83}Se	0.62	0.03	^{116}In	−0.01	−0.50
^{42}K	−0.95	−3.28	^{80}Br	1.76	3.20	^{113}Sn	0.50	0.22
^{41}Ca	0.45	0.65	^{82}Br	0.15	−0.50	^{115}Sn	0.35	0.53
^{43}Ca	1.26	1.35	^{79}Kr	−0.14	−0.50	^{117}Sn	0.44	0.38
^{44}Ca	0.08	2.35	^{81}Kr	0.05	−1.00	^{118}Sn	0.21	0.67
^{45}Ca	0.66	1.05	^{84}Kr	−0.54	1.14	^{119}Sn	0.47	0.07
^{46}Sc	−0.07	0.05	^{85}Kr	0.84	0.78	^{120}Sn	0.04	0.33
^{47}Ti	−0.31	−0.65	^{86}Rb	−0.24	−0.15	^{121}Sn	−0.02	−0.16
^{48}Ti	−0.16	0.23	^{88}Rb	−0.12	0.01	^{125}Sn	3.35	1.37
^{49}Ti	0.21	0.37	^{85}Sr	0.15	−0.69	^{122}Sb	−0.29	−0.92
^{50}Ti	−0.38	0.53	^{87}Sr	0.06	−0.17	^{124}Sb	−0.40	−1.21
^{51}Ti	0.00	0.00	^{88}Sr	−0.26	−0.13	^{123}Te	−0.12	0.58
^{51}V	−0.21	0.74	^{89}Sr	0.58	1.35	^{124}Te	0.34	0.66
^{52}V	−0.10	−0.20	^{90}Y	−0.21	0.28	^{125}Te	0.11	−0.46
^{51}Cr	0.04	0.57	^{91}Zr	−0.05	0.28	^{126}Te	0.30	0.58
^{53}Cr	−0.43	−0.90	^{92}Zr	−0.24	0.60	^{127}Te	0.09	0.13
^{54}Cr	0.03	0.67	^{93}Zr	0.01	0.83	^{129}Te	0.37	−0.06
^{55}Cr	2.26	1.75	^{94}Zr	0.14	1.34	^{131}Te	0.81	0.51
^{56}Mn	−0.41	−1.34	^{95}Zr	0.33	0.82	^{128}I	−0.37	−0.80
^{55}Fe	−0.13	0.81	^{94}Nb	−0.24	0.01	^{130}I	1.26	1.72
^{57}Fe	−0.15	−0.38	^{93}Mo	−0.07	0.26	^{129}Xe	−0.03	−0.27
^{58}Fe	−0.50	−0.23	^{95}Mo	0.00	0.00	^{130}Xe	0.03	0.96
^{59}Fe	−0.13	−0.28	^{96}Mo	−0.41	0.90	^{131}Xe	0.33	−0.09
^{60}Co	−0.34	−0.59	^{97}Mo	−0.09	−0.33	^{132}Xe	0.22	0.51
^{59}Ni	−0.22	0.17	^{98}Mo	−0.26	0.31	^{133}Xe	0.45	0.16
^{60}Ni	−0.80	−0.31	^{99}Mo	0.02	−0.56	^{135}Xe	0.59	0.97
^{61}Ni	−0.20	−0.54	^{101}Mo	−0.19	−0.95	^{137}Xe	2.96	1.09
^{62}Ni	−0.75	−1.62	^{100}Tc	−0.14	−0.56	^{134}Cs	0.00	0.00
^{63}Ni	0.10	0.05	^{100}Ru	0.02	0.33	^{131}Ba	0.06	0.10
^{65}Ni	0.70	0.83	^{102}Ru	−0.11	0.71	^{133}Ba	0.36	0.05
^{64}Cu	−0.04	0.27	^{103}Ru	−0.55	−0.77	^{135}Ba	0.16	−0.18
^{66}Cu	−0.27	−0.25	^{105}Ru	−0.36	−0.29	^{136}Ba	0.03	0.72
^{65}Zn	−0.23	−0.36	^{104}Rh	−0.05	−0.55	^{137}Ba	0.36	0.72
^{67}Zn	−0.18	−0.20	^{105}Pd	−0.13	−0.64	^{138}Ba	0.48	1.18
^{68}Zn	−0.31	0.13	^{106}Pd	−0.09	0.79	^{139}Ba	0.27	0.45
^{69}Zn	0.23	−0.34	^{107}Pd	−0.20	−0.40	^{139}La	0.17	−0.19

Table 19
Local level density parameters c and p for HFM

Nuc	c	p	Nuc	c	p	Nuc	c	p
^{140}La	−0.09	−0.16	^{167}Er	−0.01	−0.03	^{198}Au	−0.46	−0.39
^{137}Ce	0.53	0.20	^{168}Er	0.13	0.47	^{199}Hg	−0.35	−0.15
^{141}Ce	0.30	0.77	^{169}Er	0.07	0.10	^{200}Hg	−0.29	0.64
^{142}Ce	0.31	0.52	^{171}Er	0.20	0.12	^{201}Hg	−0.66	−0.01
^{143}Ce	0.14	0.21	^{170}Tm	−0.09	0.04	^{202}Hg	−0.44	0.41
^{142}Pr	−0.24	−0.26	^{171}Tm	0.06	0.23	^{204}Tl	−0.31	0.38
^{143}Nd	0.25	0.44	^{169}Yb	0.44	0.18	^{206}Tl	−0.36	0.43
^{144}Nd	−0.06	0.65	^{170}Yb	0.18	0.28	^{205}Pb	0.20	0.03
^{145}Nd	0.29	0.33	^{171}Yb	0.00	0.24	^{207}Pb	0.94	1.84
^{146}Nd	−0.13	0.55	^{172}Yb	0.40	0.57	^{208}Pb	0.38	0.10
^{147}Nd	0.09	−0.10	^{173}Yb	0.12	0.02	^{209}Pb	0.08	0.57
^{148}Nd	0.45	0.82	^{174}Yb	0.58	0.62	^{210}Bi	−0.26	0.52
^{149}Nd	0.08	−0.53	^{175}Yb	0.26	0.09	^{227}Ra	0.61	−0.09
^{151}Nd	0.68	0.00	^{177}Yb	0.31	0.12	^{229}Th	0.58	−0.26
^{148}Pm	0.04	−0.21	^{176}Lu	−0.03	0.16	^{230}Th	0.35	0.48
^{145}Sm	−0.20	0.24	^{177}Lu	0.13	0.35	^{231}Th	0.47	−0.05
^{148}Sm	−0.02	0.68	^{175}Hf	−0.03	0.00	^{233}Th	0.65	0.08
^{149}Sm	0.05	−0.35	^{177}Hf	0.12	0.02	^{233}Pa	−0.17	−0.14
^{150}Sm	0.27	0.69	^{178}Hf	0.77	0.45	^{233}U	0.42	0.08
^{151}Sm	−0.07	−0.02	^{179}Hf	0.09	0.25	^{234}U	0.49	0.55
^{152}Sm	0.24	0.24	^{180}Hf	0.12	0.46	^{235}U	0.13	−0.04
^{153}Sm	−0.12	−0.35	^{181}Hf	0.38	0.36	^{236}U	0.61	0.50
^{155}Sm	0.15	0.15	^{181}Ta	0.39	0.98	^{237}U	0.25	0.20
^{152}Eu	0.24	−0.52	^{182}Ta	−0.15	0.13	^{238}U	0.15	0.48
^{153}Eu	−0.29	−0.03	^{183}Ta	−0.17	0.48	^{239}U	0.37	0.54
^{154}Eu	0.14	−0.28	^{181}W	−0.01	0.19	^{237}Np	−0.25	−0.13
^{155}Eu	−0.09	0.13	^{183}W	−0.12	0.27	^{238}Np	0.35	0.04
^{156}Eu	−0.28	−0.07	^{184}W	0.30	0.82	^{239}Np	0.19	−0.07
^{153}Gd	0.11	−0.45	^{185}W	0.32	0.31	^{239}Pu	0.45	0.18
^{155}Gd	−0.15	−0.07	^{187}W	0.55	0.45	^{240}Pu	0.63	0.58
^{156}Gd	−0.05	0.57	^{186}Re	0.23	0.02	^{241}Pu	0.17	0.21
^{157}Gd	−0.28	0.15	^{188}Re	0.19	0.00	^{242}Pu	1.21	0.67
^{158}Gd	−0.08	0.31	^{187}Os	0.42	0.06	^{243}Pu	0.98	0.20
^{159}Gd	−0.11	0.12	^{188}Os	−0.60	0.72	^{245}Pu	1.11	0.53
^{161}Gd	−0.04	0.36	^{189}Os	−1.12	−0.08	^{242}Am	0.01	0.18
^{160}Tb	−0.55	0.05	^{190}Os	−0.49	0.69	^{243}Am	0.54	0.16
^{157}Dy	0.42	−0.02	^{191}Os	−0.95	−0.40	^{244}Am	0.77	0.15
^{159}Dy	−0.01	−0.13	^{193}Os	−0.11	0.39	^{243}Cm	0.22	0.60
^{161}Dy	−0.38	0.25	^{192}Ir	−0.44	−0.43	^{244}Cm	0.45	0.61
^{162}Dy	0.32	0.37	^{193}Ir	−0.49	−0.16	^{245}Cm	0.39	0.14
^{163}Dy	−0.16	−0.42	^{194}Ir	−0.27	−0.27	^{246}Cm	0.82	0.61
^{164}Dy	−0.07	0.11	^{193}Pt	−0.25	−0.24	^{247}Cm	−0.13	0.06
^{165}Dy	0.20	−0.08	^{195}Pt	−0.94	−0.56	^{248}Cm	0.61	0.70
^{166}Ho	−0.20	0.05	^{196}Pt	−0.39	0.49	^{249}Cm	0.04	0.29
^{163}Er	−0.11	0.11	^{197}Pt	−1.04	−0.43	^{250}Bk	0.22	−0.06
^{165}Er	−0.26	−0.21	^{199}Pt	−0.72	0.11	^{250}Cf	0.52	0.65

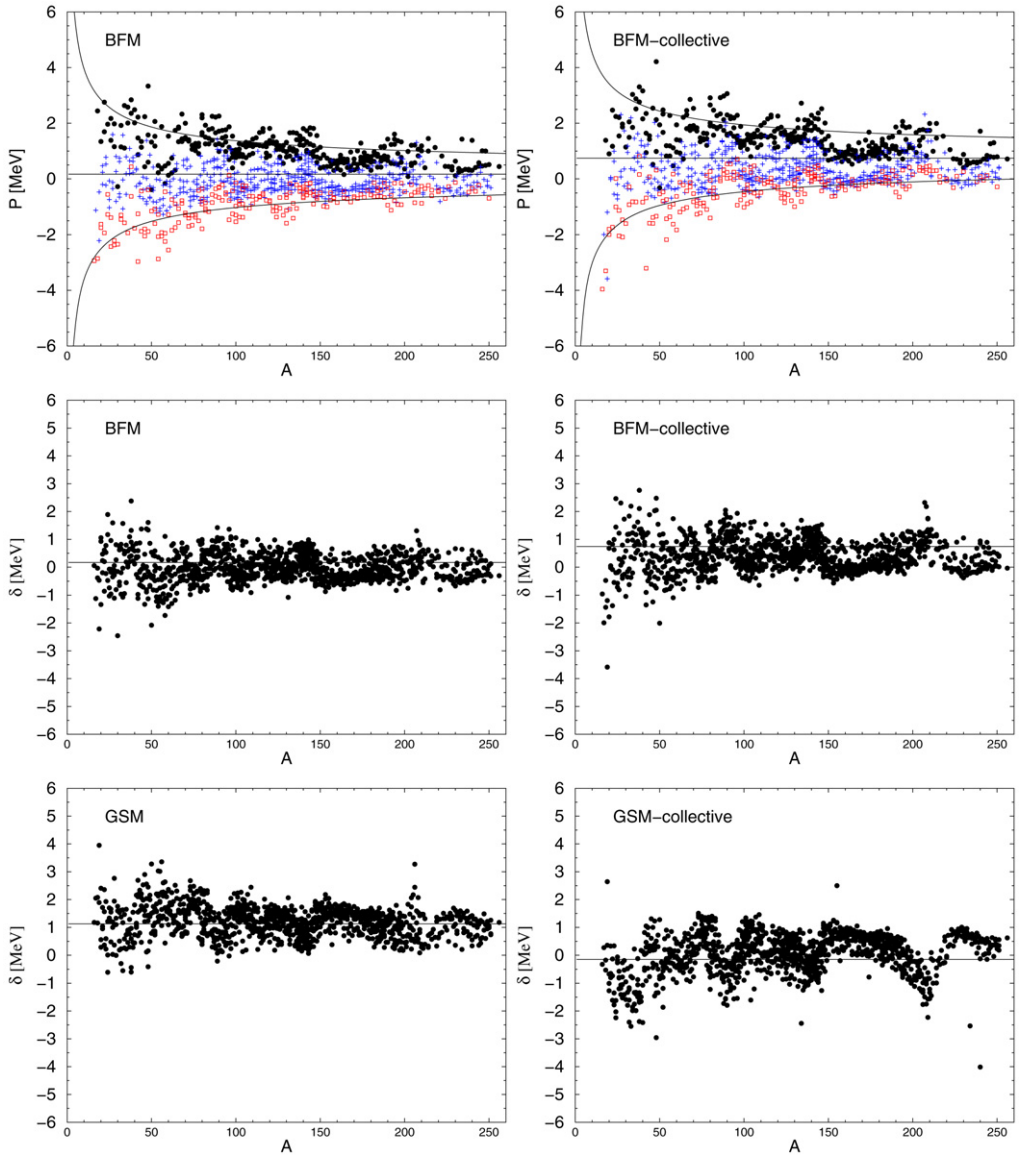

Fig. 4. Panels at the top: Pairing energy for the BFM without and with explicit collective enhancement. The closed circles represent the values for even nuclides, the crosses for odd nuclides, and the open circles for odd–odd nuclides, respectively. The solid lines represents the global systematical values for the pairing energy for these three subsets. Other 4 panels: Adjustable pairing shift parameters δ for the BFM and GSM without and with explicit collective enhancement. The solid line represents δ_{global}, the global value for δ.

different level density models on cross section, emission spectra, etc. calculations. For this paper, we have performed default ("blind") calculations with TALYS, for each level density model separately, for neutrons on all stable nuclides of the periodic table of elements and for energies up to 40 MeV. We have compared the resulting excitation curves with each other and with experimen-

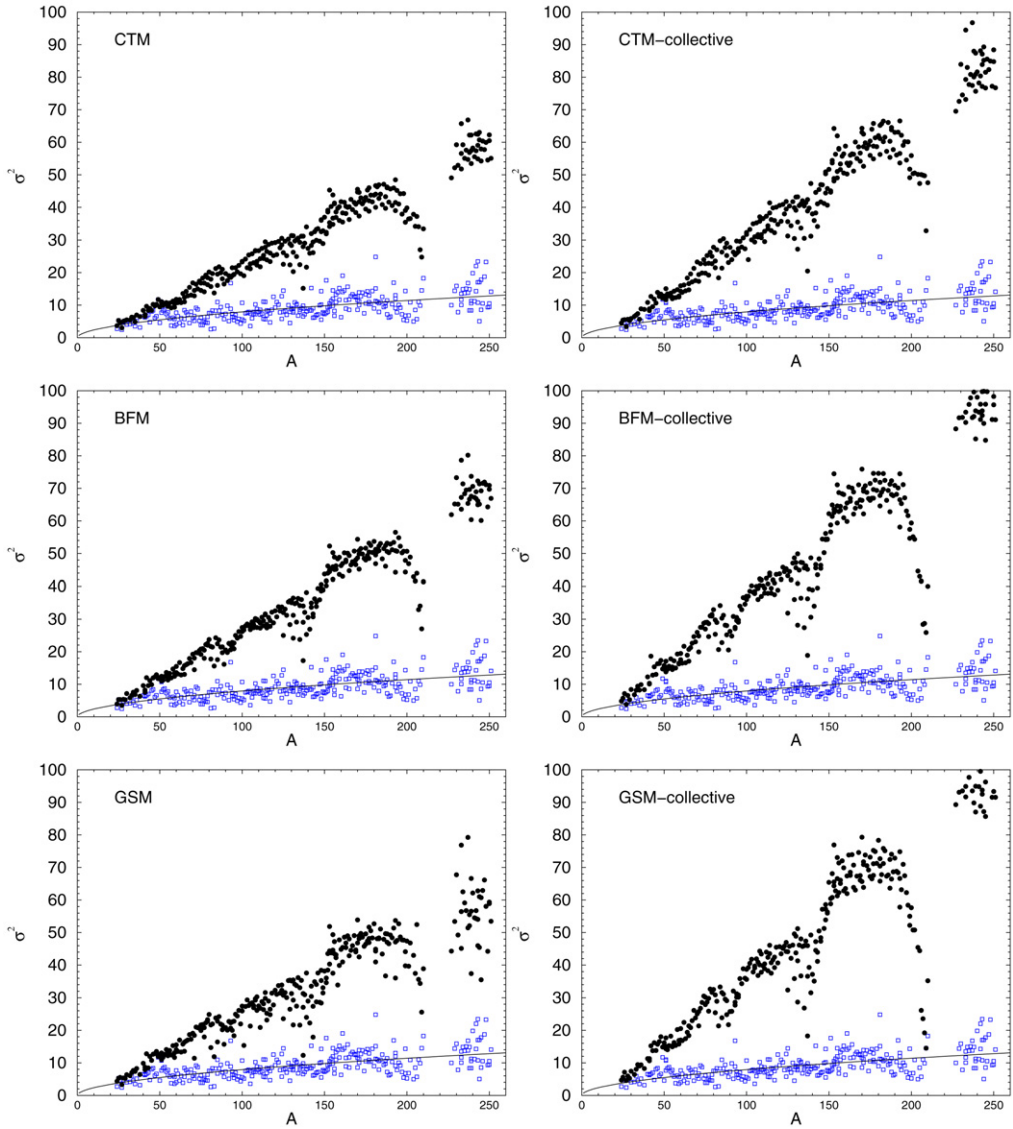

Fig. 5. Spin cut-off parameter σ^2 for the CTM, BFM and GSM without and with explicit collective enhancement. The open squares represent the values for the discrete level region. The closed circles represent the values at the neutron separation energy S_n, using the optimal values for the level density parameter a. The solid line represents the global value for σ^2 in the discrete level region. Only values for which an experimental D_0 value exists are plotted.

tal data. Apart from changing the level density model in each calculation for a particular target nucleus, all other nuclear model parameters where kept at their default parameters, i.e. the KD03 potential for the optical model [7], the standard pre-equilibrium parameterization of Ref. [8], and the gamma-ray strength parameters from the RIPL library [6]. Hence, no attempt was made to fit available experimental reaction data since the only objective here is to study the variation of the results as function of the level density model. Fig. 9 displays the results for a few reactions

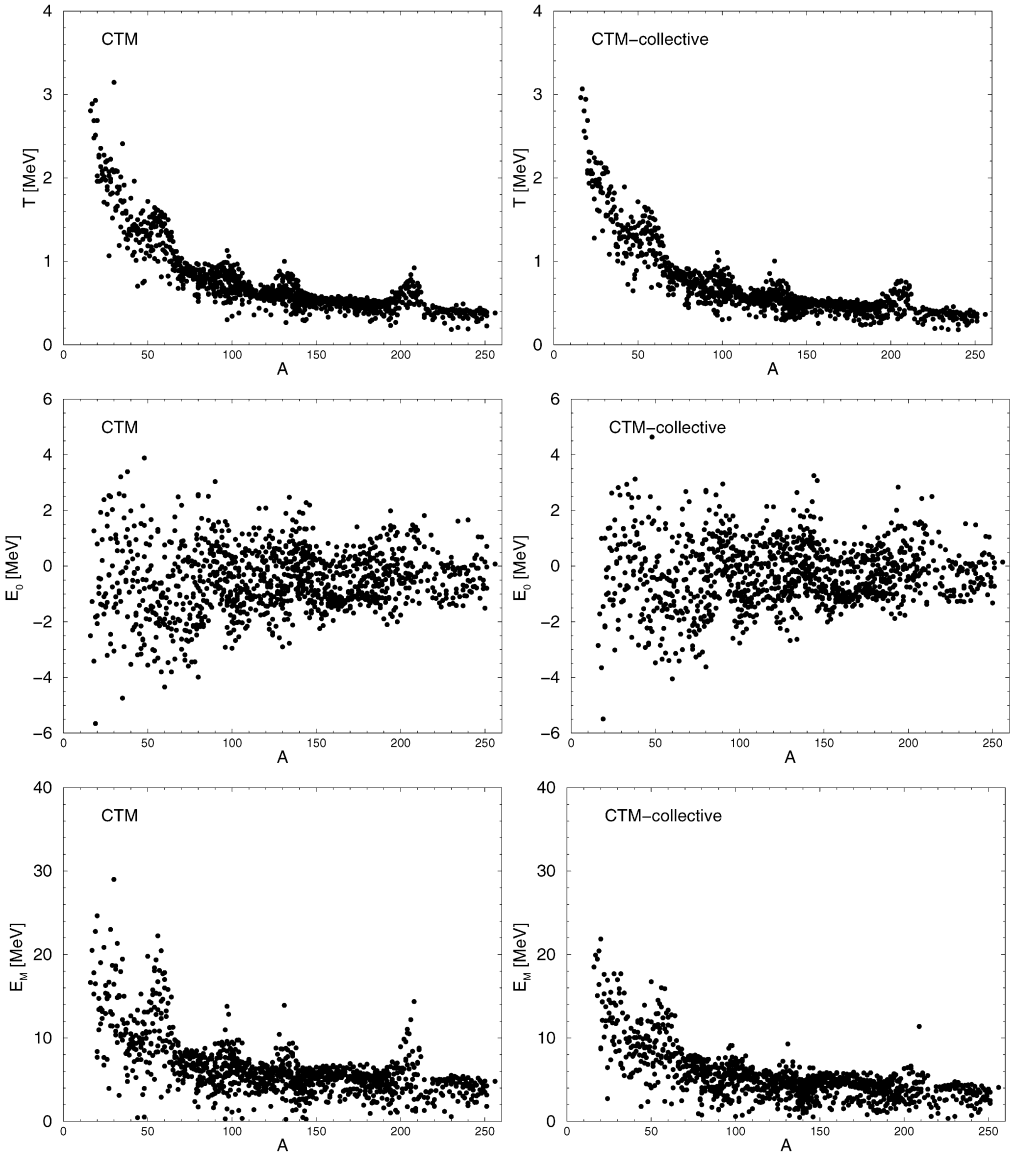

Fig. 6. Temperature T, energy shift E_0, and matching energy E_M for the CTM without and with explicit collective enhancement.

on ^{92}Zr for all level density models considered in this paper. It can be seen that while our level density models were constructed from nuclear structure information only, the resulting curves for cross sections are rather close together. Comparisons like this shed light on the uncertainty of model calculated cross sections that can be expected from uncertainties in the level density prescription. For example, global level density models account for about 5% variation of the $(n, 2n)$ results (the optical model and pre-equilibrium component also contribute to the total uncertainty of the $(n, 2n)$ cross section, which is generally about 10%) and about 30% of the (n, γ)

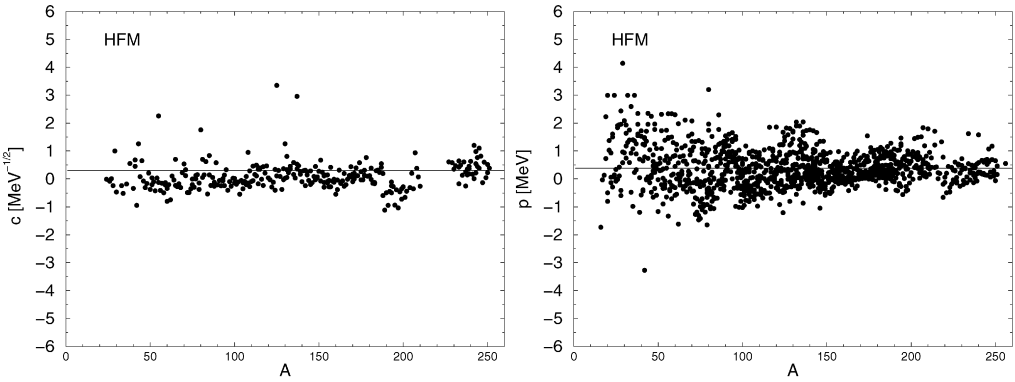

Fig. 7. HFM parameters c and p.

results. The entire collection of (n, γ), $(n, 2n)$, (n, p), (n, d) and (n, α) cross section figures for all nuclides for both local and global level density models can be found at [31]. Somewhat more relative sensitivity can be expected when considering neutron emission spectra, as displayed in Fig. 10, for the low-energy part of the emission spectra of the ^{93}Nb(n, xn) and ^{197}Au(p, xn) reactions, respectively. The evaporation spectrum resulting from the Hauser–Feshbach formalism is approximately of Maxwellian shape, having its peak around an emission energy of 1 MeV. The "temperature" of such a Maxwellian can be related to the level densities considered in this paper. For these two cases, the dispersion is about 30%, and similar values are found for other nuclides.

7. Summary

Nuclear reaction calculations require complete and clearly defined nuclear level densities. For this reason, we have set up a procedure to create consistent level density parameter sets for the three major phenomenological models and a recent Hartree–Fock–Bogolyubov based microscopic approach. For each of the models we have obtained local and global level density parameters on the basis of recent experimental D_0 and discrete level data. This variety of level density models can now be used with confidence in nuclear reaction calculations. To prove that statement, we have gone beyond the usual testing of level densities against basic observables (discrete levels and mean resonance spacings) and also directly test our results in cross section calculations. The scattering of the results, which is relatively small, indicates that all level density models, together with their parameterization, span up a space of results that is rather constrained. This does not necessarily hold for nuclides far away from the dripline and at very high energies, since experimental data is missing to constrain our parameters in these regions.

This paper describes three phenomenological models: CTM, BFM and GSM. Each of them can be considered as (i) an effective model, with all collective effects included in the level density parameter a, or (ii) as a model which explicitly includes collective effects, whereby an intrinsic level density function is multiplied by vibrational and rotational enhancement factors. Moreover, each of these six models can be used with local parameters, whereby experimental data of the nucleus under consideration is used to obtain parameters for that nucleus only, and with global parameters, whereby the level density model for the entire nuclide chart is defined in terms of a few global parameters. As usual, the order of priority in nuclear model calculations is to first use local parameters when they are available, i.e. for the nuclides of Table 4, and to resort to global

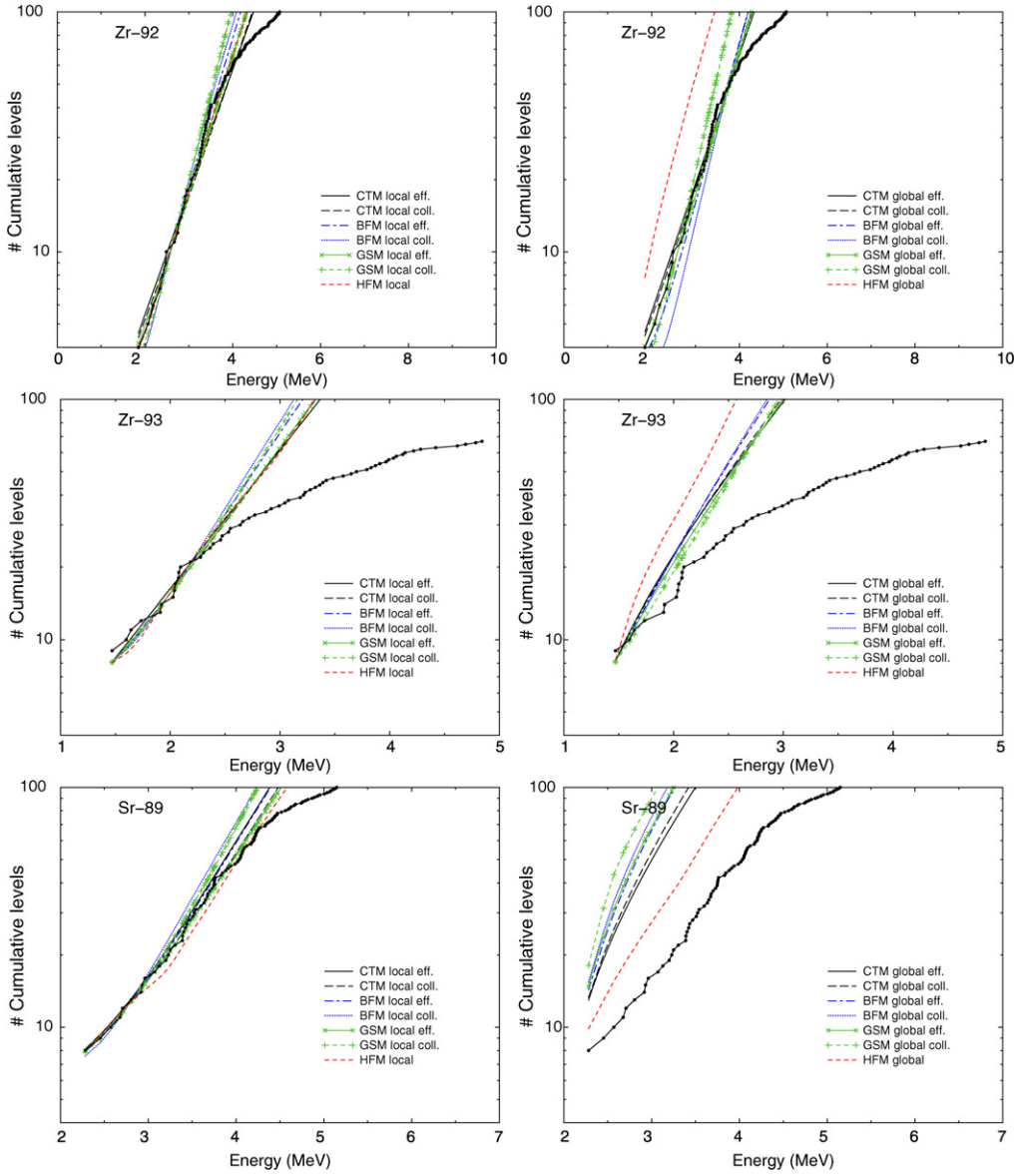

Fig. 8. Comparison between the calculated and experimental cumulative number of levels for local and global level density models, for a few nuclides.

parameters otherwise. The entire formalism, including parameter collections, is implemented in the TALYS code. The optimization of the level density parameters took place by comparing the TALYS level density results directly with experimental data. This ensures that the results produced in this paper are also actually used in nuclear model calculations.

While the BFM and GSM employ two adjustable parameters, the CTM has three: a, E_0 and T. Not surprisingly, the combined description of discrete level values and D_0 values is thus best for

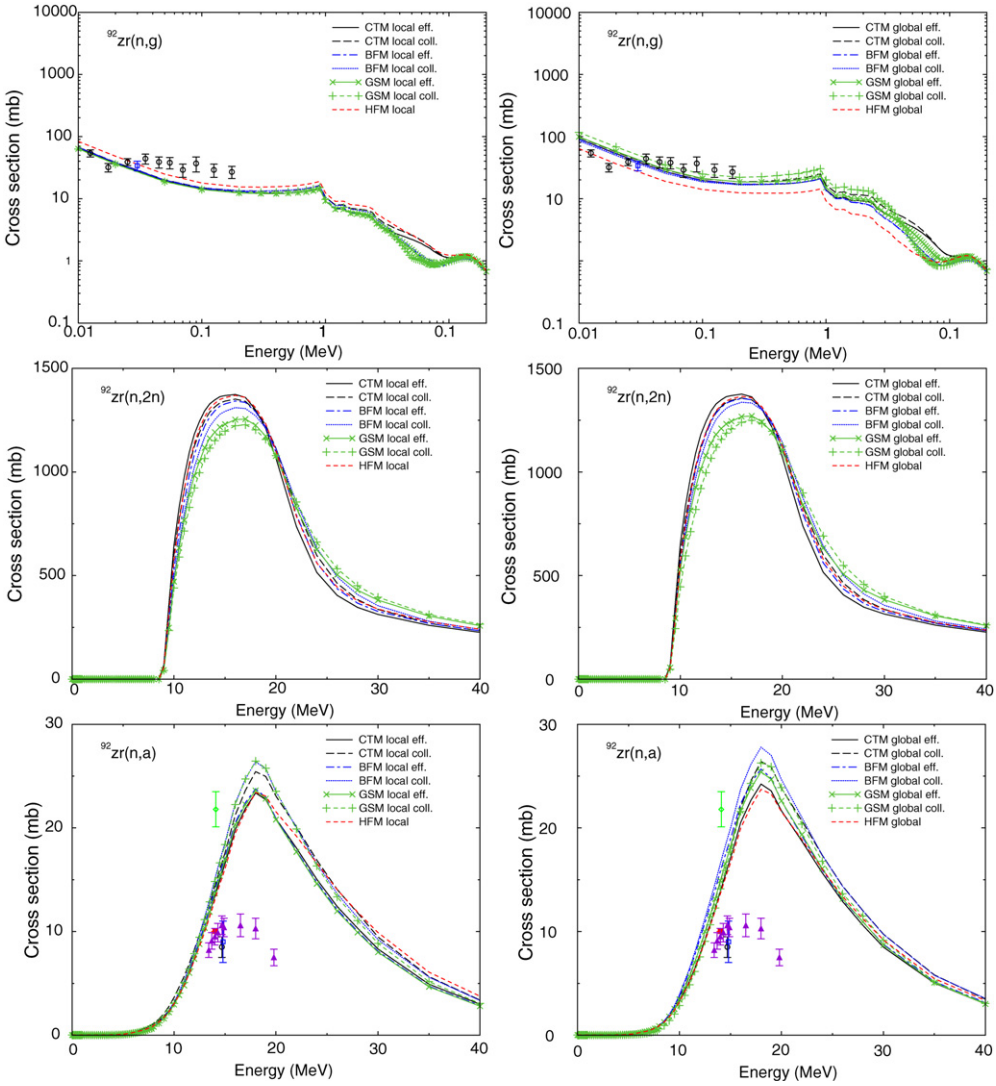

Fig. 9. Comparison between calculated and experimental cross sections, for the different local and global level density models, for a few reactions on ^{92}Zr.

the CTM, and some of these authors (the astrophysical calculations of S.G. invariably use unadjusted microscopic level densities) therefore recommend to use the effective CTM in detailed nuclear reaction calculations. For fissile nuclides, the collective CTM is proposed, bearing in mind that the results are then much more sensitive to level density values than the cross sections considered in this paper.

Relative simple post-adjustment expressions are sufficient to renormalize fully microscopic level densities to experimental data. This is important for the evolution of theoretical nuclear reaction calculations. It should be possible to replace all phenomenological ingredients of nuclear model calculations, such as the expressions for the optical model, gamma-ray strength functions,

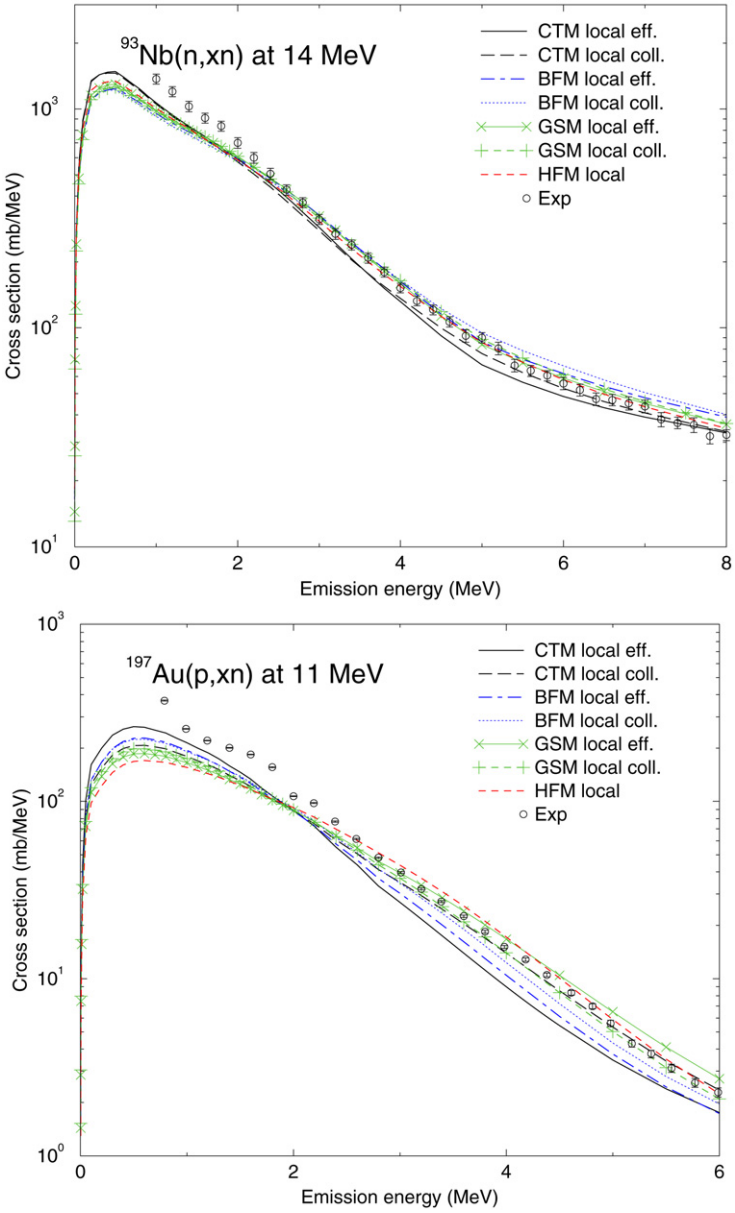

Fig. 10. Comparison between calculated and experimental neutron emission spectra sections, for the different local level density models.

pre-equilibrium contribution, level densities and fission barriers, by microscopic tables, which could then be adjusted by an appropriate expression using at most an equal number of parameters as for the phenomenological models. In this paper, such a first step has been set for level densities, through Eq. (75).

Acknowledgements

The authors acknowledge valuable discussions with Tamas Belgya, Roberto Capote, Marieke Duijvestijn, Mike Herman and Anatoly Ignatyuk.

Appendix A. The discrete spin cut-off parameter

Since the state density as function of the spin projection M is assumed to follow a Gaussian distribution [9], the spin cut-off parameter $\sigma^2(E_x)$ for a given excitation energy E_x can be written as

$$\sigma^2(E_x) = \sum_M M^2 \frac{\omega(E_x, M)}{\omega^{\mathrm{tot}}(E_x)}, \tag{A.1}$$

where $\omega^{\mathrm{tot}}(E_x)$ is the total state density and $\omega(E_x, M)$ is the state density with a specified spin projection M. To calculate the discrete spin cut-off parameter we approximate the formal expression of ω^{tot} as

$$\omega^{\mathrm{tot}}(E_x) = \frac{dN_s(E_x)}{dE_x}, \tag{A.2}$$

where $N_s(E_x)$ is the cumulated number of excited *states* of the nucleus up to the excitation energy E_x. If the discrete level energy range is small enough, an acceptable approximation to Eq. (A.2) is

$$\omega^{\mathrm{tot}}(E_U) = \frac{N_s(E_U) - N_s(E_L)}{E_U - E_L}, \tag{A.3}$$

and a similar approximation holds for $\omega(E_x, M)$. In this case, we can replace Eq. (A.1) by an expression for the discrete spin cut-off parameter σ_d^2,

$$\sigma_d^2 = \frac{1}{N_s(E_U) - N_s(E_L)} \sum_{M_d} \big[N_s(E_U, M_d) - N_s(E_L, M_d)\big] M_d^2, \tag{A.4}$$

where the sum runs over all the projections M_d of the discrete *levels* with spins J_i, and $N_s(E_U, M_d)$ is the number of levels in the energy interval $[0, E_U]$ yielding a state with a projection M_d. The contribution from the $[0, E_L]$ interval is subtracted from this. Since each excited level with spin J yields $2J + 1$ excited states with projections $M_1 = -J, M_2 = -J + 1, \ldots, M_{2J+1} = J$, the total number of states $N_s(E_U)$ reads

$$N_s(E_U) = \sum_{i=1}^{N_U} 2J_i + 1, \tag{A.5}$$

and similarly for $N_s(E_L)$, and the sum over M_d in Eq. (A.4) becomes

$$\sum_{M_d} N_s(E_U, M_d) M_d^2 = \sum_{i=1}^{N_U} \sum_{M=-J_i}^{M=J_i} M^2, \tag{A.6}$$

and similarly for $N_s(E_L, M_d)$. With the identity

$$\sum_{i=1}^{N} i^2 = \frac{1}{6} N(N+1)(2N+1), \tag{A.7}$$

we obtain Eq. (24).

References

[1] P. Demetriou, S. Goriely, Nucl. Phys. A 695 (2001) 95.
[2] S. Hilaire, S. Goriely, Nucl. Phys. A 779 (2006) 63.
[3] A. Gilbert, A.G.W. Cameron, Can. J. Phys. 43 (1965) 1446.
[4] W. Dilg, W. Schantl, H. Vonach, M. Uhl, Nucl. Phys. A 217 (1973) 269.
[5] A.V. Ignatyuk, K.K. Istekov, G.N. Smirenkin, Sov. J. Nucl. Phys. 29 (4) (1979) 450.
[6] T. Belgya, O. Bersillon, R. Capote, T. Fukahori, G. Zhigang, S. Goriely, M. Herman, A.V. Ignatyuk, S. Kailas, A. Koning, P. Oblozinsky, V. Plujko, P. Young, IAEA-TECDOC-1506: Handbook for calculations of nuclear reaction data: Reference Input Parameter Library-2, IAEA, Vienna, 2005. Available online at http://www-nds.iaea.org/RIPL-2/.
[7] A.J. Koning, J.P. Delaroche, Nucl. Phys. A 713 (2003) 231.
[8] A.J. Koning, M.C. Duijvestijn, Nucl. Phys. A 744 (2004) 15.
[9] T. Ericson, Adv. Phys. 9 (1960) 425.
[10] D. Mocelj, T. Rauscher, G. Martínez-Pinedo, K. Langanke, L. Pacearescu, A. Faessler, F.-K. Thielemann, Y. Alhassid, Phys. Rev. C 75 (2007) 045805.
[11] Y. Alhassid, G.F. Bertsch, S. Liu, H. Nakada, Phys. Rev. Lett. 84 (2000) 4313.
[12] J.R. Huizenga, L.G. Moretto, Annu. Rev. Nucl. Sci. 22 (1972) 427.
[13] H. Bethe, Rev. Mod. Phys. 9 (1937) 69.
[14] H. Baba, Nucl. Phys. A 159 (1970) 625.
[15] A.V. Ignatyuk, G.N. Smirenkin, A.S. Tishin, Sov. J. Nucl. Phys. 21 (3) (1975) 255.
[16] G. Audi, A.H. Wapstra, Nucl. Phys. A 729 (2003) 129.
[17] A. Mengoni, Y. Nakajima, J. Nucl. Sci. Technol. 31 (1994) 151.
[18] W.D. Myers, W.J. Swiatecki, Nucl. Phys. 81 (1966) 1.
[19] S. Goriely, Nucl. Phys. A 605 (1996) 28.
[20] S. Hilaire, PhD thesis, unpublished, 1997.
[21] S.F. Mughabghab, C. Dunford, Phys. Rev. Lett. 81 (1998) 4083.
[22] A.S. Iljinov, M.V. Mebel, N. Bianchi, E. De Sanctis, C. Guaraldo, V. Lucherini, V. Muccifora, E. Polli, A.R. Reolon, P. Rossi, Nucl. Phys. A 543 (1992) 517.
[23] O.T. Grudzevich, A.V. Ignatyuk, V.I. Plyaskin, A.V. Zelenetsky, in: Proceedings of the Nuclear Data for Science and Technology, Mito, JAERI, 1988, p. 187.
[24] A.R. Junghans, M. de Jong, H.-G. Clerc, A.V. Ignatyuk, G.A. Kudyaev, K.-H. Schmidt, Nucl. Phys. A 629 (1998) 635.
[25] G. Hansen, A.S. Jensen, Nucl. Phys. A 406 (1983) 236.
[26] A.J. Koning, S. Hilaire, M.C. Duijvestijn, TALYS: Comprehensive nuclear reaction modeling, in: R.C. Haight, M.B. Chadwick, T. Kawano, P. Talou (Eds.), Proceedings of the International Conference on Nuclear Data for Science and Technology – ND2004, Santa Fe, USA, 26 September–1 October, 2004, in: AIP, vol. 769, 2005, p. 1154.
[27] EXFOR: Experimental Nuclear Reaction Data Retrievals, available at http://www.nea.fr/html/dbdata/x4/welcome.html.
[28] M.K. Grossjean, H. Feldmeier, Nucl. Phys. A 444 (1985) 113.
[29] A.V. Ignatyuk, J.L. Weil, S. Raman, S. Kahane, Phys. Rev. C 47 (1993) 1504.
[30] RIPL-3 database, to be published at the IAEA.
[31] TALYS website, www.talys.eu.